NOTICE

The quality of this microform is heavily dependent upon the quality of the original thesis submitted for microfilming. Every effort has been made to ensure the highest quality of reproduction possible.

If pages are missing, contact the university which granted the degree.

Some pages may have indistinct print especially if the original pages were typed with a poor typewriter ribbon or if the university sent us an inferior photocopy.

Reproduction in full or in part of this microform is governed by the Canadian Copyright Act, R.S.C. 1970, c. C-30, and subsequent amendments.

AVIS

La qualité de cette microforme dépend grandement de la qualité de la thèse soumise au microfilmage. Nous avons tout fait pour assurer une qualité supérieure de reproduction.

S'il manque des pages, veuillez communiquer avec l'université qui a conféré le grade.

La qualité d'impression de certaines pages peut laisser à désirer, surtout si les pages originales ont été dactylographiées à l'aide d'un ruban usé ou si l'université nous a fait parvenir une photocopie de qualité inférieure.

La reproduction, même partielle, de cette microforme est soumise à la Loi canadienne sur le droit d'auteur, SRC 1970, c. C-30, et ses amendements subséquents.

Canada

ON THE CHARACTERIZATION OF THE VISCOELASTIC RESPONSE OF A CLASS OF MATERIALS USING ACOUSTO-ULTRASONICS - A PATTERN RECOGNITION APPROACH

by
SRINIVASAN IYER

A thesis submitted to the Faculty of Graduate Studies and Research in partial fulfilment of the requirement for the degree of Master of Applied Science in Mechanical Engineering

Department of Mechanical Engineering
University of Ottawa
Ottawa, Canada

May, 1993

ISBN 0-315-89605-1

Canada

UNIVERSITÉ D'OTTAWA
UNIVERSITY OF OTTAWA

ABSTRACT

This thesis describes the experimental work carried out at the University of Ottawa for characterizing linear viscoelastic materials using acousto-ultrasonic wave propagation technique. The objective of the research program is to asses the feasibility of utilizing acousto-ultrasonics in the characterization of mechanical response and strength prediction of solid polymers as a class of engineering materials.

The basic principles of acousto-ultrasonic technique, the instrumentation involved, and the factors affecting waveform measurements are described. A review on the analysis of the resultant acousto-ultrasonic waveform using statistical pattern recognition methodology is presented. The time-dependent properties of creep, and stress-relaxation of linear viscoelastic materials are reviewed. Also, fatigue, macromechanical defects and yielding of polymers are discussed.

Experimental results obtained in a series of acousto-ultrasonic characterization tests performed on Polyvinylchloride (PVC) and Polycarbonate (PC) specimens are presented. Good correlation was obtained between the acousto-ultrasonic parameter (AUP) and stress in material during a time-dependent stress relaxation testing for a particular strain level. The acousto-ultrasonic parameter (AUP) was seen to decrease with increasing stress levels during uniaxial tensile loading. Also, induced fatigue states in the material and macromechanical defect states were seen to have good correlation with the AUP. Statistical pattern recognition classifiers were designed for all characterization experiments performed and tested with unknown samples and found to be very effective. Acousto-Ultrasonics (AU), combined with statistical pattern recognition methodology applied in real time environment, proves to be an efficient non-destructive quantitative evaluation process for the class of solid polymers investigated.

ACKNOWLEDGEMENT

I wish to express my sincere gratitude to my research supervisor Prof. Y.M. Haddad of the University of Ottawa. The successful completion of this thesis depended solely on his useful ideas and constant encouragement. The timely guidance and assistance provided by the staff of Tektrend International, Montreal, Canada are deeply appreciated. Also, I would like to thank the staff of the Department of Mechanical Engineering, University of Ottawa for their continued assistance.

I am grateful to the Natural Sciences and Engineering Research Council of Canada (NSERC) for the financial support provided for this research through the operating grant of my research supervisor. The tuition fee waiver and the entrance scholarship granted to me by the University of Ottawa during my Masters program is sincerely appreciated.

The support and encouragement given by my wife Ms. Jayashree Iyer has helped in many respects towards the completion of this thesis.

TABLE OF CONTENTS

1.	INTRODUCTION		1
1.1	Introduction		1
1.2	Problem Definition		3
1.3	Objective and Presentation of the Research Work		4
	1.3.1	Objective of the research	4
	1.3.2	Formal presentation of the research	6
2.	REVIEW OF NON-DESTRUCTIVE TESTING (NDT) TECHNIQUES		10
2.1	Introduction		10
2.2	NDT Techniques Using Ultrasonic Wave Propagation		11
	2.2.1	Pulse echo	11
	2.2.2	Through-transmission	13
	2.2.3	Interface and plate waves	14
	2.2.4	Resonance	14
	2.2.5	Ultrasonic spectroscopy	15
	2.2.6	Acoustic emission (AE) technique	15
2.3	Acousto-Ultrasonic (AU) Technique		18
	2.3.1	Introduction	18
	2.3.2	Acousto-Ultrasonic characterization of engineering materials	19
	2.3.3	Principle of acousto-ultrasonics	20
	2.3.4	Acousto-Ultrasonics applied to viscoelastic materials	20
	2.3.5	Experimental set-up for viscoelastic material characterization	21
2.4	Acousto-Ultrasonic Waveform Parameters		23
	2.4.1	Ring down stress wave factor (SWF)	23
	2.4.2	Peak voltage SWF	24
	2.4.3	Energy SWF	25

2.5 Factors Affecting the Acousto-Ultrasonic Waveform Measurement 27

2.5.1 External parameters affecting AU measurements 27
2.5.2 Internal parameters affecting AU measurements 29

2.6 Conclusion 30

3 SIGNAL ANALYSIS TECHNIQUES FOR ACOUSTO-ULTRASONICS 31

3.1 Introduction 31

3.2 Homomorphic Processing 31

3.3 Pattern Recognition Method 32

3.4 Pattern Recognition Method for Signal Analysis 33

3.4.1 Introduction 33
3.4.2 Principle of pattern recognition 33
3.4.3 Decision functions 39
3.4.4 Pattern classification by distance functions 42
3.4.5 Minimum-distance pattern classification 43
3.4.6 Extension of minimum-distance pattern classification concepts 45
3.4.7 Empirical Bayesian classifier 46
3.4.8 Training and evaluation of the classifier 48

3.5 Conclusion 49

4 ON THE VISCOELASTIC RESPONSE BEHAVIOUR OF MATERIALS 51

4.1 Introduction 51

4.1.1 Assumptions of linear viscoelastic materials 51

4.2 Linear Viscoelastic Behaviour 52

4.2.1 Creep function 52
4.2.2 Stress-relaxation 54
4.2.3 Mathematical treatment of linear viscoelastic behaviour 54
4.2.4 The stress-relaxation modulus 57

4.2.5 Relationship between creep and stress-relaxation 57

4.3 The Formal Structure of Linear Viscoelasticity 59

4.4 Yield Behaviour in Polymers 61

4.4.1 Necking and the ultimate stress 62

4.5 Fatigue in Polymers 64

4.6 Macromechanical Defects in a Polymer 66

4.7 Conclusion 67

5 ACOUSTO-ULTRASONIC EVALUATION OF STRESS-RELAXATION IN POLYMERS 68

5.1 Introduction 68

5.2 Experimental Procedure and Apparatus 69

5.2.1 Material and test specimen 69
5.2.2 Acousto-Ultrasonic testing system 70

5.3 Stress-Relaxation Testing for Polycarbonate Specimens 72

5.3.1 Acousto-Ultrasonic measurements 73
5.3.2 Stress-relaxation at different strain levels 73

5.4 Stress-Relaxation Testing for Polyvinylchloride Specimens 74

5.4.1 Acousto-Ultrasonic measurements 74
5.4.2 Stress-relaxation at different strain levels 74

5.5 Results and Discussion 75

5.5.1 Polycarbonate (PC) specimens 75
5.5.2 Polyvinylchloride (PVC) specimens 76
5.5.3 Discussion of the results obtained 76

5.6 Pattern Recognition Methodology Applied for Signal Analysis 78

5.6.1 Polycarbonate (PC) specimens 78

5.6.2 Polyvinylchloride (PVC) specimens 82

5.7 Conclusion 85

6 EVALUATION OF STRESS LEVELS IN VISCOELASTIC SPECIMENS SUBJECTED TO UNIAXIAL TENSILE LOADING 87

6.1 Introduction 87

6.2 Experimental Apparatus and Procedure 88

6.2.1 Material and test specimen 88
6.2.2 Acousto-Ultrasonic testing system 89

6.3 Mechanical Testing 89

6.3.1 Acousto-Ultrasonic measurements 90

6.4 Results and Discussion 90

6.5 Pattern Recognition Methodology Applied for Signal Analysis 92

6.5.1 Training and evaluation of the classifier 96
6.5.2 Testing of the classifier 97

6.6 Conclusion 97

7 FATIGUE TESTING OF A SOLID POLYMER SPECIMEN 99

7.1 Introduction 99

7.2 Experimental Apparatus and Test Procedure 101

7.2.1 Material and test specimen 101
7.2.2 Acousto-Ultrasonic testing system 101

7.3 Mechanical Fatigue Testing 101

7.3.1 Acousto-Ultrasonic measurements 102

7.4 Results and Discussion 103

7.5 Pattern Recognition Methodology Applied for Signal Analysis 104

7.6 Conclusion 107

8 TESTING FOR A MACROMECHANICAL DEFECT IN A SOLID POLYMER SPECIMEN 108

8.1 Introduction 108

8.2 Experimental Apparatus and Procedure 109

8.2.1 Material and test specimen 109
8.2.2 Acousto-Ultrasonic testing system 110

8.3 Mechanical Testing 110

8.3.1 Acousto-Ultrasonic measurements 110

8.4 Results and Discussion 111

8.5 Pattern Recognition Methodology Applied for Signal Analysis 113

8.6 Conclusion 117

9 CONCLUSION AND FUTURE RECOMMENDATIONS 119

REFERENCES 122

APPENDIX A 129

FIGURES 130

LIST OF FIGURES

2.1 Ultrasonic pulse echo technique.

2.2 Ultrasonic through transmission technique.

2.3 Interface and plate waves technique.

2.4 Ultrasonic resonance technique.

2.5 Acoustic emission testing system.

2.6 A schematic diagram of the acousto-ultrasonic test set-up.

2.7 Acousto-ultrasonic experimental set-up.

2.8 Measurement of acousto-ultrasonic waveform parameters.

2.9 Calculation of acousto-ultrasonic parameter (AUP) [26,37].

2.10 Illustration of constant force clamps for acousto-ultrasonic set-up.

2.11 Variation of acousto-ultrasonic parameter (AUP) with the change in the coupling medium between transducers and the specimen.

2.12 Variation of AUP with inter-transducer distance.

3.1 A sample of the received acousto-ultrasonic signal as the raw data vector for pattern classification.

3.2 Two disjoint pattern classes.

3.3 A simple decision function for two pattern classes.

3.4a Patterns classifiable by proximity concept.

3.4b Minimum distance classifier applied to classes with varying sizes.

3.5 Patterns not easily classifiable by proximity concept.

3.6 Decision boundary of two classes characterized by minimum distance classification approach.

3.7 Nearest Neighbour classifier.

3.8 Empirical Bayesian classifier.

3.9 Schematic illustration of the training processes in a pattern classifier using normalized feature values.

3.10 Schematic illustration of the evaluation process in a pattern classifier using normalized feature values.

4.1 Creep curves.

4.2 Comparison between a linearly elastic and linearly viscoelastic material response for the same type of loading program.

4.3 Boltzmann's superposition principle.

4.4 Schematics of a stress-strain relationship for a solid polymer undergoing uniaxial tension.

4.5 Conventional (engineering) and true stress-strain curves for a solid polymer undergoing uniaxial tension test.

4.6 The Conside're construction [57].

4.7 Fatigue response of a solid polymer.

5.1 Specimen for uniaxial tensile stress-relaxation testing.

5.2 Acousto-ultrasonic experimental set-up.

5.3 A sample of acousto-ultrasonic waveform with test parameters chart.

5.4 Stress-relaxation curves for Polycarbonate (PC) specimens under 4% uniaxial (tensile) strain.

5.5 Stress-relaxation curves for Polycarbonate (PC) specimens under different uniaxial (tensile) strain levels of 1% - 7%.

5.6 Stress-relaxation curves for Polyvinylchloride (PVC) specimens under 4% uniaxial (tensile) strain.

5.7 Stress-relaxation curves for Polyvinylchloride (PVC) specimens under different uniaxial (tensile) strain levels of 1% - 6%.

5.8a Correlation between the normalized relaxed stress and the normalized acousto-

ultrasonic parameter (AUP) of the waveform at different stress levels for Polycarbonate (PC) specimens.

5.8b Correlation between the normalized relaxed stress and the normalized acousto-ultrasonic parameter (AUP) of the waveform at different stress levels for Polyvinylchloride (PVC) specimens.

5.9a Plot illustrating the separation of pattern classes in a two-dimensional feature space for Polycarbonate (PC) specimens.

5.9b Plot illustrating the separation of pattern classes in a two-dimensional feature space for Polycarbonate (PC) specimens.

5.9c Plot illustrating the separation of pattern classes in a two-dimensional feature space for Polyvinylchloride (PVC) specimens.

5.9d Plot illustrating the separation of pattern classes in a two-dimensional feature space for Polyvinylchloride (PVC) specimens.

6.1 Stress-Strain diagram for uniaxial tension test for Polyvinylchloride (PVC) specimens at a cross head speed of 2.5 mm/min.

6.2 The Conside're construction for the ultimate strength of the PVC specimen under Uniaxial tension test.

6.3 Correlation between the normalized stress and the normalized acousto-ultrasonic parameter (AUP) of the waveform at different stress levels.

6.4a Plot illustrating the separation of pattern classes in a two-dimensional feature space.

6.4b Plot illustrating the separation of pattern classes in a two-dimensional feature space.

7.1 Stress (σ) - Number of cycles for failure (N) diagram for fatigue testing.

7.2 Correlation between the normalized acousto-ultrasonic parameter and cyclic loading levels causing fatigue.

7.3 Plot illustrating the separation of pattern classes in a two-dimensional feature space.

7.4 Plot illustrating the separation of pattern classes in a two-dimensional feature space.

8.1 Specimen for evaluation of reduced tensile strength in uniaxial tensile testing.

8.2 Correlation between the normalized acousto-ultrasonic parameter and normalized tensile strength.

8.3 Correlation between tensile strength and defect size.

8.4a Plot illustrating the separation of pattern classes in a two-dimensional feature space.

8.4b Plot illustrating the separation of pattern classes in a two-dimensional feature space.

LIST OF SYMBOLS

A	Instantaneous cross-sectional area of the specimen
A_o	Original cross-sectional area of the specimen
AUP	Acousto-Ultrasonic Parameter
C	Digital counter output of the digitizer
C_i, C_{i+1}	Digital counter outputs at i th and i + 1 th levels respectively
C'	Length of a crack initiated in a fatigued specimen
e(t)	Strain at time 't' for a one dimensional viscoelastic specimen
F(t)	creep function
G	Strain energy release rate
N	Number of cycles of cyclic loading of a fatigue specimen
p	Pulse repetition rate of an ultrasonic pulsar
P	Load applied to a uniaxial tensile testing specimen
R	Reset time of an ultrasonic pulsar
R(t)	stress relaxation function
R(t-τ)	Stress relaxation modulus
S_i, S_k	Reference pattern vectors for nearest neighbour classifier
S_{rms}	Function of frequency of the acousto-ultrasonic wave in frequency domain
SWF	Stress wave factor
U	Stored energy in a viscoelastic specimen

V_p	Peak amplitude of the ultrasonic waveform
V_{max}	Maximum voltage swing observed in an acousto-ultrasonic waveform
V_{rms}	Root Mean Square voltage of the time varying waveform
W_{ik}	Weights associated with discriminant classification functions
$\sigma(t)$	Stress at time 't' for a one dimensional viscoelastic specimen
λ'	Draw ratio for a polymer
ϱ	Density of a material
ω_1, ω_2	Pattern classes represented in feature space

Chapter 1

INTRODUCTION

1.1 Introduction

The role of polymeric materials in engineering applications continues to increase throughout industries where metals were historically the major useful choices. The advantages in cost, weight, ease of fabrication and often strength of polymeric base systems are accepted today, and the development of specialized polymers with specific properties is accelerating.

A thorough understanding of the nature of mechanical behaviour is essential for designing with 'solid polymers', since the stress-strain response of polymers are fundamentally different from that of conventional engineering materials. For instance, polymeric materials often exhibit viscoelastic creep under loading, whereby the gradual deformation of a polymer based component might render the structure nonfunctional if the occurring geometrical variation is beyond a critical limit. Similarly, viscoelastic materials, when heated above their glass transition temperatures, behave like liquids and, hence, the response characteristics in this phase, are very much different from those of the original solids. As it is impractical to perform destructive tests on structural components in service, non-destructive testing represents a viable concept for evaluating the strength of such material systems.

Acousto-Ultrasonics is a non-destructive evaluation technique that involves generating ultrasonically, stress waves inside the material and allowing these waves to travel through the test specimen. The resultant waveform which contains

information regarding the nature of the microstructure of the material is then captured and analyzed for material property variations using several statistical and analytical techniques. When applied to a viscoelastic material (of a loading history) suitably at different times, the resultant stress waves would contain 'features' which are peculiar to the time-dependent mechanical properties such as creep and stress-relaxation of the material. The acousto-ultrasonic waveform that had travelled through the material specimen at various defect states, fatigue states and at various stress levels, would give out information pertaining to the overall mechanical response characteristics of the specimen.

The analysis of such waveforms could be performed using statistical pattern recognition methods. In a pattern recognition approach, the normalized feature co-ordinates of the waveforms are plotted in n-dimensional feature space forming distinct clusters or groups pertaining to various problem states such as different fatigue or different stress levels. By using samples of known values at these states, a discriminating classifier is first created. Then, the feature values of a given wave form of an unknown mechanical state could be matched by plotting them in the n-dimensional feature space and judging as to which cluster they would belong to, so that the material state would be classified from the statistical inference. This entire process is termed as the 'design' of a pattern classifier for the particular mechanical state of the material specimen under consideration.

1.2 Problem Definition

The extensive use of solid polymeric materials such as Polyvinylchloride (PVC) over the past years have resulted in an enormous amount of polymeric structural components in aerospace, automobile and other industrial structures (as both original equipment parts and spares). These components, designed for the particular performance requirements of the given application, would come across various time-dependent changes such as creep and stress-relaxation. This is in addition to the structural defects such as cracks and voids that would effectively reduce the strength of these solid polymers and could hinder their performance as structural components. Another important aspect is the cyclic loading that can induce fatigue in the polymer and consequently may reduce its overall structural performance. Thus, each of the above mentioned effects would constitute a degradation state that could reduce the strength of the material. Therefore, it is necessary to identify in course of time the defect state for any structural component made of solid polymeric material.

All of the above said material deterioration states that correspond to changes in material properties may be evaluated globally within the material specimen. A classifier designed for various material states with known samples of a particular polymer would serve this purpose adequately, i.e., by classifying the unknown sample as to which state it belongs to, thereby, giving an indication to the nature of its structural ability and strength. In this, the various material states characterized by selected features of an ultrasonic waveform that have already travelled in the material would form different clusters in n-dimensional feature space. The unknown sample

can then be matched to one of the clusters and evaluated for its structure worthiness. This poses a typical pattern classification problem, whereby different statistical pattern classification techniques may be used. By using discriminating statistical values, e.g., mean, standard deviation and probability density function of the feature distribution in n-dimensional feature space, the discriminatory function could be designed. The following section describes in more details the above said mechanical response characteristics and the formal structure of presenting the experimentation.

1.3 Objective and Presentation of the Research Work

1.3.1 Objective of the research

Polymeric materials often exhibit time-dependent deformation for a given level of loading. This response behaviour is referred to as 'creep'. When the strain level is maintained constant, the stress in the material relaxes over a period of time. This response phenomenon is referred to as 'stress-relaxation'. The response behaviour of relaxed stress and deformation constitute distinct time-dependent strain and stress states. A classifier may be designed for various states that can identify a structural member to its strain state in the creep phase or, alternatively, to its stress state in the relaxation phase. A pattern classifier could effectively discriminate the various discrete stress levels and the unknown sample could be matched to one of the discrete stress level, it is experiencing in real-time service.

The response behaviour of a polymeric material, when subjected to a uniaxial tensile loading, is similar to that of elastic materials except for the large plastic plateau

phase after its yield point. Structural components made of polymeric materials experience stresses due to static loads imposed on them. It is thus necessary to evaluate these stresses by a NDT-technique. Acousto-Ultrasonic (AU) technique could provide quantitative information on the stress level experienced by the polymeric member. The evaluation of stress levels could be achieved by designing a pattern classifier using the acousto-ultrasonic waveforms that had been passed through the microstructure of the material, while the material is loaded. Acousto-ultrasonic waveforms received from unknown samples could then be classified to their respective class using the designed pattern classifier.

Another important mechanical response characteristic of polymeric materials is fatigue, caused by cyclic loading. Thus, through repeated cyclic loading, a known fatigue state can be created. Different number of cycles would constitute various fatigue states that may be discriminated using a pattern classification technique. For this, a pattern recognition classifier may be built based on the feature values and could be used to discriminate the various fatigue states.

Macro-mechanical defects such as voids and rivet holes play an important role in reducing the strength of the polymeric materials. Thus the reduction in the strength of the material, due to different sizes of the defect, pose a pattern recognition problem. The necessary feature values required for such discrimination are obtained by employing acousto-ultrasonic experimental procedure through induced defects.

Classifiers such as mentioned above, when applied to an unknown material specimen would then give a prediction of its mechanical state, e.g., mechanical

strength, ability to resist further deformation, creep state etc. The waveforms necessary for such an approach are obtained by employing an acousto-ultrasonic technique.

1.3.2 Formal presentation of the research

The experimental technique used in this research is the acousto-ultrasonic (AU) technique. This is a new non-destructive technique characterizing quantitatively the mechanical response behaviour of engineering materials. The concept of the AU technique, its suitability for characterizing engineering materials, the experimental set-up, factors that affect the waveforms and its employment by other researchers are reviewed in Chapter 2.

The analysis of the resultant AU waveform obtained from the material characterization experiment is discussed in Chapter 3. Several parameters used to quantify the information obtained from the resulting signal are discussed. The use of such parameters by different researchers is reviewed. In this research, the information from the resulting AU signal is quantified, by first using a parameter known as acousto-ultrasonic parameter (AUP). The resulting signal is then analyzed using statistical pattern recognition methods. In Chapter 3, both these techniques are discussed. A detailed mathematical description and reviews from the available literature on statistical pattern recognition methodology is presented. Different algorithmic approaches, the hypotheses and software and hardware environments necessary to perform such an analysis are reviewed.

Chapter 4 deals with the response characteristics of linear viscoelastic materials.

The mechanical properties of linear viscoelastic materials that are critical to the strength of engineering structural components are discussed. This includes the time-dependent properties of creep and stress-relaxation. Yield behaviour of linear viscoelastic materials during uniaxial tensile loading is also discussed. Another important property that reduces the strength of the structural components subjected to cyclic loading, i.e., fatigue of polymeric components, is discussed and the available literature in this area is reviewed. Further, it is of interest to obtain prior knowledge regarding the reduction in strength of the polymeric component in structure due to the presence of defects such as holes. A discussion regarding this is also given in Chapter 4.

Chapter 5 deals with the experimental investigation of a number of solid polymeric materials using acousto-ultrasonics. This experiment is carried out at different stress levels during a stress-relaxation for a prescribed strain level. First, a family of stress-relaxation curves are generated at various strain levels. Then for a particular strain level, the characterization using acousto-ultrasonic waveforms is performed. The acousto-ultrasonic parameter is correlated with the relaxed stress levels observed during the time period of the experiment. The pattern recognition methodology is used to discriminate between various stress states. Acousto-Ultrasonic waveforms obtained from samples of unknown stress states are then tested using the pattern classifier and classified to their respective classes.

Chapter 6 deals with the experimental investigation involving different stress levels a polymeric specimen experiences while undergoing uniaxial tensile loading.

Ultrasonic pulses are injected and the resulting acousto-ultrasonic waveforms are captured at different stress levels. The acousto-ultrasonic parameter is correlated with the increasing stress level the material experiences, during the uniaxial tensile loading experiment. Statistical pattern recognition methodology is used to design a pattern classifier that would discriminate between the stress states based on the features extracted from the resulting acousto-ultrasonic waveform.

Chapter 7 involves the experimental investigation of a solid polymeric material for various fatigue states. These fatigue in the polymeric specimens were initiated by subjecting them to various levels of tensile cyclic loading between zero and a particular stress level. The acousto-ultrasonic parameter was correlated with different fatigue levels. A classifier designed using the pattern recognition methodology is used to discriminate these fatigue states. Acousto-Ultrasonic waveforms obtained from unknown specimens subjected to similar fatigue damage are then tested with the designed pattern classifier.

Chapter 8 deals with the experimental investigation involving the prediction of the reduction in strength of solid polymeric specimens containing a macro-mechanical defect. This defect is intentionally created in the form of a hole. The size of the hole was varied so that the ultimate tensile strength of the material could be varied when tested destructively in uniaxial tensile testing. Specimens having the same hole size, thus, constitute a group with a particular tensile strength. Several such groups of specimens were prepared by varying the size of the hole. Acousto-Ultrasonic measurements were taken prior to the testing of the specimens destructively.

Acousto-Ultrasonic (AU) waveforms received from specimens belonging to each group, thus represents the specimen with a particular strength level. The acousto-ultrasonic parameter is correlated with the reduction in tensile strength. Statistical pattern recognition methodology is then used to discriminate the reduced strength levels by designing a pattern classifier using the resulting AU waveforms. Finally, unknown samples were tested and classified to their respective class using the classifier.

Experiments conducted in Chapters 5, 6 and 7 utilize the same specimen geometry. Experiments for Chapter 8 also utilizes similar specimen geometry, but with a defect initiated in the form of a hole. For the purpose of stress-relaxation testing, explained in Chapter 5, two kinds of polymers, Polycarbonate (PC) and Polyvinylchloride (PVC) were chosen. The uniaxial tensile loading experiment, discussed in Chapter 6 and the fatigue testing explained in Chapter 7 were conducted using polyvinylchloride (PVC) specimens. Polycarbonate (PC) specimens were used for evaluating the reduction in strength due to the presence of the initiated defect in the form of a hole as explained in Chapter 8. The acousto-ultrasonic test set-up was maintained the same for all the experiments.

Finally, chapter 9 contains the concluding remarks and recommendations for future research.

Chapter 2

REVIEW OF NON-DESTRUCTIVE TESTING (NDT) TECHNIQUES

2.1 Introduction

Traditionally the vast majority of material property characterization techniques have been destructive, e.g., chemical composition analysis, metallographic determination of microstructure, destructive mechanical testing, etc. The present day engineering requirements need new techniques to meet them. The development of high quality low porosity ceramics capable of performing reliably at high temperatures, the improvement of metallic super-alloys and the evolution of high performance structural plastics and composites require proper application of non-destructive testing techniques (NDT) for material characterization (i.e., to monitor and control the different stages of the production process of such materials). Also, the need to evaluate the response of these materials in structures for different situations of loading without destroying the structure itself in the process of testing, calls for more reliable and accurate non destructive evaluation (NDE) methods.

The above said need is addressed by several NDE techniques developed to detect critical defects, flaws and anomalies of the microstructure of engineered materials. These techniques usually use sonic vibration, radiation, optical lasers and liquid penetration, among others as principle methods. The methods based on such principle are Ultrasonics, Sonic Vibration, Acoustic Emission, Radiology, Optical Holography, etc. A much newer technique combining the desirable properties of ultrasonic wave propagation and Acoustic Emission methodology, known as Acousto-Ultrasonics has

been found to address the requirement of non-destructively evaluating the overall performance of the material [1].

The following sections give a brief introduction to several NDT techniques using ultrasonic wave propagation and deals with the Acousto-Ultrasonic technique more elaborately.

2.2 NDT Techniques Using Ultrasonic Wave Propagation

Although numerous material testing methods are available under the broad terminology of NDT techniques, the ones discussed below are based on the principle of interrogating the material using ultrasonic wave propagation. All of these techniques use some type of a piezoelectric transducer to generate and inject 'ultrasonic waves' into the test specimen and capture the resulting wave after interaction with the material using another piezoelectric transducer.

As the name implies, ultrasonic techniques utilize high frequency (0.5-20 MHZ) waves to interrogate the quality of the test material. Ultrasonic methods have been used widely due to their flexibility and effectiveness. Some of the methods which use the ultrasonic principle are summarized below.

2.2.1 Pulse echo

A repetitive ultrasonic pulse is transmitted into the test specimen through a transducer and the same transducer receives the reflected signals from any voids or flaws which are responsible for such reflection (Fig 2.1). Acoustic coupling necessary between the transducer and test specimen is achieved by a layer of gel or immersing

the whole set up in water bath. On following closely with the description of the experimental set up mentioned in [2], this method can be described as follows.

As illustrated in (Fig 2.1), Pulse echo technique comprises of a single piezoelectric transducer coupled to the test specimen through a suitable coupling medium such as gel or grease, capable of generating and transmitting ultrasonic waves. Repetitive ultrasonic pulses are injected into the specimen which is partly refracted and absorbed, but a majority of it gets reflected from the presence of any voids. The latter is captured using the same transducer (capturing the echoes of the injected pulse) before the next wavelet is passed into the material. The same pulse triggers a time base generator, so that the pulse of ultrasound starts to move through the specimen at the same time as a spot starts to move across the cathode ray tube (CRT), display screen. Variations in voltage in the transducer due to the ultrasonic wave are passed to the amplifier and applied to the Y-axis of the CRT to produce a transmission signal, which represents the shape of the generated ultrasonic pulse. The spot continues to move across the screen of the CRT as the ultrasonic pulse travels through the specimen until the ultrasonic pulse reaches a reflecting or scattering surface. The reflected portion of the ultrasonic pulse returns to the transducer, which vibrates, causing a small alternating voltage which is fed to the amplifier. After amplification, it is fed to the CRT and produces the echo pulse from the flaw. Further ultrasonic energy in the transmitted pulse may continue to the bottom surface of the specimen and be reflected back to the transducer, producing the bottom surface echo.

Since the ultrasonic signals may be weak or strong, the amplifier need to have a calibrated gain control. For testing metals, ultrasonic probe frequencies from about 1 to 10 MHZ are used and much of the equipment is designed to use a slightly wider range of frequencies, from 250 KHZ to 20 MHZ. The gain control should be calibrated in decibels so that any signal can be increased or decreased in display amplitude by a known amount. Discontinuities in bonded joints were successfully detected using the pulse echo method [3]. Alers et. al., [4] found a correlation between the cohesive shear strength of an aluminium lap joint and the longitudinal velocity of sound in the adhesive bond line. Also Kline et.al., [5] examined the ultrasonic attenuation and phase velocity in adhesively bonded steel specimens.

2.2.2 Through transmission

Here the transmitting and receiving transducers are positioned on opposite sides of the test specimen (Fig.2.2). Both the transducers need to be exactly aligned for effecting through transmission. Difficulties are often encountered in probe alignment and in establishing good contact on both sides of the joint [2]. Ultrasonic waves are injected through the test specimen by the transmitting transducer and captured by the receiving transducer at the other end of the specimen. By incorporating automatic C-scan [6], a 2-D image of the defect can be produced. However simple the ultrasonic through transmission technique may look, there are practical difficulties involved [7]. Because of diffraction around the edges of the defect, the acoustic wavelength in the object must always be less than the diameter of the smallest defect to be detected. Good and consistent acoustic coupling must be ensured, otherwise the received

ultrasonic wave will vary regardless of the presence or absence of any flaw.

2.2.3 Interface and plate waves

When an incident ultrasonic beam strikes the material at an oblique angle rather than normal incidence as in conventional technique, information about interfacial material properties might be obtained from the velocity and attenuation of these waves [8]. In this technique, plate and interface waves propagate along the interlaminar bond line (Fig.2.3), thereby the changes in the properties of interfaces may be effectively monitored using this method [9]. Kline and Hashemi [10] monitored the fatigue damage development in single-lap aluminium specimens using interface waves and termed them as 'guide waves'. Chapman [11] used Lamb waves to evaluate the bond quality of fibreglass reinforced plastic bonded joints.

2.2.4 Resonance

In this method, the frequency of a continuous ultrasonic wave injected locally to a test specimen is changed until a resonance condition is produced. 'Standing waves' as shown in Fig.2.4 are generated during resonance and are an indication of resonant phenomenon in the test specimen [11]. At resonant frequency, the wavelength of the standing wave is twice the thickness of the specimen [11,12], given by

$$\lambda_D = 2D = v/f_D; \quad or \quad f_D = v/2D \qquad (2.1)$$

When there is a void, the changed resonant frequency is $f_d = v/2d$; where f_d is the changed frequency due to the void, with a new overall effective thickness 'd', v is the velocity of the ultrasonic wave in the test specimen. As shown in Fig.2.4, when there is a defect inside the test specimen such as a void, the resonant frequency will

change sharply due to the presence of a gap which is "seen" by the transducer as change of thickness. Therefore the corresponding resonant frequency at the new thickness, d, is then $f_d = v/2d$.

For measuring very thin sheets with high accuracy, a new type of thickness gauge based on resonance was developed at the Non-destructive Testing Centre, Harewell, called the ultrasonic micrometer [14], which is based on the resonance principle of changed frequency due to the changed thickness for standing waves to occur.

2.2.5 Ultrasonic spectroscopy

Conventional ultrasonic techniques use a narrow frequency band. Thus the information obtained from the ultrasonic signals has to be deducted solely from appropriate variations. Ultrasonic spectroscopy however uses broad band ultrasonic transducers. These techniques are generally carried out by using pulse echo method at different frequencies of 0.5 to 10 MHZ. The echoes from the interfaces are then analyzed in time and frequency domain. Material variations are regressed against different bands of a continuous frequency or time spectrum of the resultant ultrasonic signal. This technique is based on the principle of constructive and destructive wave interference [15]. The technique has been found to be useful in determining the quality variations in aluminium alloy bonded joints due to fabrication processes [16,17] and/or hydrothermal degradation [18].

2.2.6 Acoustic Emission (AE) Technique

Acoustic Emission is a spontaneous emission of sound pulses from materials subjected to external stresses as a result of sudden relaxation of stresses within the

material [19,22]. In accordance with the development of wave equation for equilibrium, the stress distributes throughout the remaining material at the velocity of sound [23]. Stress relaxation in any material producing acoustic emission can occur as a result of the nucleation and propagation of cracks. It can also occur as a result of such elastic and plastic deformation processes as the slip of the existing dislocations in metal, the activation of dislocation sources, twinning and slip of grain boundaries [23]. The emitted energy consists of two components:

(i) A low level, high frequency component which appears as an increasing noise as the stress continues to be applied and

(ii) A discontinuous burst type component or pulse. The high frequency component is believed to be induced by dislocation pinning during slip formation, mechanical twinning and/or the formation of cracks [23].

The sound level of acoustic emission is very low and depends upon the stress level at which it is produced, neglecting strain rates and volume effects. The loading mechanism used to stress the material must be carefully designed so that it does not generate sufficient noise to mask the acoustic emission [24,25].

The frequency spectrum of acoustic emission depends upon how the sound is produced. The frequencies range from the audible to the ultrasonic frequencies in the megahertz range. Sometimes frequency is used to denote rate of emission or the number of bursts or counts per second.

The microstructure and therefore the processing treatment that a metal has been subjected to, affects the acoustic emission. Deformation may cause a random signal

which is strain rate dependent with an average frequency being discernible. Along with the random signal, spontaneous bursts of higher frequency corresponding to brittle fracture produces burst signals of much higher frequency.

When a metal is stressed to a value near or above the yield stress, unloaded, and then stressed again up to the previous level, the emission that had been observed during the first load cycle would be absent or very much reduced during the second application of a load up to the previous stress level. However, when the previous stress level is exceeded, acoustic emission is again evident. This phenomenon has been called the 'Kaiser effect' (See, e.g., [19]). It should be noted that acoustic emission in reality is a destructive testing method, though conventionally it is treated as a non- destructive testing method.

The basic equipment required for applying acoustic emission practice for testing engineering structures, comprises of a loading machine such as the Universal testing machine, a pickup piezoelectric transducer and a signal processing system. This is illustrated schematically in Fig.2.5.

On detecting the acoustic emission events, it is necessary to amplify, possibly filter and then employ some type of signal processing to format and present the data obtained. The usual features that are inferred from the raw data are ring down count, burst rate, energy rate, rise time, event duration, frequency content and amplitude distribution amongst many others. A detailed description of different features that may be extracted from an acoustic emission experiment is given in [20].

Amongst the above measures, for the purpose of analyzing the data using

conventional methods, 'ring down count' is perhaps the most widely used (See, e.g., [19]). This consists of counting the number of times the amplified acoustic emission signal crosses a preset trigger level voltage. The results can be reported either as a rate, (counts/unit time), or as an accumulation of the measured count (summation of counts). A much newer approach is by using the method of statistical pattern recognition [19,20]. For both time and frequency domains of the signal, the method of statistical pattern classification can be applied. This technique is of most value when noises and signals do not occur simultaneously. A detailed theoretical background for interpretation of the results using statistical pattern recognition is explained in Chapter 3. Also it has been shown in [19] that the percentage of quiet time in monitoring acoustic emission event by a transducer is a good indication of the success probability of a pattern recognition approach.

Acoustic Emission is widely applied for monitoring pressure vessels [21], aerospace components [22,23] and for monitoring growth of cracks in engineering materials such as ceramics [24]. Inspection of welds can also be monitored using acoustic emission methodology [25].

2.3 Acousto-Ultrasonic Technique

2.3.1 Introduction

'Acousto-Ultrasonics' may be taken as a short form for 'Acoustic Emission simulation with ultrasonic wave generation', as it is a combination of the desirable aspects of acoustic emission practice and ultrasonic material characterization

methodology. In this technique, stress waves are 'simulated' that resemble acoustic emission waves but without disrupting the material (i.e., without loading) [1].

2.3.2 Acousto-Ultrasonic characterization of engineering materials

The waves that are generated by a piezo-transducer and transmitted into the material are affected by internal abnormalities in the material. Acousto-Ultrasonic waveform has been shown to be very sensitive to interlaminar and adhesive bond strength variations [26]. It has been proven to be useful in assessing micro-porosity and micro-cracking produced by fatigue cycling [27]. This technique is shown to be particularly useful in estimating the variation in strength of structural composites [28-30], as well as in estimating their residual strength and degradation from cyclic fatigue and impact damage [27,31]. The technique has also been used to evaluate the strength of wire ropes [32] and tension in nylon ropes [33]. The filler content in wood and paper products had been predicted using acousto-ultrasonics [34]. Strength of ceramic materials and the effect of hydrothermal aging on composites have been successfully evaluated using this approach [35].

In addition to providing quantitative information on the characterization of the materials, acousto-ultrasonics also offer some practical advantages. This technique requires the need for only one side of the specimen unlike other ultrasonic techniques [1,28 & 41]. Also, the technique overcomes the high attenuation posed by materials which are viscoelastic in nature, e.g., the matrix of a polymeric base composite material and viscoelastic materials in general [41]. This may be primarily due to the high sensitivity provided by the acoustic emission sensor.

2.3.3 Principle of acousto-ultrasonics

In the acousto-ultrasonic technique, shown in Fig. 2.6, a broad band transducer is employed to transmit a repetitive series of ultrasonic pulses into the test specimen. A receiving acoustic emission transducer is placed at a specific distance from the transmitting transducer to intercept the propagating stress waves resulting from the injected ultrasonic pulses. Although the transmitting transducer injects longitudinal waves normal to the specimen surface, the sound waves radiated into the material will produce oblique reflections and shear waves [36]. The resultant stress waves which consist of longitudinal and transverse components, will propagate in the material interacting with a significant portion of the microstructure along their path. Thus, they can be affected by those microstructural and morphological properties which also determine structural performance. In many situations it is possible to obtain information on the mechanical behaviour from the stress wave propagation data. (See, e.g., Tanary [26] and Tanary et. al.,[37]).

2.3.4 Acousto-Ultrasonics applied to viscoelastic materials

Non-destructive characterization of viscoelastic materials often involves evaluating the change in material properties with the change in environmental factors. The Acousto-Ultrasonic (AU) technique suits this purpose as it is concerned with the overall change of mechanical properties of materials, unlike the ultrasonic pulse-echo technique used for mechanical flaw detection. Also, the AU technique is totally non-destructive unlike the Acoustic Emission (AE) which is a one time destructive technique.

The AU waveform which travels through a viscoelastic test specimen while the material changes its properties continuously to the change in environmental factors such as loading, temperature etc., would result in a wave comprising of many features that are peculiar to the material state due to that particular loading or temperature condition. On analyzing these waveform features and using an Artificial Intelligence technique like pattern recognition method, it is possible to build an intelligent discriminant function that can be used in real time to predict the state of the material.

2.3.5 Experimental set-up for viscoelastic material characterization

Acousto-Ultrasonic (AU) technique involves generating ultrasonic waves and letting them pass through the material under test. The resultant waveform which travels through the material is captured through a receiving piezoelectric transducer. Although a number of test configurations are possible, the most desired test configuration is the one in which the sending and receiving transducers are located on the same side of the test specimen. This is widely adopted by many researchers [37-38].

The AU experimental set up used in the present research is shown in Fig.2.7. The pulsar-sender PCPR-100[1] is a printed circuit board with microelectronic components and solid state devices intended for pulse generation, connected to the mother board of a PC-386[2]. It sends in electric voltage pulses to the piezoelectric transducer at

---

1 PCPR-100 is the trademark of General Research Corporation, California.

2 PC-386 is the Central Processing Unit of Intel Corporation, used in the Hewlett Packard Computer Model Vectra RS/25C.

pre-determined rates and times. The acousto-ultrasonic wave is typically an ultrasonic or acoustic pressure wave sent periodically. The time between the successive waveforms is determined by the digitization rate. The first wave starts and interacts with the material thoroughly before being captured by the receiving transducer, which is connected to the preamplifier and in turn to the acoustic emission testing equipment (AET 5500[3]). The latter, The acoustic emission testing equipment, receives the waveform, converts the signal from analog to digital form and transfers the data to a digitization board STR-825[4] (a solid state circuit board connected to the mother board of the PC-386, which possess the signal processing capability through the signal processing chip TMS 32010[5] and the software SKY 321- PC[6] required to effect it), which digitizes the signal with the use of 'ARIUS™'[7] (A real-time data acquisition and signal processing software) [39]. The moment this signal is digitized, the STR-825 - digitizer triggers the pulsar again for sending the next wave form, which interacts with the material and the whole sequence repeats. The number of times the pulsar emits the waveform is determined by the 'repetition rate' utility,

---

3 AET 5500 is the trademark of acoustic emission testing equipment of Hartford Steam Boiler Technologies, California.

4 STR-825 is the trademark of Sonotek Inc.

5 TMS 32010 is the trademark of Texas Instruments.

6 SKY 321-PC is the trademark of SKY Computers Inc., MA.

7 ARIUS™ is the trademark of Tektrend Inc., Montreal.

which is controlled by the ARIUS™ software and can be manually set in DOS[8] environment. Also, ARIUS™ allows easy selection of threshold setting, setting of gates and their values, damping, frequency, etc., which initialises the waveform generation and reception. The digitized waveform is stored in the computer hard disk in separate data files for later analysis. A detailed instruction regarding digitization of waveform , sampling of waveform, computer hardware, software, and the operating system requirements can be found in [39-40]. Other parameters such as the gain factor, gates, etc., are selected after repeated trials for the given geometry, and material of the specimen in order to obtain reproducible results of the waveform.

2.4 Acousto-Ultrasonic Waveform Parameters

The following parameters are used in the present research for AU waveform analysis of engineering materials [1].(see Fig.2.8).

2.4.1 Ring down Stress Wave Factor (SWF)

Ring down Stress Wave Factor is defined as

$$SWF = P\,R\,C \qquad (2.2)$$

where, P is the repetition rate of an ultrasonic pulsar,

R is the reset time, and

C is the digital counter output.

A threshold voltage setting is the basis for counting the number of ring-down

---

[8] DOS is the trademark of Microsoft Inc.

oscillations per wave form. Defined this way, the SWF measures the relative signal strength.

AU signals that resemble acoustic emission bursts are readily characterized by a ring down count or count rate [41]. The threshold voltage is usually set at just above the noise level. The pulse repetition rate, P, is set so that each signal rings down below the threshold before a new one starts. The reset time, R, allows averaging a predetermined number of signals into the count, C.

A modified form to the stress wave factor was originally proposed in [27] and subsequently adopted for verification of adhesive shear strength in bonded joints [26]. It is termed as 'Acousto-Ultrasonic parameter' (Fig.2.9), and expressed as follows:

$$AUP(V_i) \quad = \Sigma_{i=0}^{p} V_i \, (C_i - C_{i+1}) \tag{2.3}$$

where V_i = Voltage at the ith level above threshold

C_i = Number of counts at the ith level and

V_p = Peak amplitude of the waveform

2.4.2 Peak voltage SWF

By using peak detection the SWF may also be defined as [41],

$$SWF = V_{max} \tag{2.4}$$

where, the SWF is based on the maximum voltage swing. This assumes that dominant oscillations always represent material variations. But smaller oscillations that precede or follow, may be more representative. An appropriate alternative based

on peak voltage might be the measurement of signal rise time or signal decay time (as in acoustic emission practice).

The pulse repetition rate, P, and the reset time, R, and settings mentioned above for ring-down SWF still apply for measuring peak voltage SWF and also for the energy SWF, described next.

2.4.3 Energy SWF

The relative energy of the acousto-ultrasonic signal can be defined in the time domain as [41],

$$SWF = (V_{rms}^2) = (1/T) \int_{t_1}^{t_2} v^2 dt \qquad (2.5)$$

where, SWF is based on root mean square (rms) voltage,

T is a time interval (t_1 to t_2), t is the time, and

v is time-varying voltage

An equivalent frequency domain definition of the SWF in terms of the root mean square of the power spectrum is,

$$SWF = (1/F) \int_{f_1}^{f_2} s^2 df \qquad (2.6)$$

where, F is a frequency interval (f_1 to f_2),

f is frequency and

s is a function of frequency.

Although it is unnecessary to set a threshold voltage, it is still necessary to specify

the size and location of the interval (i.e., T or F) in the time or frequency domain that will most closely associate with material variations. While using the previous definitions of the SWF (see sections 2.4.1-2.4.3), it has been shown that it is useful to normalize the values of the different quantities obtained for comparison with material property variations [41]. Further it may be practical to normalize against the maximum asymptotic value found for these quantities for a given material, structure, and (or) probe configuration. Care must be taken while performing the experiment concerning the interaction of vibration of the test specimen and the imposed frequency of AU transducer. Resonant frequencies due to natural vibration modes of the structure can dominate the spectral content. Further location of the receiver in relation to nodal lines may influence the spectrum of the acousto-ultrasonic waveform [1].

The acousto-ultrasonic approach attempts to ensure that the interrogating waves interact freely with many material parameters [41]. Then, a major signal analysis problem in acousto-ultrasonics is needed for separating interactive waveform components. It becomes necessary to sort out those components that are most relevant to the particular material property or the internal condition that has to be assessed. Alternatively, there may be instances where it is better not to separate waveform components but to deal with the whole signal as a multivariate data set. Several powerful approaches to acousto-ultrasonics signal analysis along both lines have been adopted and are presented in Chapter 3.

2.5 Factors Affecting the Acousto-Ultrasonic Waveform Measurement

Several important parameters relating to the experiment affect the waveform parameters other than the material property variations. These may be grouped as being 'external' to the system (i.e., the pressure applied on the transducers, the type of couplant used and the distance between the transducers) and 'internal' to the system [87] (i.e., frequency of the propagating wave 'gain' used to amplify the signal and the threshold voltage above which the signal is digitized). These parameters are discussed in detail in the following sections.

2.5.1 External parameters affecting acousto-ultrasonic measurements

The pressure applied on the transducer is one of the prime factor affecting the data obtained. It has been reported [42] that a large force must be applied on the transducer to couple it with the test specimen. A special kind of fixture to hold the transducers were used in [26] for obtaining repeatable results for different specimens. In this research, 'constant force clamps' as illustrated in Fig.2.10, were employed to couple the transducers to the specimen. A series of experiments were conducted to verify their effectiveness. The results for eight readings of acousto-ultrasonic parameter were calculated from the resultant AU waveform from the polymeric test specimen used for this purpose. The tests were repeated by removing the transducer after each test, cleaning the surface, applying fresh couplant and finally, clamping the transducer back for the next reading. Table 2.1 illustrates the values of acousto-ultrasonic parameter (AUP) for these tests with their mean and standard deviation. It is seen that while keeping all other parameters constant, the use of constant force

clamps (Fig.2.10) gives sufficiently accurate results.

Trial Number	Value of AUP (volts)
1	.928
2	.864
3	.96
4	.928
5	.896
6	.928
7	.896
8	.96
Mean :	9.2
Standard Deviation:	0.3098

The type of couplant used to create continuity between the transducer and the specimen is also a factor that affects the resultant waveform [26,87]. The experimental results for the comparison of different couplants are given in Fig.2.11. By varying only the type of couplant, the variation in the acousto-ultrasonic parameter (AUP) was studied. This experiment was conducted using acoustic emission gel (SC-2, water and petroleum jelly) for a defect free specimen. It is seen from Fig.2.11, that SC-2 gives high and consistent readings of AUP. Thus, the SC-2 was chosen over water and petroleum jelly so that, the lower values of AUP obtained from defective specimens would fall well within the calibration range of instrumental settings.

The change in distance between the transducers affects the data to a great extent [87], as it changes the total amount of microstructure through which the ultrasonic

waveform travels. The experiment conducted for this purpose involves varying the distance between the sending and the receiving transducers and capturing the resulting acousto-ultrasonic waveforms. The variation of AUP with the distance between the transducers is shown in Fig.2.12. A distance of 25.4 mm between the transducers is chosen to get a high but consistent reading on an undamaged test specimen, so that, the lower value for a damaged material could be obtained using the same distance, but still would fall within the instrument settings.

2.5.2 Internal parameters affecting acousto-ultrasonic measurement

The acousto-ultrasonic parameter (AUP) changes with the change in hardware settings, such as gain and frequency of the injected wave [26]. Following the discussions given in [26 & 87], the optimization of the instrumental settings were carried out to find the best combination of transmitting frequency and amplitude gain. The system gain was selected on the basis of sensitivity of the transmitting and receiving transducers. The set value was chosen, so that the signal to noise ratio was sufficiently high, while the maximum signal amplitude was held below the saturation level of the receiving instruments.

The frequency of the acousto-ultrasonic waveform was set at 750 KHZ to arrive at the optimum condition for acousto-ultrasonic measurements [26,41]. This frequency falls well within the band width of the broad band pulsar and receiving transducers (175 KHZ - 2 MHZ). This enables the sampling rate to be set at a high level of 3.125 MHZ and still capture significant number of waveforms without exceeding the memory space of the digitizer.

2.6. Conclusion

Several non-destructive techniques utilizing ultrasonic wave propagation are illustrated. The advantages of acousto-ultrasonic technique over others for evaluating the overall material property variations has been discussed. The experimental set up and the selection of test parameters are experimentally investigated and selected. On reviewing the available literature on acousto-ultrasonic technique, it has been found that the signal processing and further analysis of the resultant waveform is of great importance for evaluating the variations in material properties. Several signal analysis techniques have been developed by various researchers [1,41]. e.g., homomorphic signal processing, which deconvolutes the overlapping individual wavelets that constitute the resultant waveform by means of special filters [1]. This technique has been successfully applied to the analysis of audio, acoustic, speech and seismic signals [41]. Other techniques include partition-regression method [41], which partitions the resultant signal and its spectra, followed by statistical regression analysis. Pattern recognition method is a whole new approach to signal processing, which is primarily used in this research for signal analysis [46,49]. This technique uses computers to reason and infer decisions from data stored in data bases [46]. All these techniques and their application to acousto-ultrasonic signal processing has been explained in detail with the reviews from available literature in Chapter 3.

Chapter 3

SIGNAL ANALYSIS TECHNIQUES FOR ACOUSTO-ULTRASONICS

3.1 Introduction

The ultimate purpose of the acousto-ultrasonic approach is to rate relative efficiencies of stress-wave propagation in a material [1]. Vary [1,28] also suggests that for many materials (e.g., fiber-reinforced composites), better stress-wave energy transfer means better transmission of dynamic strain and better load distribution in the material. In such situations, it is necessary to quantify the information to obtain meaningful correlations between the variations of the material response characteristics and the variations of the acousto-ultrasonic signal obtained. The techniques widely used, in this context, by different researchers [41,43,77] are reviewed. Further, a much newer technique, namely the statistical pattern recognition methodology, has been presented in detail since it is used in this thesis to discriminate the acousto-ultrasonic wave forms resulting from the change in the material properties of the test materials.

3.2 Homomorphic Processing

One of the most promising means for dealing with the signal deconvolution problem is provided by homomorphic signal processing [43]. This method selects and isolates the important components of a waveform such as a distinct peak or the peak position. This is then compared with the material property variation. Karagülle et.

al., [43] has discussed in detail about the way in which this method isolates the key components in waveforms. It has been successfully applied to the analysis of audio acoustic, speech, and seismic signals [1,41]. Homomorphic processing is necessary for waveforms, whose Fourier transforms overlap. Homomorphic filters provide the means for separating such waveform components. This method leads to the improved evaluation of the stress wave factor (SWF) by isolating key components in waveforms that consist of superimposed multiple echo systems (as in thin composite laminates) [38].

3.3 Partition-Regression Method

This technique is based on partitioning waveforms and their spectra followed by regression analysis [41]. The basic assumption of the partition-regression method is that relevant signal components and their frequency bands can be separated with simple linear filters [1,36]. In this procedure, the time and frequency domain records of the waveform are divided into a large number of equal segments [36]. The SWF for each segment is regressed against a material property of interest to find corresponding time and frequency segments that correlate with that property [41]. The procedure is iterated until the correlation between the material property of interest and the SWF of time domain and frequency domain is optimized to obtain the best fit between the two.

3.4 Pattern Recognition Method for Signal Analysis

3.4.1 Introduction

Statistical pattern recognition method is one of the most powerful Artificial Intelligence techniques in discriminating various pattern classes . This method utilizes statistical tools implemented as computer softwares to reason and infer decisions from data stored in data bases. Pattern matching is the universal generic human problem solving method. It is analogous to humans who look for a pattern when they encounter a new and complex situation. Mathematically, a pattern is defined as an ordered array consisting of elements which may just be numbers (e.g., voltage reading from a piezo-transducer at time t). These patterns are characterised by features which are characteristic of a particular pattern class. A pattern class is a group of patterns with common feature values.

In the pattern recognition methodology, pattern values are classified into their respective classes by plotting their common feature values in the 'feature space'. The feature space is the Euclidean space where the co-ordinate axes are the common feature values of interest to the problem being analyzed. The following sections describe the application of this methodology to ultrasonic signal analysis.

3.4.2 Principle of pattern recognition

The design of an automatic pattern recognition system generally involves several steps. The first step is concerned with the representation of input data which can be measured from the objects to be recognized. Fig.3.1 illustrates the sensed data in the form of an acousto-ultrasonic signal in time domain. This signal represents the raw

data values necessary for pattern classification process. Each point in this signal would be a characteristic feature in time domain. It can be seen from Fig.3.1, that the primitive measurements of this acousto-ultrasonic waveform could become very large. Each of this 'primitive measurements' carry a small portion of 'information' about the microstructure of the material which has been interrogated by the stress wave [1,41]. For the purpose of pattern recognition analysis, it is necessary to form an Euclidean space, where each of the co-ordinate axes are represented by the 'characteristic feature' obtained from the signal illustrated in Fig.3.1. A large number of information obtained from such a signal would constitute a 'multi-dimensional' Euclidean space. Such high dimensionality makes pattern recognition problems very difficult [50]. If the analogy of the way humans recognize a pattern is considered, it is surprisingly based on very small number of patterns (e.g., a base ball is recognized from a foot ball based on its approximate shape and size than on its intricate geometrical measurements and weight). Thus it is necessary to 'extract' important 'features' from the primitive measurements. Each of these measurements carry a small, but significant information for classification purposes and is usually selected according to the physics of the problem.

As the number of inputs become smaller, the design of the classifier becomes simpler. This is achieved through a process known as the 'feature extraction' [50]. This involves in 'mapping' from the primitive 'n-dimensional' space to a lower dimensional space, without loosing any of the information pertaining to the pattern class [50].

For the purpose of mathematical treatment, let the primitive measurement vector be defined as '$\boldsymbol{a}$'. This is a vector comprising of a large number of primitive measurements (see Fig. 3.1). Let '**x**', be defined as the feature vector, which comprises of the 'important features' extracted from the primitive measurement vector. This vector is a subset of the 'primitive measurement vector ' or the 'raw data vector' '$\boldsymbol{a}$'. As a matter of convention, the 'feature' or 'pattern' vectors are usually denoted by lower case bold face letters, such as **x**, **y** and **z** [44].

Fig.3.1 shows an acousto-ultrasonic signal in time domain. In this case, the patterns are continuous functions of the time variable 't'. If these functions are sampled at discrete points $t_1, t_2, \ldots, t_n$, then a pattern vector could be formed by letting

$$x_1 = f(t_1),\ x_2 = f(t_2),\ \ldots,\ x_n = f(t_n).$$

Thus the pattern vector of an acousto-ultrasonic waveform can be denoted by a column vector, such as

$$\boldsymbol{x} = \begin{bmatrix} x_1 \\ x_2 \\ . \\ . \\ x_n \end{bmatrix} \qquad (3.1)$$

When the measurements (i.e., $x_1, x_2, \ldots, x_n$) yield information in the form of real numbers, it is often useful to think of a pattern vector as a point in an Euclidean space. For simplicity, let the pattern be characterized by two common feature values (i.e., peak amplitude of and the inter-peak distance of the acousto-ultrasonic

waveform).

The pattern vectors are, therefore, of the form

$$\boldsymbol{x} = \begin{bmatrix} x_1 \\ x_2 \end{bmatrix} \qquad (3.2)$$

where x_1 represents peak amplitude and x_2 represents the inter-peak distance of the acousto-ultrasonic waveform. Each pattern vector may be viewed as a point in 2-dimensional space. The axes of this two-dimensional space are represented by two common feature values. For comparing different quantities that are used as features in acousto-ultrasonic wave form analysis, they are normalized. In the present work, normalization is carried out as follows [20]

$$\boldsymbol{x}_i(norm) = \frac{\boldsymbol{x}_i - \mu}{S_i}$$

where $\mathbf{x}_i$ is the unnormalized feature value

μ is the mean of feature values of all the feature vectors for the problem

and S_i is the variance of feature values of all the feature vectors for the problem.

The set of patterns belonging to the same class corresponds to a group of points scattered within some region of the measurement space. A simple example of this is shown in Fig.3.2 for two pattern classes denoted by ω_1 and ω_2. Let ω_1 represent a class (e.g., acousto-ultrasonic waveform that had been passed through an undamaged test specimen). Similarly, let ω_2 represent another material class (e.g., acousto-ultrasonic waveform that had been passed through a damaged test

specimen).

Referring to Fig.3.2, it is seen that acousto-ultrasonic measurements for undamaged and damaged test specimens form distinct clusters. In practical situations, however, one is not always able to specify measurements that will result in clearly disjoint sets. For instance, there would be considerable overlap in the classes of damaged and undamaged material states, if the values of the features chosen as criteria for discrimination have changed little or remains unchanged by the damage in the material.

The second step in pattern recognition concerns the extraction of characteristic "features" or attributes from the received input data for the reduction of the dimensionality of pattern vectors. This is often referred to as the 'preprocessing and feature extraction' problem [50]. The commonly used features for acousto-ultrasonics, amongst many other NDT- techniques are the greatest peak amplitude and the greatest peak position, etc.,. A detailed list of the features that are extracted using ICEPAK™* for pattern recognition problems involving acousto-ultrasonics is given in [20]. If a complete set of discriminatory features for each pattern class can be determined from the measured data, then, the recognition and classification of patterns will present little difficulty and automatic recognition may be reduced to a simple matching process [44]. However, in most pattern recognition problems which arise in practise, the determination of a complete set of discriminatory features is extremely difficult [44,50]. To address this problem, well developed algorithms for

---

* ICEPAK™ is the trademark of Tektrend International Inc., Montreal, Canada.

the extraction of features from primitive measurements have been developed and discussed in [47,50].

In the present research work, we adopt the commercial software package, ICEPAK™, for analyzing the received stress waveform. This software extracts a total of 108 standard features normally used for waveform analysis [20]. The software uses an algorithm that works on the concept of 'Fisher distances'. A Fisher distance [46] is a statistical distance that can be computed between two sets of scalar numbers. Essentially, the definition of the Fisher distance is based on the difference between the two set averages [46]. Following [46], mathematical formulation of the Fisher distance or Fisher discriminatory ratio [F_{xy}] can be expressed as

$$F_{xy} = \frac{[MEAN(\boldsymbol{x}) - MEAN(\boldsymbol{y})]^2}{\sigma(\boldsymbol{x})^2 - \sigma(\boldsymbol{y})^2} \qquad (3.3)$$

where $\mathbf{x} = [x_1, x_2, \ldots, x_m]$ and $\mathbf{y} = [y_1, y_2, \ldots y_n]$ are the two sets of feature vectors and σ_x and σ_y are the standard deviations of sets **x** and **y**. Each set represents a class and the vectors represent one individual feature value in the n-dimensional feature space.

As the two classes become better separated, their Fisher distance will increase [20]. In the case where there are more than two classes say **x**, **y** and **z**, then for one particular feature, a summation of Fisher distances is carried out [20,47]. i.e.,

$$F_{\Sigma} = F_{xy} + F_{xz} + F_{yz} .$$

The ranking done in this manner enables the software to select the features automatically, e.g., in a descending order of greater separability to lower separability [20,46].

The third step in pattern recognition system design involves an optimum decision procedure that is needed in the classification process. After the observed data from the patterns to be recognized have been expressed in the form of pattern points or measurement vectors in pattern space, the next step is to decide as to which pattern class these data belong. On assuming that a machine is to be designed to recognize 'M' different pattern classes denoted by $\omega_1, \omega_2, \ldots, \omega_M$, then, the pattern space can be considered as consisting of M regions, each of which encloses the pattern point of a class.

The recognition problem can now be viewed as that of generating the decision boundaries which separate the 'M' pattern classes on the basis of the observed measurement vectors. This is explained in the following sections.

3.4.3 Decision functions

The principal function of a pattern recognition system is to yield decisions concerning the class membership of the patterns with which it is confronted. In order to accomplish this task, it is necessary to establish some rules upon which to base these decisions [50]. One important approach to this problem is the use of decision functions. Fig.3.3 illustrates two pattern classes, separated by a line in the feature space.

Let $d(\mathbf{x}) = w_1x_1 + w_2x_2 + w_3 = 0$ be the equation of the separating line, where x_1, x_2 are the general co-ordinate variables and w_1, w_2, and w_3 are the unknown parameters to be identified. It is clear from the figure that any pattern **x** belonging to class ω_1 will yield a positive quantity when substituted into $d(\mathbf{x})$. Thus, $d(\mathbf{x})$ can be

used as a discriminant function, since, given a pattern **x** of unknown classification, it can be said that **x** belongs to ω_1 if $d(\mathbf{x})>0$, or ω_2 if $d(\mathbf{x})<0$. If the pattern lies on the separating boundary, an intermediate condition of **x** is obtained. Thus the success of foregoing pattern classification scheme depends both on the form of $d(\mathbf{x})$ and the determination of coefficients (w_1, w_2, w_3, etc.) [44].

The simple 2-dimensional decision function introduced in the foregoing can be extended to a generalized n-dimensional case. Thus, a general linear decision function may be expressed in the form

$$d(\boldsymbol{x}) = w_1x_1 + w_2x_2 + \ldots + w_nx_n + w_{n+1} \qquad (3.4)$$

which can be rewritten as

$$d(\boldsymbol{x}) = \mathbf{W}_0'\boldsymbol{x} + w_{n+1} \qquad (3.5)$$

where $\mathbf{W}_0 = (w_1, w_2, \ldots, w_n)'$. This vector is the transposed 'weight' or 'parameter' vector' [44]. The weight vector $\mathbf{W}_0$ is transposed in Eqn.3.5, so that the rules of matrix multiplication could be effected (i.e., the number of rows in the second matrix must be equal to the number of columns in the first matrix). This operation of transposition is indicated by (') for a particular column vector. Also, to write the column vector in text, it is transposed and written as a row vector. The transposition operation and the writing of column vector as a transposed row vector are used after following the conventions in statistical pattern recognition texts [44-49]. It is also a widely accepted convention to add the numeral '1' after the last component of all pattern vectors [44] and express Eqn.3.4 in the form

$$d(\boldsymbol{x}) = \boldsymbol{W}' \boldsymbol{x} \qquad (3.6)$$

where $\mathbf{x} = (x_1, x_2, \ldots, x_n, 1)'$ is the transposed pattern vector and $\mathbf{W} = (w_1, w_2, \ldots, w_n, w_{n+1})'$ is the weight vector [44].

In the two-class case, a decision function d(**x**) is assumed to have the property

$$d(\boldsymbol{x}) = \boldsymbol{W}' \boldsymbol{x} = \begin{cases} >0 \ if \ \boldsymbol{x} \in \omega_1 \\ <0 \ if \ \boldsymbol{x} \in \omega_2 \end{cases} \qquad (3.7)$$

When there are more than two classes, denoted by $\omega_1, \omega_2, \ldots, \omega_M$, a multi-class pattern recognition case arises. In this case, each pattern class is separable from the other classes by more than one decision function [44]. For instance, in the two dimensional space, separation between three pattern classes would involve at least two decision functions in the form of lines. Utilizing M decision functions with the property,

$$d_i(\boldsymbol{x}) = \boldsymbol{W}_i / \boldsymbol{x} = \begin{cases} >0 \ if \ \boldsymbol{x} \in \omega_i \\ <0 \ otherwise \end{cases}, i=1,2,\ldots,M \qquad (3.8)$$

where $\mathbf{W}_i = (w_{i1}, w_{i2}, \ldots, w_{in}, w_{i,n+1})'$ is the weight vector associated with the ith decision function.

The classifier using such a linear function is called Linear discriminant classifier [44]. It defines lines in two-dimensional feature space and planes in three-dimensional feature space [50]. Since it involves linear operations of matrices, it is very simple to design. It is also very efficient in computer memory space since matrices could be easily treated as two dimensional arrays in the computer memory. It is also quick with respect to the computing time since it involves standard matrix operations

normally performed by computer programs [20,46]. But this type of classification has some limitations. This uses lines and planes to discriminate between the classes. So if some class samples are distributed in a strange shape that cannot be separated by lines or planes, then this type of classification cannot be applied. For such situations, pattern classification using 'distance functions' may be used [44].

3.4.4 Pattern classification by distance functions

The most obvious way of establishing a measure of similarity between pattern vectors is by determining their proximity to their respective class. This is illustrated in Fig.3.4a which shows that **x** belongs to class ω_i on the basis that it is closer to the pattern of this class. This method of pattern classification by 'proximity' concept or 'distance functions' can be expected to yield practical and satisfactory results only when the pattern classes tend to have 'clustering' properties [44, 50-51]. i.e., the intra-class pattern vectors group together and are well separated from other classes. This can be seen by comparing Figs.3.4a & 3.5. In the first figure, it is seen that there would be little difficulty in classifying **x** into ω_i because of its proximity to this class. In the second figure, although the two pattern populations are perfectly disjoint, **x** could be easily classified into either class based on a measure of the proximity of its pattern to both the classes.

The above concepts are generalized and developed in a mathematical framework in the following sections. Since the proximity of an unknown pattern to the patterns of a class will serve as a measure for its classification, the term 'minimum-distance pattern classification' is commonly used to characterize this particular approach [44].

Pattern classification by distance functions is one of the earliest concepts in automatic pattern recognition [44]. This simple classification technique is considered to be an effective tool for the solution of problems in which the pattern classes exhibit a reasonably limited degree of variability [44,48].

3.4.5 Minimum-distance pattern classification

An important classification relation is that of the distance between the input pattern and a set of pattern vectors which act as reference vectors in the feature space [46-47]. This classification criterion for each class can be represented by the arithmetic mean of all patterns in the class [44]. Since it is a rather simple representation of the class, this type of linear classifier is fast but not robust while the classification is performed by computers. This is represented in Fig. 3.4b. For instance, a two-class classification problem might arise, in which the size of one class is considerably larger than the other. In such a situation, an unknown pattern vector could be falsely identified as belonging to the opposite class based on the distance measured from the arithmetic mean (representing the centroid of the group of patterns) of the classes. Thus, this classifier assigns the same importance to each class, regardless of its size or spread [20,46].

In some situations, patterns of a class tend to 'cluster' tightly about a typical or representative pattern for that class. Such a pattern vector is the 'prototype' or the 'mean' vector of that particular pattern class. Considering M pattern classes and assuming that these classes are representable by prototype patterns $\mathbf{z}_1, \mathbf{z}_2, \ldots, \mathbf{z}_M$, the Euclidean distance between an arbitrary pattern vector $\mathbf{x}$ and the ith prototype is given

by [44]

$$D_i = \|\boldsymbol{x}-\boldsymbol{z}_i\| = \sqrt{(\boldsymbol{x}-\boldsymbol{z}_i)'(\boldsymbol{x}-\boldsymbol{z}_i)} \qquad (3.9)$$

A minimum-distance classifier computes the distance from a pattern **x** of unknown classification to the prototype of each class, and assigns the pattern to the class to which it is closest [52]. In other words, first, the Euclidean distance between '**x**' and the prototype of each class (i.e., ω_i and ω_j) is computed. For a two-class problem this would be two distance measures (D_i and D_j). **x** is assigned to class ω_i if D_i is less than D_j, for all $j \neq i$.

All terms of Eqn.3.9 can be squared and expressed as

$$D_i^2 = \|\boldsymbol{x}-\boldsymbol{z}_i\|^2 = (\boldsymbol{x}-\boldsymbol{z}_i)'(\boldsymbol{x}-\boldsymbol{z}_i) \qquad (3.10a)$$

On simplifying this further

$$D_i^2 = \boldsymbol{x}'\boldsymbol{x} - 2\boldsymbol{x}'\boldsymbol{z}_i + \boldsymbol{z}_i'\boldsymbol{z}_i \qquad (3.10b)$$

which can also be written as

$$D_i^2 = \boldsymbol{x}'\boldsymbol{x} - 2\left(\boldsymbol{x}'\boldsymbol{z}_i - \frac{1}{2}\boldsymbol{z}_i'\boldsymbol{z}_i\right) \qquad (3.10c)$$

Choosing the minimum value of D_i^2 is equivalent to choosing the corresponding minimum value D_i, since only the absolute values of the distances are taken into account (i.e., all the numerical values of the Euclidean distances are positive). From Eqn.3.10c, it is seen that the term **x'x** is independent of 'i' in all D_i^2, $i = 1,2,..,M,$. Thus, choosing the minimum D_i^2 would be equivalent to choosing the maximum of the expression in parentheses ($\mathbf{x}'\mathbf{z}_i - 1/2\mathbf{z}_i'\mathbf{z}_i$). Consequently, decision functions can be

defined as [44]

$$d_i(\boldsymbol{x}) = \boldsymbol{x}'\boldsymbol{z}_i - \frac{1}{2}\boldsymbol{z}_i'\boldsymbol{z}_i, \quad i=1,2,\ldots,M \tag{3.11}$$

Eqn. (3.11) represents a linear decision function which is represented by a line in a two-dimensional feature space (See, e.g., references [44,47]). The decision boundary of a two-class example is shown in Fig.3.6. The class prototype for each of the classes ω_i and ω_j is chosen as the arithmetic mean of all the pattern vectors in the respective classes. For the two class problem illustrated in a two-dimensional feature space, the decision boundary is represented by a line whose generalized equation is given in Eqn. (3.11).

3.4.6 Extension of minimum-distance classification concepts

Although the ideas of small number of prototypes and familiar Euclidean distances are geometrically attractive, they are not limiting factors in the definition of the minimum-distance classification concept [44]. To explore the general properties of this scheme, following the arguments in [44,50], a set of 'sample patterns of known classification', $\{s_1, s_2,\ldots,s_n\}$ is considered. Here, it is assumed that each pattern belongs to one of the classes $\omega_1, \omega_2, \ldots, \omega_M$. In the nearest neighbour (NN) classification rule, the distance between an unknown pattern class **x** and that of the known pattern vector from the sample s_k belonging to the sample set $s_i \in \{s_1, s_2, .., s_k, s_N\}$ is measured. If this distance is the least amongst the set $s_i \in \{s_1, s_2, .., s_k, s_N\}$, then s_k may be termed as the nearest neighbour to **x**. This is illustrated in Fig 3.7. The analogy of the minimum distance classifier concept could

be seen from Fig. 3.7. For example, in the minimum distance classifier, distances are measured always between **x** and the prototype of a particular class (represented by the arithmetic mean of all the pattern vectors belonging to that class). It is further extended to obtain the distance measure between **x** and s_k, where this distance is the least amongst the sample set s_i. Mathematically, it can be represented as,

$$d(\boldsymbol{x}, s_i) = Min\|\boldsymbol{x} - s_i\| \qquad (3.12)$$

where d is any distance measure definable over the feature space.

This scheme is known as the 1-NN rule since it employs only the classification of 'one' of the nearest neighbour to **x**. Similarly extending this concept to 'K-nearest neighbours' to **x**, the decision function for this type of classifier could be formulated as follows [44,48].

$$d(\boldsymbol{x}, s_i) = Min\|\boldsymbol{x} - s_i^K\|, \qquad K=1,2,\ldots,u_{jK} \qquad (3.13)$$

where $d(\mathbf{x},s_i)$ is essentially the decision function adopted for K-nearest neighbour classifier.

3.4.7 Empirical Bayesian classifier

This classifier is based on parametric classification theories (See, e.g., [48, 51-52]). For designing with this classifier, prior knowledge of the probability density distributions of the classes should be known before hand [48]. They can also be assumed to follow a certain distribution relationship [48]. To illustrate this, a set of pattern vectors $x_1, x_2, x_3, \ldots, x_n$ is considered where x_i is the measurement of the ith feature. For each pattern class ω_j, j = 1,...,M, the 'probability density function' of

the feature vector **x** can be then expressed as $p(\mathbf{x}/\omega_j)$, provided that the probability of occurrences of ω_j and $p(\omega_j)$ are known. On the basis of this prior information pertaining to the probability of occurrence of the feature and the nature of its distribution, the function of a classifier would be to minimise the probability of misrecognition between the classes [51,52]. Accordingly, a statistical hypothesis testing problem is formulated by defining a decision function $d(\mathbf{x})$, where $d(\mathbf{x}) = d_i$ means that the hypothesis $\mathbf{X} \sim \omega_i$ is accepted [52]. Assuming, for instance (See [48]), that the conditional loss or conditional risk of misclassifying a class ω_j belonging to ω_i is given by the following integral

$$r(\omega_i, d) = \int_{\Omega_x} L(\omega_i, d)\, p(\boldsymbol{x}/\omega_i)\, d\boldsymbol{x} \qquad (3.14)$$

then it can be shown that the average loss of the decision d for the given feature measurements **x** can be expressed as

$$R(P, d) = \int_{\Omega_x} p(\boldsymbol{x})\, r_X(P, d)\, d\boldsymbol{x} \qquad (3.15)$$

where $r_X(P,d)$ is defined as the 'posteriori conditional average loss of the decision-d' for the given feature vector **x**. The next step is thus to choose a proper decision d_j, $j = 1,2,\ldots,M$ to minimise the average loss R(P,d). The optimal decision rule which minimizes the average loss is the Bayes' rule [48]. The latter is briefly interpreted as follows:

If d^* is an optimal decision in the sense of minimizing the average loss, then the Bayesian classifier becomes $d^* = d_i$, $\mathbf{x} \sim \omega_i$ and the classification function becomes

$$P(\omega_i)p(\boldsymbol{x}/\omega_i) \geq P(\omega_j)p(\boldsymbol{x}/\omega_j) \quad for\ all\ j=1,\ldots,m \qquad (3.16)$$

The above classification rule determines the decision surface for the Bayesian classifier which takes the form of a hyper plane in the feature space [48,50]. The concept of Empirical Bayesian classifier is illustrated in Fig.3.8. From Fig. 3.8, it could be seen that for a two-class problem, the classification is done by minimizing the overlap between the probability density distributions pertaining to the two classes. The minimization of this overlap corresponds to the integral given in Eqn. 3.15 representing the 'posteriori conditional average loss of the decision-d' for the given feature vector **x**.

3.4.8 Training and evaluation of the classifier

If the patterns from different classes are linearly separable (i.e., by a plane in the feature space), then with the correct values of the coefficients in Eqn.3.4, a perfectly correct recognition is possible to be achieved [46]. However, in practice, the proper values of these coefficients are usually not available. Under such circumstance, it is proposed that the classifier be designed to have the capability of estimating the 'optimum values' of these coefficients from a set of input patterns [46,50]. The basic idea is that, by observing patterns with known classifications, the classifier can automatically adjust the parameter or weight vector **Wi** (see Eqn.3.8 in section 3.4), in order to achieve correct recognitions. The performance of the classifier is supposed to improve as more and more patterns are used as input or 'training' patterns [46]. This process, termed as training or learning, uses pattern classes that have known decision boundaries (e.g., by supplying the raw data vector from a known material

state such as damaged or undamaged, as shown in Fig.3.2).

ICEPAK™ uses one of the simplest training rules [20], i.e., the software splits the input data values into two separate files after normalizing it with respect to its variance (see section 3.2). The first file that contains the values of the normalized feature vectors is used to create the boundary between the pattern classes. Once the boundary is established, the classifier is evaluated using the second set. These processes of training and evaluation are schematically illustrated in Figs. 3.9 & 3.10. The results of the training and evaluation processes are expressed as percentage of success in forming distinct clusters in the feature space from the known pattern vectors. The power of such a classifier is tested using a raw data set taken from an unknown sample creating a pattern vector in the feature space that need to be classified to its respective class [20,46].

3.5 CONCLUSION

Statistical pattern recognition technique is a process of forming the raw data vector, extracting features and building of various discriminant functions by which the different pattern classes could be classified. This takes into account many mathematical models that are based on the concepts of the theories of probability and statistics [44-52]. The basic formulations of decision functions, such as, Linear Discriminant Classifier, Minimum Distance Classifier, K-Nearest Neighbour Classifier, and Empirical Bayesian Classifier were discussed. The linear discriminant classifier, is simple to design because of the nature of matrix operations involved. It is very

economical in terms of computer memory space and speed of operation. If the pattern classes are distributed in a strange shape that cannot be discriminated using a simple linear decision function, then classification using distance concepts such as the minimum distance and K-nearest neighbours could be applied. The latter consumes more memory space and is very slow in execution. This is due to the fact that, it has to estimate the distance between the unknown feature vector **x** and at least more than one reference vectors for each of the pattern classes. But this type of classification offers considerable accuracy over the linear decision function and the minimum distance classification function. The Empirical Bayesian type of classifier is useful if the nature of distribution of the feature values are known or at least can be assumed. In this thesis, all of the above mentioned classifiers were tried for classification. The one that gave the highest classification rate was then chosen.

Chapter 4

ON THE VISCOELASTIC RESPONSE BEHAVIOUR OF MATERIALS

4.1 Introduction

The response characteristics of viscoelastic materials are different from that of Hookean solids and Newtonian liquids. These materials maintain a constant deformation under constant stress, but go on deforming with time or 'creep'. When such a body is constrained at constant deformation, the stress required to hold it diminishes gradually or 'relaxes'. If both strain and rate of strain are infinitesimal, one likely encounters linear viscoelastic behaviour of the test material. Then, in a given experiment, the ratio of stress to strain is a function of time alone and not of the magnitude of input loading.

4.1.1 Assumptions of linear viscoelastic materials

The following assumptions are used in deriving the relations for the theory of linear viscoelasticity [53,56].

1. Material is homogeneous, i.e., same constitutive relations apply to all positions.
2. Material is isotopic, i.e., same constitutive relation applies to all directions.
3. Isothermal condition is maintained during the entire loading of the material.
4. The criteria of superposition of input histories is applied to the linear viscoelastic material, i.e.,

$$f(\sigma(t_1),\sigma(t_2),\ldots,\sigma(t_n)) = f(\sigma(t_1)) + f(\sigma(t_2)) + \ldots + f(\sigma(t_n)) \quad (4.1)$$

4.2 Linear Viscoelastic Behaviour

4.2.1 Creep function

In uniaxial tension, the extensional behaviour of materials such as metals, may be characterized in the region of small strains by its elastic modulus. This type of characterization alone cannot represent the response characteristics of polymers. The essential difference between the behaviour of polymers and metals is shown by the fact that when a polymeric specimen is loaded, the resulting strain depends not only on the magnitude of the imposed stress, but also on the length of time during which the load is applied [53-57].

The dependence of strain on time, as well as on stress, is conveniently established in tensile creep experiments, where the increase in strain with time is observed at constant values of the imposed uniaxial stress, or, usually, at constant load. The results of such an experiment is schematically illustrated in Fig.4.1, which shows three different creep curves, i.e., curves of strain versus the logarithm of the time for different values of the constant imposed stress.

The results obtained in creep tests with solid polymers may be expressed, within certain limits of strain and time, by the equation [56-57]

$$e = \sigma_n f(t) \qquad (4.2)$$

This particular relationship between strain, stress and time implies linear viscoelasticity and the polymers to which it applies are, therefore, classified as linear viscoelastic materials.

Fig.4.2 illustrates the fundamental difference between a linearly elastic material

response and a linearly viscoelastic material response to step loading. For an elastic solid, the following is observed at the two levels of stress, σ_0 and $2\sigma_0$. The strain follows the pattern of the loading program exactly and in exact proportionality to the magnitude of the loads applied. The effect of applying similar loading program to a linear viscoelastic solid has several similarities. In the most general case, the total strain 'e' is the sum of three separate parts e_1, e_2 and e_3. e_1 and e_2 are often termed the immediate elastic deformation and the delayed elastic deformation respectively [56]. e_3 is the Newtonian flow, i.e., that part of the deformation which is identical with the deformation of a viscous liquid obeying Newton's law of viscosity [56].

Because the material shows linear behaviour, the magnitude of the strains e_1, e_2 and e_3 are exactly proportional to the magnitude of the applied stress. Thus the simple loading experiment defines a creep compliance F(t) which is only a function of time [57].

$$\frac{e(t)}{\sigma} = F(t) = F_1 + F_2 + F_3 \qquad (4.3)$$

where F_1, F_2 and F_3 correspond to e_1, e_2 and e_3 respectively.

The term F_3 which defines the Newtonian flow, can be neglected for solid polymers at ordinary temperatures, because their flow viscosities are very large. At any given temperature, the separation of compliance into terms F_1 and F_2 are the compliances corresponding to immediate and relaxed responses of the linearly viscoelastic material [57].

4.2.2 Stress-relaxation

The relaxation response of a viscoelastic material is the converse of creep response. i.e., the input is strain instead of stress. The decay of stress (σ_t) with time is observed for a constant strain e. Through the assumption of linear viscoelastic behaviour, the stress relaxation modulus R(t) is defined as [57]

$$R(t) = \frac{\sigma(t)}{e} \qquad (4.4)$$

4.2.3 Mathematical treatment of linear viscoelastic behaviour

Creep compliance

The Boltzmann superposition principle is the first mathematical statement of linear viscoelastic behaviour [53-57]. This principle proposes that the creep in a specimen is a function of the entire loading history and that each loading step makes an independent contribution to the final deformation and that the final deformation can be obtained by the simple addition of each contribution [57].

Consider a several-stage loading program (Fig.4.3) in which incremental stresses $\Delta\sigma_1$, $\Delta\sigma_2$, $\Delta\sigma_3$, etc., are added at times τ_1, τ_2, τ_3, etc., respectively. The total creep at time t is then given by [53-57]

$$e(t) = \Delta\sigma_1 F(t-\tau_1) + \Delta\sigma_2 F(t-\tau_2) + \Delta\sigma_3 F(t-\tau_3) + \ldots, \qquad (4.5)$$

where F(t-τ) is the creep compliance function. The contribution of each loading step is the product of the incremental stress and a general function of time, the creep compliance, which depends only on the interval in time between the instant at which

the incremental stress is applied and the instant at which the creep is measured. Eqn.4.5 can be generalized to give the integral [54,55]

$$e(t) = \int_{-\infty}^{t} F(t-\tau)\, d\sigma(t) \qquad (4.6)$$

This integral given in Eqn.4.6 is known as Duhamel integral, and it is a useful illustration of the consequences of the Boltzmann superposition principle to evaluate the response for a number of simple loading programmes [57]. Recalling Eqn.4.6, it can be seen that the Duhamel integral is most simply evaluated by treating it as the summation of a number of response terms. To illustrate this, three specific loading programs are considered (see for example, Fig.4.2)

1. Single-step loading of a stress σ_0 at time $\tau=0$. For this case

$$F(t-\tau)=F(t) \quad and \quad e(t)=\sigma_0 F(t)$$

2. Two-step loading, a stress σ_0 at time $\tau=0$, followed by an additional stress σ_0 at time $\tau=t_1$. For this case

$$e_1=\sigma_0 F(t), \quad e_2=\sigma_0 F(t-\tau_1)$$

give the creep deformations produced by the two-loading steps, and

$$e(t)=e_1+e_2=\sigma_0 F(t)+\sigma_0 F(t-t_1) .$$

This shows that the additional creep $e'_{creep}(t-t_1)$ produced by the second loading step is given by

$$e_{creep}(t-t_1) = \sigma_0 F(t) + \sigma_0 F(t-t_1) - \sigma_0 F(t) = \sigma_0 F(t-t_1) \qquad (4.7)$$

Further Eqn.4.6 can be generalized and written as [54,57]

$$e(t) = \left[\frac{\sigma}{R_u}\right] + \int_{-\infty}^{t} F(t-\tau)\,\frac{d\sigma(\tau)}{d\tau}\,d\tau \qquad (4.8)$$

where the 'immediate elastic' contribution to the compliance is included in terms of an elastic modulus R_u (R_u is the unrelaxed modulus) and the integral term is written in its more correct mathematical form. It is to be noted that the integral is taken from $-\infty$ to t. This follows from the hypothesis of Boltzmann principle, that all previous elements of loading history were to be taken into account. In all actual experiments, a conditioning procedure may be required to destroy the long term memory of the specimen [56]. This illustrates one consequence of Boltzmann principle, which is, that the additional creep, $e'_{creep}(t-t_1)$, produced by adding the stress σ_0 is identical with the creep which would have occurred had this stress σ_0 been applied without any previous loading at the same instant in time t_1.

3. In the case of creep and recovery, the stress σ_0 is applied at time $\tau=0$ and removed at time $\tau=t_1$. The deformation e(t) at time $t>t_1$ is given by the addition of two terms $e_1=\sigma_0 F(t)$ and $e_2=-\sigma_0 F(t-t_1)$, which express the application and removal of the stress σ_0 respectively. Thus,

$$e_{recovery}(t) = \sigma_0 F(t) - \sigma_0 F(t-t_1)\,.$$

The recovery $e_{recovery}(t-t_1)$ will be defined as the difference between the

anticipated creep under the initial stress and the actual measured response [57].

$$e_{recovery}(t-t_1) = \sigma_0 F(t) - [\sigma_0 F(t) - \sigma_0 F(t-t_1)] = \sigma_0 F(t-t_1)$$

It can be seen that this is identical with the creep response to a stress σ_0 applied at time t_1. This demonstrates a second consequence of the Boltzmann superposition principle, that the creep and recovery responses are identical in magnitude [56].

4.2.4 The stress-relaxation modulus

Stress-relaxation behaviour can be represented in an exactly complementary fashion using the Boltzmann superposition principle [53-55]. Consider a stress-relaxation programme in which incremental strains Δe_1, Δe_2, Δe_3,k etc., are added at times τ_1, τ_2, τ_3, etc., respectively. The total stress at time t is then given by [57]

$$\sigma(t) = \Delta e_1 R(t-\tau_1) + \Delta e_2 R(t-\tau_2) = \Delta e_3 R(t-\tau_3) + \ldots, \qquad (4.9)$$

where $R(t-\tau)$ is the stress relaxation modulus. The above equation may be generalized similar to Eqn.4.6-4.8 and following the discussions in section 4.2.3, Eqn.4.9 can be written as [57]

$$\sigma(t) = [G_{relaxed} e] + \int_{-\infty}^{t} R(t-\tau) \frac{de(\tau)}{d\tau} dt \qquad (4.10)$$

where $G_{relaxed}$ is the equilibrium or relaxed modulus.

4.2.5 Relationship between creep and stress-relaxation

The following set of equations illustrate the principle that creep is the converse of stress-relaxation in a general case [54,57]. Rewriting Eqn.(4.6) gives,

$$e(t) = \int_{-\infty}^{t} F(t-\tau)\, d\sigma(t) \qquad (4.11)$$

$$e(t) = \int_{-\infty}^{t} F(t-\tau)\, \frac{d\sigma(t)}{d\tau}\, d\tau \qquad (4.12)$$

Usually a conditioning procedure is effected to destroy the long term memory of the specimen before conducting the experiment [57]. This enables the limits of integration to be set from 0 to t instead from $-\infty$ to t [56,57]. Let the stress program start at time $\tau=0$. The stress decreases exactly as the relaxation function R(*r*) [54]. In this case the corresponding strain must remain constant as in a typical stress relaxation experiment. Thus, if

$$\frac{d\sigma(\tau)}{d\tau} = \frac{dR(\tau)}{d\tau} \qquad (4.13)$$

then,

$$\int_{0}^{t} \frac{dr(t)}{d\tau} F(t-\tau)\, d\tau = k' \qquad (4.14)$$

where K′ is a constant.

For simplicity the definitions of R(t) and F(t) are normalised so that the constant is unity, which can then be written as follows [57]

$$\int_{0}^{t} \frac{dR(t)}{d\tau} F(t-\tau)\, d\tau = 1 \qquad (4.15)$$

and it may be written in any one of the following forms [57].

$$\int_0^t R(t)\,F(t-\tau)\,d\tau = t \qquad (4.16)$$

$$F(t) \approx [R(t)]^{-1} \qquad (4.17)$$

$$\frac{dl_n(F(t))}{dl_n t} = -\frac{dl_n(R(t))}{dl_n(t)} \qquad (4.18)$$

4.3 The Formal Structure of Linear Viscoelasticity

Gross [66] has discussed the formal structure of the theory of linear viscoelasticity. A summary of his treatment is presented here as a suitable conclusion to the theoretical treatment. Following closely the arguments given in [66], two groups of experiments could be defined:

Group 1: Experiments which take place under a given stress, either fixed or alternating. These define the stress relaxation modulus or the complex compliance.

Group 2: Experiments which take place under a given strain, either fixed or alternating. These define the stress relaxation modulus or the complex modulus.

Within each group the viscoelastic functions exist in three levels:

(a)	Top level	Complex compliance	Group 1
		Complex Modulus	Group 2
(b)	Medium level	Creep function	Group 1

		Relaxation function	Group 2
(c)	Bottom level	Retardation spectrum	Group 1
		Relaxation spectrum	Group 2

To go up a level, one applies either a Laplace transform or a one-sided complex Fourier transform. To go down a level, one applies either an inverse Laplace transform or an inverse Fourier transform.

The relationships between the groups vary in complexity. At the top level, the complex compliance is merely the inverse of the complex modulus. The relationships between the creep function and the relaxation function and between the retardation spectrum and the relaxation spectrum involve integral equations and integral transforms respectively.

In this thesis, stress-relaxation testing was carried out on two linearly viscoelastic materials, i.e., Polycarbonate (PC) and Polyvinylchloride (PVC). Test specimens made from these polymeric materials were subjected to constant input strain and the stress in the material was allowed to decay. Acousto-Ultrasonic measurements were taken by injecting an ultrasonic pulse into the test material, and capturing the resultant acousto-ultrasonic waveform. These waveforms that had passed through the microstructure of the polymeric specimens, would contain information pertaining to the changes effected on the specimen [1,41]. Thus the changes effected by the stress-relaxation phenomenon, would reflect the changes effected on the acousto-ultrasonic waveform. By designing a pattern classifier, distinct relaxed stress states could be discriminated in the feature space based on the features extracted from the

resultant acousto-ultrasonic waveforms.

4.4 Yield Behaviour in Polymers

Until recently, the yield behaviour of polymers has not been treated as a distinct mode of mechanical behaviour, i.e., different in kind from either the viscous flow process which occur at high temperatures or the large extensions observed in the temperature range above the glass transition. The yield process in a polymer was often considered to be softening due to a local rise in temperature and was referred to as a localized melting [57].

Some polymers show 'necking' and 'cold-drawing' while others are brittle and fail catastrophically [67]. A salient point to recognize is that polymers in general show all these types of behaviour depending on the exact conditions of test.

The most dramatic manifestation of yield is seen in tensile test (ASTM D-638M-91a) when a neck or deformation band occurs. In these cases, the plastic deformation is concentrated either entirely or primarily in small region of the specimen. The precise nature of the plastic deformation depends both on the geometry of the specimen and on the nature of the applied stresses [57,67].

Fig.4.4 illustrates the phenomenon of elastic-plastic failure in polymers. Referring to Fig.4.4, it is seen that during the initial elongation of the specimen, homogeneous deformation occurs and the conventional load-extension curve shows a steady increase in load with increasing elongation. After this initial elongation, the specimen thins to a smaller cross section at some point, i.e. a neck is formed. Further

elongation brings a fall in load. Continuing extension is achieved by causing the shoulders of the neck to travel along the specimen as it thins from the initial cross-section to the drawn cross-section [57]. The existence of a finite or natural draw ratio is an important aspect of polymer deformation [67-68] and is discussed below.

4.4.1 Necking and the ultimate stress

Necking and cold drawing are accompanied by a non-uniform distribution of stress and strain along the length of the test specimen by considering the true stress-strain curve of the specimen rather than the conventional applied tension to overall elongation. The cross section of the sample is decreasing with increasing extension. But the true stress may be increasing when the apparent or conventional stress or load may be remaining constant or even decreasing. This has been well discussed by Nadai [67] and his argument will be followed here.

Fig.4.5 illustrates the conventional and true stress-strain curves for a polymer. The ordinate is equal to the stress σ_a obtained by dividing the load P by the original cross sectional area A_0. i.e.,

$$\sigma_a = \frac{P}{A_0} \qquad (4.19)$$

The load reaches its maximum value at the instant the uniform extension of the sample stops. At this elongation, necking begins and consequently the load falls as shown by the last part of the stress strain curve. Finally, the sample fractures at the narrowest point of the neck.

By plotting the true tensile stress σ = P/A rather than the apparent stress σ_{ao}. The

true stress is σ = P/A (where A is the cross section at any time) and assuming that the deformation takes place at constant volume as in plastic deformation, then Al = $A_0 l_0$, and if l/l_0 is expressed as 1 + e where e is the elongation per unit length,

$$A = \frac{A_0 l_0}{l} = \frac{A_0}{1+e} \qquad (4.20)$$

The true stress is given by

$$\sigma = \frac{P}{A} = \frac{(1+e)\ P}{A_0} = (1+e)\,\sigma_a \qquad (4.21)$$

This gives the load

$$P = \frac{A_0 \sigma}{1+e} \qquad (4.22)$$

By knowing the true stress, σ,as a function of ε from the true stress-strain curve, load 'P' can be computed for any elongation and P_{max}, the maximum load is defined by the condition $dP/d\varepsilon = 0$, i.e.,

$$\frac{dP}{de} = \frac{A_0}{(1+e)^2}\left[(1+e)\,\frac{d\sigma}{de} - \sigma\right] = 0 \qquad (4.23)$$

or

$$\frac{d\sigma}{de} = \frac{\sigma}{1+e} \qquad (4.24)$$

The measured ultimate stress can be obtained from the true stress-strain curve by the simple construction shown in Fig.4.6 [57]. The ultimate stress is obtained by drawing a tangent line to the true stress-strain curve from point -1 on the elongation axis. The

slope ($d\sigma/d\varepsilon$) is given by the liner portion of the curve. The angle α in Fig.4.6 is defined by [57]

$$\tan\alpha = \frac{d\sigma}{de} = \frac{\sigma}{1+e} = \frac{\sigma}{\lambda'} \qquad (4.25)$$

where λ is the draw ratio. This construction is called the 'Conside're construction' and is used in analyzing the necking and cold-drawing of polymers [57]. The detailed construction of this is given in Chapter 6 for the yielding of the test specimen. This explains the importance of yield stress in many plastics, defining the practical limit of behaviour much more than the ultimate strength, unless the plastic fails by brittle fracture [57,67] (see also [68,69]).

4.5 Fatigue in Polymers

Fatigue occurs due to the cyclic application of stresses, the stress levels being much below the yield stress. The effect of such cyclic stresses is to initiate microscopic cracks at the centres of stress concentration within the material or on the surface, and subsequently enable these cracks to propagate, leading to eventual failure [70-79].

Early studies of fatigue in polymers concentrated on stress cycling of un-notched specimens [74,77] to produce S versus N plots, similar to those which have proved so useful for characterizing fatigue in metals (S being the maximum loading stress, N the number of cycles to failure). Later studies [70-72] used specimens with known cracks and applying conventional fracture mechanics concepts, the nature of crack

propagation was examined (Fig.4.7). The first studies of fatigue in polymers of quantitative nature concentrated on rubbers, where Thomas [70], and later Lake and Thomas [71] applied the tearing energy concept of fracture proposed by Rivilin and Thomas [72] to fatigue crack propagation. Thomas [70] showed that the fatigue crack growth rate could be expressed in the form of an empirical relationship,

$$\frac{dc}{dN} = AT^n \qquad (4.26)$$

where 'c' is the crack length, 'N' is the number of cycles, and 'T' is the surface work parameter which is analogous to the strain energy release rate 'G' in linear elastic fracture mechanics. For a single-edge notch specimen [57]

$$T = 2k_1 cU \qquad (4.27)$$

where 'c' is the crack length and 'U' = $\sigma^2/2E$ is the stored energy density for a linear elastic material. k_1 is a constant which varies from π at small extensions (the linear elastic value) to approximately unity at large extensions [77]. A and n are constants which are dependent on the material and generally vary with test conditions such as temperature. The exponent n usually lies between 1 and 6 and for rubber is approximately 2 for anything other than very small dc/dN.

A strong sensitivity of fatigue crack growth to molecular weight was noted. In a study of fatigue behaviour in Polycarbonate, Pitman and Ward [78] has also brought out the similarity between fatigue and fracture. A recent development by Williams [79], attempts to model the fatigue crack propagation in terms of the plastic zone analysis of the crack tip. On reviewing the literature on the fatigue of polymer, it can

be concluded that it is difficult to assign physical significance to the parameters causing fatigue damage. Further development in this area requires a more distinctly physical approach.

Thus, acousto-ultrasonic waves when injected at different fatigue levels of the solid polymeric specimen, would likely give a more abstract, but a clear correlation between the physical variables such as the number of cycles causing the fatigue level at a particular stress level. Chapter 7 deals with the experimental analysis of the polymeric specimen for different fatigue levels by acousto-ultrasonics.

4.6 Macromechanical Defects in a Polymer

Macromechanical defects such as holes, reduce the strength of any engineering material. This is particularly true for a polymeric material which is extensively used in structures. The structural components are fastened to each other by employing fasteners and rivet holes. Although these factors are taken into consideration during the designing process, it is instructive to develop a method by which the reduction in the strength of these polymeric components could be characterized. Acousto-Ultrasonics can provide quantitative information on such reductions in the strength of initiated defects [1,26 & 41].

Tanary et.al., [26] have extended such a study for adhesively bonded joints undergoing deformation. A newer approach of pattern recognition methodology can be effectively used where the classifiers are first trained to recognize the defect state. The non-dimensionalized values of discriminating features of the resulting acousto-

ultrasonic waveforms are used to discriminate unknown samples containing similar defects. Chapter 8 deals with this aspect. Samples containing known defect states i.e., in the form of holes of varying diameter are prepared to simulate the defect state. A classifier is built by using the resultant acousto-ultrasonic waveforms with the pattern recognition methodology.

4.7 Conclusion

The behaviour of linearly viscoelastic materials differs considerably from that of conventional elastic materials used in engineering structures. The time-dependent properties of creep and stress-relaxation are the important response characteristics, that need to be evaluated non-destructively on polymeric structural components. It is instructive to evaluate the stress levels in polymers, fatigue response and the reduction in strength due to the presence of defects by a non-destructive testing technique. Acousto-Ultrasonics, a non-destructive technique, can provide quantitative information on the above mentioned properties of polymers. The following chapters deal with this experimentally. Both destructive and non-destructive testing, using acousto-ultrasonics, are employed to characterize the viscoelastic response of solid polymers for the time-dependent property of stress-relaxation and various types of loading.

CHAPTER 5

ACOUSTO-ULTRASONIC EVALUATION OF STRESS-RELAXATION IN SOLID POLYMERS

5.1 Introduction

The utilization of solid polymeric materials in critical engineering structural applications as replacement for conventional metallic components has increased significantly in recent years. The time-dependent response characteristics of these materials (i.e., creep or stress relaxation) play an important role in the structural integrity of the components, thereby affecting the total strength of the structure itself. The wave propagation characteristics of the viscoelastic material might be affected by the microstructural changes effected on the test specimen (e.g., when the material is subjected to an increased level of stress, the microstructural bonds of the material are either broken or stretched due to the application of the stress). The acousto-ultrasonic waveform is known to be affected by the microstructural changes effected on the material [1,28 & 41]. During stress-relaxation, the microstructure of a viscoelastic material undergoes changes (See, e.g., 56-57 for details). It is instructive, for instance, to know the stress status of the material at a constant strain level. In other words, it would be beneficial to know the extent of stress-relaxation in a given polymeric structural component for a given strain level. Thus, it is essential that non-destructive evaluation methods be available to ensure that the structural performance of the polymeric components meet the design and service requirements. As discussed in Chapter 2, the majority of non-destructive testing (NDT) techniques

using ultrasonic wave propagation available today can readily detect physical discontinuities in terms of their location and sizes, but few NDT-techniques are available that could provide quantitative information on the overall performance of the mechanical response of the materials in general, and hence that of, polymeric structural materials undergoing, for instance, creep or relaxation. Acousto-Ultrasonics (AU), as discussed in Chapter-2, has the capability of providing quantitative information on the mechanical response of engineering materials.

This chapter provides the experimental results on the characterization of two different linear viscoelastic materials for their time-dependent viscoelastic properties using the acousto-ultrasonic technique. Results for the time-dependent stress relaxation behaviour of the viscoelastic material under the applied strain level is used to construct a pattern classifier. Unknown samples are characterized using acousto-ultrasonics (AU) and classified as to which stress state they may belong to.

5.2 Experimental Procedure and Apparatus

5.2.1 Material and test specimen

Two different linear viscoelastic materials, Polycarbonate (PC) and Polyvinylchloride (PVC), belonging to the class of solid polymersused in structural applications, are chosen for the purpose of present investigation. An uniaxial tensile test specimen configuration is adopted for performing stress- relaxation experiments in the INSTRON Universal Testing Machine (MODEL 4202). Twenty two specimens were prepared with dimensions as shown in Fig 5.1. Eleven specimens of

Polycarbonate (PC) and eleven specimens of Polyvinylchloride (PVC) were cut by careful machining to obtain defect free boundaries and dimensional accuracy. Close tolerances were maintained as per ASTM D-638 guidelines and also in accordance with ASTM D-2990 (specification for tensile creep testing). The surface of the specimen was guarded against any scratches for visible defects. The 'flat specimen configuration' as shown in Fig.5.1 was adopted and preferred over the 'dog-bone' type in order to simplify as much as possible the boundary effects on the mode of stress wave propagation through the specimen.

5.2.2 Accousto-Ultrasonic testing system

The acousto-ultrasonic (AU) testing technique involves generating ultrasonic waves and letting them pass through the test specimen. The resultant waveform is captured after travelling through the material by means of a receiving piezoelectric transducer. Although a number of test configurations are possible, the most desired test configuration is the one in which the sending and receiving transducers are located on the same side of the specimen [1,26 & 37]. Such a configuration is advantageous while inspecting structural components that are already in service (e.g., It would be impractical to access both sides of a wing structure of an aircraft for the placement of the transducer). Also, the transmitting and receiving transducers can be aligned parallel to the major load-carrying direction. Thus, the measured ultrasonic parameters will be more directly responsive of the material condition in the direction of loading, as opposed to measuring through-the-thickness properties as with the other ultrasonic techniques already discussed in Chapter 2. In this thesis, the latter

configuration is adopted due to its advantages as discussed in the foregoing; see also [30-37].

A specially designed acousto-ultrasonic (AU) experimental set-up for characterizing an engineering material is shown in Fig. 5.2. The pulsar-receiver sends in electric voltage pulses to the piezoelectric transducer at pre-determined rates and times. The acousto-ultrasonic wave is typically an ultrasonic wave sent periodically. The time between the successive waveforms is determined by the "digitization rate". The first wave starts and interacts with the microstructure of the material specimen thoroughly before being captured by the receiving transducer. The latter is connected to the preamplifier and in turn to the acoustic emission testing equipment (AET 5500) which eventually receives the waveform.

The acoustic emission testing equipment receives the wave form, amplifies the signal and transfers the data to a digitization board. This digitization board possess signal processing capability. The signal is digitized with the use of a commercial software 'ARIUS^{TM1}'. As soon as the first signal is digitized, the digitizer triggers the pulsar again for sending the next wave form, which interacts with the material and the cycle is repeated. The number of times the pulsar emits the wave form is determined by the 'repetition rate' utility, which is controlled by the ARIUS^{TM} software and can be manually set in DOS environment. ARIUS^{TM} allows further easy selection of threshold setting, setting of gates and their values, damping, frequency, etc., which initialises the waveform generation and reception. The digitized waveform is

---

1 ARIUS^{TM} is the Trademark of Tektrend International Inc., Montreal, Canada.

stored in the computer hard disk in separate data files for later analysis. A sample of the acousto-ultrasonic wave form obtained through ARIUS™ is illustrated in Fig.5.3 along with the test parameters chart. The latter shows the hardware settings used for experimentation.

The nominal central frequency of the sending transducer is set at 750 KHZ which is twice the central frequency of the receiving transducer. The sampling rate is set at 3.125 MHZ, since sampling rate must be at least twice that of the pulsar frequency to avoid 'aliaising' or false recreation of the waveform (See e.g., [40]. Other parameters such as the gain factor, gates, etc., are selected after repeated trials for the given geometry and material of the specimen in order to obtain reproducible results of the waveform.

5.3 Stress-Relaxation Testing for Polycarbonate Specimens

The specimens for stress relaxation testing, as shown in Fig.5.1, were loaded in the universal testing machine using screw type self-tightening wedge action grips. After initializing the parameters such as gauge length of 110 mm and speed of the cross head at 300 mm/min (keeping in accordance with the hypothesis that the stress should be applied at an infinitesimally short time [53-54]), the specimen was loaded to reach 4% of strain (i.e., 4.4 mm). The latter corresponds to an initial stress input of 34.971 MPa. The cross head of the tensile testing machine was, then, fixed at this position to maintain a constant strain level of 4%. The stress in the material was allowed to relax for a time period of up to 100000 sec. A chart recorder was used

to record the stress vs. time curve under the input level of strain. The x-axis of the recorder was set at a scale of 10 mm of chart distance for each 85.67 minutes. The y-axis of the chart recorder was set at a scale of 10 mm for 400 N of load acting on a cross-sectional area of the specimen of 120.9 mm^2.

5.3.1 Acousto-Ultrasonics measurements

The acousto-ultrasonic waves were injected into the specimen when the stress level was observed to be 34.971 MPa. The resulting acousto-ultrasonic (AU) wave was captured by the receiving transducer which was located at a fixed distance of 25.4 mm from the pulsar transducer. The resulting waveforms were captured and stored in separate data files on the hard disk of the computer. Acousto-ultrasonic measurements were carried out when the stress levels were observed to be 34.971, 33.203, 32.708, 31.660, 30.536 and 28.832 MPa corresponding to 1, 10, 100, 1000, 10000, and 100000 sec. respectively. From the start of the stress-relaxation experiment, five identical specimens were tested according to the procedure mentioned above (Fig.5.4). All other parameters concerning both the acousto-ultrasonic and tensile testing were maintained constant for all specimens. The coupling fluid "acoustic emission testing gel SC-2" was used for creating an effective continuity between the transducers and the test specimens.

5.3.2 Stress-relaxation at different strain levels

After completing the acousto-ultrasonic and stress-relaxation testing at 4% strain level as indicated in the foregoing, a number of stress-relaxation experiments were carried out at different strain levels (1%-7%). The family of stress-relaxation curves

obtained are shown in Fig.5.5. A new specimen was tested for each strain level. As shown in Fig.5.5, the values of relaxed stresses were recorded at 1, 10, 100, 1000, 10000, and 100000 sec. for each strain level.

5.4 Stress-Relaxation testing for Polyvinylchloride Specimens

In an identical fashion, polyvinylchloride (PVC) specimens were loaded at 4% strain level and the values of the relaxed stress were recorded at different instances of time for a time period of up to 100000 sec (Fig 5.6). Acousto-Ultrasonic measurements were taken as explained for polycarbonate specimens and totally five specimens were tested.

5.4.1 Acousto-Ultrasonic Measurements

The acousto-ultrasonic waveforms were injected and received as explained in section 5.3.1, when the relaxed stress values were observed to be 40.69, 36.227, 33.051, 31.644, 28.915 and 25.309 MPa at 1, 10, 100, 1000, 10000 and 100000 sec. respectively.

5.4.2 Stress-relaxation at different strain levels

The experimentation for obtaining the stress-relaxation curves at different strain levels were also carried out for polyvinylchloride (PVC) specimens, the results of which are shown in Fig.5.7. The relaxation experiments were carried out in a similar fashion as that of Polycarbonate specimens at 1%, 2%, 3%, 4%, 5% and 6% of the strain levels. The relaxed stresses were recorded at different instances of time for a time period of up to 100000 sec. for each of the strain levels (Fig.5.7).

5.5 Results and Discussion

5.5.1 Polycarbonate (PC) specimens

Fig.5.4 illustrates the relaxed stress values obtained at 4% strain level for polycarbonate specimens. These values were obtained when the stress in the material relaxes with time at the input strain level considered. For the five specimens tested, the experimental values are fitted using 'least square method', a obtain curve as shown in Fig.5.4. The nature of this curve is in accordance with the time-dependent stress-relaxation curves seen usually for polymeric materials of the same class [56-58]. Mercier et.al., [60], for instance, obtained similar curves for Bis-phenol Polycarbonate specimens, but for a longer period of time.

Fig.5.5 illustrates the stress-relaxation curves obtained at different strain levels for Polycarbonate specimens. The values are obtained when the stress in the material relaxes with time at different input strain levels. This exercise was carried out to create a family of stress-relaxation curves for up to 7% input strain levels. As the strain level was increased, the initial unrelaxed stress in the material also increased (e.g., the stress at 4% strain level was higher than the one obtained at 3%).

The acousto-ultrasonic parameter was normalized with respect to the maximum of the average of values obtained for five specimens as per the following equation.

$$AUP_{norm} = \frac{AUP\ measured\ for\ a\ relaxed\ stress\ level}{Maximum\ of\ the\ average\ values\ of\ AUP} \quad (5.1)$$

where AUP_{norm} is the normalized value of the acousto-ultrasonic parameter.

The relaxed stress in the material is also normalized with respect to the maximum

of the average of values obtained for the five specimens.

$$\sigma_{norm} = \frac{Value\ of\ the\ relaxed\ stress\ in\ a\ specimen}{Maximum\ of\ the\ average\ of\ stresses} \quad (5.2)$$

where σ_{norm} is the normalized value of the relaxed stress.

These normalizations are carried out to eliminate the material variations and to compare the values of stresses obtained through different specimens. Fig.5.8a illustrates the correlation between the normalized acousto-ultrasonic parameter (AUP) (Eqn. 5.1) and the normalized relaxed stress (Eqn.5.2) for polycarbonate (PC) specimens at 4% strain level. It was found that the values of the normalized AUP increases, as the stress in the material relaxes.

5.5.2 Polyvinylchloride (PVC) specimens

Fig.5.6 illustrates the stress-relaxation curves obtained for PVC specimens at 4% strain level, while Fig.5.7 illustrates the stress-relaxation curves for PVC specimens at different strain levels. It can be seen from Fig.5.7, that the nature of the relaxation curves at different strain levels have a similar trend to those of Polycarbonate specimens. Fig.5.8b illustrates the correlation between the normalized acousto-ultrasonic parameter (AUP) and the normalized relaxed stress for Polyvinylchloride (PVC) specimens. A correlation similar to the one obtained for Polycarbonate specimens could be seen between the normalized AUP and the normalized relaxed stress.

5.5.3 Discussion of the results obtained

During the initial unrelaxed stress state, obtained immediately after fixing the cross

head of the testing machine at a given level of strain input, the material is in a state of higher stress and the micromechanical bonds inside the specimen are stretched [57]. Some of these bonds might be already broken due to internal mechanisms such as slip and excessive local deformations [56].

For an efficient transfer of stress-wave energy, the propagation of the acousto-ultrasonic signal inside of the material specimen would depend on the integrity of the micromechanical bonds [1,28-30&38]. Thus the change in the value of the normalized AUP, which represents the transfer of stress-wave energy across the microstructure of the specimen, is changed between the unrelaxed and relaxed states. This might be attributed to the changes effected in the microstructure of the material.

On reviewing the available literature, it has been revealed that no research has been carried out for correlating the acousto-ultrasonic parameter with the time-dependent behaviour, e.g., stress-relaxation of viscoelastic materials. Vary [1,28,36 & 38]] and Vary and Lark [30], however, obtained similar correlations for AUP with respect to the reduction in tensile strength of fibre reinforced composites. In evaluating adhesive bonded joints under tensile loading, Tanary [26] obtained a straight line fit for normalized AUP that decreased with the increase in stress level. Williams et. al., [33], also noticed the change in AU measurement of nylon ropes as the tension of the rope was increased (i.e., the stress wave factor was found to decrease with the increase in the stress level). AUP was, thus, found to decrease with the increase in stress level in the experiments carried out to assess the stress levels in engineering materials [1,26,28,30,33,36].

5.6 Pattern Recognition Methodology Applied for Signal Analysis

5.6.1 Polycarbonate specimens

The resultant acousto-ultrasonic waveforms for the five specimens were captured at six different material stress states (34.971, 33.203, 32.708, 31.660, 30.536 and 28.832 MPa) for Polycarbonate specimens. These values of relaxed stresses were recorded at different instances of time, i.e., at 1, 10, 100, 1000, 10000, and 100000 sec. respectively. For the purpose of discriminating these stress states, three pattern classes (i.e., the resultant acousto-ultrasonic waveforms belonging to three different stress states) were chosen for designing a pattern classifier. The acousto-ultrasonic waveforms obtained at these stress states represent the raw data values for the pattern recognition analysis.

The number of wave form features (e.g., peak amplitude or the distance between two adjacent peaks in the resulting waveform) that could be inferred from the raw data vector would be enormous. However, most of the features may not be required for the purpose of particular pattern classification and only few features would be sufficient to fulfil the task. The commercial software used for pattern recognition analysis in this thesis, ICEPAK™[2], selects a total of 108 waveform features [20]. These are in five domains of the wave form (i.e., time, phase, power, cepstral[3] and

---

[2] ICEPAK™ is the trade mark of Tektrend International Inc., Montreal, Canada.

[3] cepstral domain provides data on spectral periodicity. i.e., this domain provides information on various wavelet arrival times that are calculated by filtering the time domain signals [1].

cross-correlation). These wave forms are automatically selected utilizing feature extraction algorithms [45,50]. To reduce these 108 features, Fisher discriminatory ratio (as explained in section 3.4.2) is used [20,46].

Important features that can readily discriminate a given waveform from other waveforms are ranked in order of their discriminatory power according to the problem being analyzed [20,46]. These selected features represent values in various domains whose units of measurement are different. Thus a normalization process is initiated that normalizes the feature vector of each of the class with respect to its mean and variance [20] (see section 3.4.2). Further, the normalized feature vectors are stored as separate files on the hard disk of the computer.

As explained in section 3.4.1, the pattern classification approach adopted in the present thesis depends on prior knowledge with respect to the decision boundaries between different classes. For the purpose of designing the classifier, the normalized feature vectors are further split into training files and evaluation files (see section 3.4.10). The normalized feature values of acousto-ultrasonic (AU) waveforms obtained from two of the five specimens tested at 4% strain level were used for the training and evaluation process. Three other specimens were treated as 'unknown specimens' and the acousto-ultrasonic waveforms obtained from them were used for testing the designed classifier. Figs.5.9a & 5.9b illustrate a two-dimensional feature space. The adopted features were selected through different 'iterations' of manual selection based on the separation of three pattern classes and on their discriminatory power as previously explained in section 3.4.2.

With reference to Figs.5.9a & 5.9b, class 1 represents the pattern class representing the unrelaxed stress state, 34.971 MPa. Class 2 represents the pattern class representing the relaxed stress state, 30.536 MPa. Class 3 represents the relaxed stress state, 28.892 MPa. It can be seen from Fig.5.9a, that the pattern vectors are spread out in the case of unrelaxed stress state, while those of the relaxed stress state cluster together. But the two pattern classes, 2 & 3 (the relaxed states), are very close to each other for two of the selected features (i.e., 'normalized 2nd greatest peak amplitude in power domain' and the normalized feature representing 'the number of peaks above the signal base line in power domain') in the feature space.

Fig.5.9b illustrates two distinct clusters of pattern vectors within class 1. Also a very high level of 'spread' is observed for pattern class 1 in the feature space for the selected features (i.e., for normalized 2nd greatest peak amplitude in power domain and the normalized feature of percentage of partial power in 3rd octant). This is probably due to the errors associated with the reproducibility of the acousto-ultrasonic waveforms for different specimens. This reproducibility problem has been cited in [1,26 & 37] and alternate methods are suggested in terms of non contact probes and laser generation of ultrasonic waves.

Table 5.1a represents the selected features for the case of Polycarbonate specimens. Also from figures 5.9a & 5.9b, it can be seen that a linear separation is no longer possible. The K-nearest neighbour classification, introduced in section 3.4.9, was therefore used. The results for training, evaluation and testing of the classifier are listed in Table 5.1b.

Table 5.1a Normalized features selected for Polycarbonate specimens

Feature Number*	Acousto-Ultrasonic feature Description	Domain of the waveform
13	inter peak distance from 1st to 2nd greatest	Time
37	Number of peaks above the signal base line	Power
43	2nd greatest peak amplitude	Power
49	% of partial power in the 3rd octant	Power
58	Greatest peak position	Phase

* Corresponding to number identification in the employed software ICEPAK™.

Table 5.1b Training, Evaluation and Testing of the classifier for polycarbonate (PC) specimens

Classification scheme: **K-Nearest Neighbour Classifier**

Stress state	Pattern class	Training (%)	Evaluation (%)	Testing of unknown specimens for all three pattern classes (%)
34.971 MPa	1	100.0	100.0	100.0
30.536 MPa	2	100.0	91.04	97.10
28.832 MPa	3	100.0	98.75	100.0

As seen from Table 5.1b, for the training and evaluation process of the designed classifier, 100% of the pattern vectors belonging to each of the three pattern classes form three separate clusters (Figs.5.9a & 5.9b). For the 2nd pattern class, the classifier misclassifies 2.9% of the waveforms belonging to this class by comparison to the classification result of pattern class 1, bringing down the classification rate in pattern class 2, to 97.10%.

5.6.2 Polyvinylchloride specimens

The resultant acousto-ultrasonic waveforms were captured when the values of relaxed stresses, in Polyvinylchloride specimens, were observed to be 40.693, 36.227, 33.051, 31.644, 28.915 and 25.309 MPa. These values of relaxed stresses were recorded at different instances of time, i.e., 1, 10, 100, 1000, 10000, and 100000 sec. respectively for the input strain of 4%. Three pattern classes, namely, the resultant acousto-ultrasonic waveforms obtained at 40.693, 28.915 & 25.309 MPa, were chosen for designing a pattern classifier. The acousto-ultrasonic waveforms obtained at these stress states represent the raw data values for the pattern recognition analysis.

As mentioned in the foregoing section, the number of waveform features that could be inferred from this raw data vector would be enormous. Thus, the waveform features are automatically selected utilizing feature extraction algorithms [45,50]. To further reduce the features, Fisher discriminatory ratio (explained in section 3.4.2) is used for ranking these features in accordance with their capability of discrimination between the captured waveforms [20,46].

Important features that can readily discriminate the waveforms belonging to one class from the others are ranked in order of their discriminatory power according to the problem being analyzed (see section 3.4.2). A normalization process, similar to the one carried out for Polycarbonate specimens is initiated, whereby, the feature vector of each of the class is normalized with respect to its mean and variance [20] (see section 3.4.2). Further, the normalized feature vectors are stored as separate

files on the hard disk of the computer.

The normalized feature values of acousto-ultrasonic waveforms obtained from two of the five specimens tested at 4% strain level were used for the training and evaluation process. Three other specimens were treated as 'unknown specimens' and the acousto-ultrasonic waveforms obtained from them were used for testing the designed classifier. Table 5.2a represents the selected features for the case of Polyvinylchloride specimens. For the purpose of designing the classifier, these features were selected through different iterations of manual selection based on the separation observed between the three classes as shown in Figs.5.9c & 5.9d.

Table 5.2a Normalized features selected for Polyvinylchloride (PVC) specimens

Feature Number*	Acousto-Ultrasonic feature Description	Domain of the Waveform
13	inter peak distance from 1st to 2nd greatest	Time
37	Number of peaks above the signal base line	Power
43	2nd greatest peak amplitude	Power
49	% of partial power in the 3rd octant	Power
58	Greatest peak position	Phase
67	% of partial power in 3rd octant	Phase
78	2nd greatest peak position	Cepstral
82	inter-peak distance from 1st to 2nd greatest	Cepstral
96	2nd greatest peak position	Cross-Correlation
100	inter peak distance from 1st to 2nd greatest	Cross-Correlation

* Corresponds to the identification number of the feature in the employed software, ICEPAK™.

Table 5.2b Training, Evaluation and Testing of the classifier for polyvinylchloride (PVC) specimens

Classification Scheme: K-Nearest Neighbour Classifier

Stress state	Pattern class	Training (%)	Evaluation (%)	Testing of unknown specimens for all three categories (%)
40.693 MPa	1	100.0	94.74	70.76
28.915 MPa	2	100.0	100.0	72.0
25.309 MPa	3	100.0	100.0	68.16

As seen from Table 5.2b, for the training process, the designed classifier classifies

100% of the pattern vectors belonging to all three classes into three separate clusters (Figs.5.9c & 5.9d). The classification rate for the training and evaluation processes for polyvinylchloride specimens falls considerably (between 68% - 72%), indicating a slightly higher misclassification of pattern classes amongst various samples. Figs.5.9c & 5.9d show well separated clusters formed from the training process. But the testing results for unknown samples indicate a considerable reduction in the testing results of the classifier. This might be attributed to either the material variations in the unknown specimens or the error associated with the reproducibility associated with the AU waveform. Such problems associated with material variations have been encountered, for instance, by Vary [1,41].

5.7 CONCLUSION

Solid polymeric specimens made of Polycarbonate (PC) and Polyvinylchloride (PVC) were prepared using flat specimen configuration for stress relaxation experiment in tensile loading configuration. Ultrasonic waves were injected in the specimens at unrelaxed initial stress state and at different relaxed stress states. The resultant acousto-ultrasonic wave forms were stored for further analysis. Eleven samples of each material were prepared. Stress-relaxation data at 4% strain level were recorded for five samples. Two of the five specimens were used for the training process in the design of the classifier. Three others were treated as 'unknown' specimens and tested with the designed classifier at 4% strain level.

For obtaining the family of stress-relaxation curves at six different strain levels, six

other specimens were utilized for Polycarbonate (PC) material. In the case of Polyvinylchloride (PVC), five specimens were used to obtain the family of stress-relaxation curves at five different strain levels.

Good correlations were obtained between the acousto-ultrasonic parameter and the relaxed stress in the material. Pattern recognition approach was used and found to be effective in discriminating different stress states while the specimen underwent stress-relaxation.

Chapter 6

EVALUATION OF STRESS LEVELS IN VISCOELASTIC SPECIMENS SUBJECTED TO UNIAXIAL TENSILE LOADING

6.1 Introduction

The utilization of solid polymeric materials in engineering structural applications has increased significantly in recent years. Although the design stresses are well within the range for which the structural components are designed for, it is possible for the stresses to exceed the maximum allowable limit. This might be due to extraneous factors (e.g., change in loading conditions). Thus, it is of interest and necessity to evaluate the stress levels of these components using a viable non-destructive testing (NDT) technique. By evaluating the strength of the structural member and setting acceptable confidence levels, a decision could be taken as to whether or not the component should be replaced.

As discussed in Chapter 2, the majority of NDT techniques available today can readily detect physical discontir.uities. Acousto-Ultrasonic (AU) technique, as discussed in Chapter 2, has the ability to provide quantitative information on the overall performance of a structural member.

The evaluation of stress level in a test specimen can be made by acousto-ultrasonic monitoring of the specimen during loading. When a material is subjected to tensile loading, it experiences microstructural changes and these changes affect the acousto-ultrasonic stress wave propagation characteristics. Hemann and Baaklini [84] observed the change in the attenuation of stress waves as the tensile stress for a

graphite/epoxy composite laminate was increased. i.e., they concluded that the attenuation of ultrasonic waves depended strongly on the tensile stress, although the relaxation between attenuation and stress was highly frequency dependent. For some frequencies, the attenuation increased with stress, while for others, the attenuation decreased with stress. They also noted a weak dependence of wave speed upon the tensile stress. William et.al., [33] found the stress wave factor to decrease with the increase in stress level, while evaluating double braided nylon ropes in tension.

This chapter provides the experimental results on the characterization of solid polymeric materials for various levels of uniaxial tensile loading using the acousto-ultrasonic (AU) technique. The change in the resulting acousto-ultrasonic (AU) wave due to the stress level in the specimen is utilized in designing a pattern classifier. Such classifier is used further to test 'unknown' specimens and to classify as to which stress state they belong. It is also intended to find the nature of correlation the acousto-ultrasonic parameter has, with the change in tensile stress levels in the material specimen.

6.2 Experimental Apparatus and Procedure

6.2.1 Material and test specimen

Twelve specimens of Polyvinychloride (PVC) with dimensions as shown in Fig.5.1 were prepared. These specimens of Polyvinylchloride were cut by careful machining to obtain defect free boundaries and dimensional accuracy. Close tolerances were maintained as per ASTM D-638 guidelines The surface of the specimen was guarded

against any scratches or visible defects. An Uniaxial tensile test specimen configuration is adopted for performing tensile loading experiments in the INSTRON Universal Testing Machine (MODEL 4202). The 'flat specimen configuration' as shown in Fig.6.1 was adopted and preferred over the 'dog-bone' type in order to simplify the boundary effects on the mode of stress wave propagation through the specimen.

6.2.2 Acousto-Ultrasonic testing system

The acousto-ultrasonic (AU) testing set-up, similar to the one explained in section 5.2.2 and illustrated in Fig.5.2, is used for the evaluation of stress levels in Polyvinylchloride (PVC) specimens. The hardware settings and the test parameters were maintained the same as the ones used for stress-relaxation testing, illustrated in Fig. 5.3.

6.3 Mechanical Testing

The specimen for uniaxial tensile testing, as shown in Fig.5.1, was loaded in the universal testing machine using screw type self-tightening wedge action grips. After initializing the parameters such as gauge length of 110 mm and speed of the cross head at 2.5 mm/min, the specimen was loaded in tension. The specimen was loaded continuously till failure. A chart recorder was used to record the stress vs. strain curve. The x-axis of the recorder was set at a scale of 10 mm of chart distance for 2mm elongation of the specimen. The y-axis of the chart recorder was set at a scale of 10 mm for 400 N of load acting on a cross-sectional area of the specimen of 120.9 mm^2.

6.3.1 Acousto-Ultrasonics measurements

Ultrasonic input pulses were injected when the stress level was observed to be 0 MPa (i.e., before stressing the specimen). The waves were let to travel inside the specimen and the resulting stress wave was captured by a receiving transducer located at 25.4 mm distance from the pulsar transducer. Both transducers were located on the longitudinal axis of the specimen. The captured waveforms were gathered and stored in separate data files on the hard disk of the computer. Further acousto-ultrasonic (AU) measurements were taken when the stress levels were 12.406, 24.813 and 39.287 MPa. All the AU measurements were taken before the yield point is reached during the tensile loading of the Polyvinylchloride (PVC) specimen. Twelve identical specimens were tested according to the procedure mentioned above (Fig.6.1). All other parameters concerning both the acousto-ultrasonic and tensile testing were maintained constant for all specimens. The coupling fluid "acoustic emission testing gel SC-2" was used for creating an effective continuity between the transducers and the test specimens.

6.4 Results and Discussion

Fig.6.1 illustrates the stress-strain curve for polyvinylchloride (PVC) specimens. These values were obtained when the specimen was continuously stressed to failure. For the twelve specimens tested, a curve was drawn using the 'least square method'. As seen from Fig.6.1, the experimental values were found to give a good fit. Fig.6.2 illustrates the true stress-strain curve. As discussed in section 4.9, a tangent to this

true stress-strain curve is drawn from the strain value of -1.0. This is known as the Consider'e construction [57]. According to this construction, the value of the ultimate tensile strength of the Polyvinylchloride specimen was found to be 40 MPa. This is the design stress that has to be used while designing structural components using Polyvinylchloride specimens (see, e.g., [57]).

The acousto-ultrasonic parameter was normalized with respect to its average of the maximum values, obtained for five specimens as per the following equation

$$AUP_{norm} = \frac{AUP\ measured\ for\ a\ stress\ level}{Maximum\ of\ the\ average\ value\ of\ AUP} \qquad (6.1)$$

where AUP_{norm} is the normalized value of the acousto-ultrasonic parameter.

The value of stress obtained during uniaxial loading in the test specimen is also normalized with respect to the average of maximum values, given by

$$\sigma_{norm} = \frac{Value\ of\ the\ stress\ in\ a\ specimen}{Maximum\ of\ the\ average\ stress} \qquad (6.2)$$

where σ_{norm} is the normalized value of the stress in the specimen.

These normalizations are carried out to eliminate the material variations and compare the values of stresses obtained from different specimens. Fig.6.3 illustrates the correlation between the normalized acousto-ultrasonic parameter (AUP) (Eqn. 6.1) and the normalized stress (Eqn.6.2). It was found that as the stress increases, the values of the normalized AUP decreases.

At increased stress levels, Acoustic emission (AE) signals are usually present (see, e.g., section 2.2.6). While evaluating the stress levels using acousto-ultrasonics (AU),

the spontaneous AE signals resulting from the loading was expected as given in [26]. This AE waveform would then combine with the resulting AU waveform to give a superimposed signal, consisting of AE and AU components. To avoid this, Tanary [26] used a waveform partitioning method. But in this thesis, this problem did not occur. This might probably be due to the attenuative nature of the viscoelastic material.

The correlation obtained in Fig.6.3 between the normalized AUP and the normalized stress for polyvinylchloride specimens is of the same nature as that observed by Tanary [26] in the case of bonded joints under tensile loading (i.e., the normalized AUP decreases with increase in stress). Williams et.al., [33], also, obtained similar relation in their study of evaluation of double braided nylon ropes using stress wave factor.

6.5 Pattern Recognition Methodology Applied for Signal Analysis

During the uniaxial tensile testing, as mentioned in section 6.3.1, ultrasonic pulses were injected in the material and the resultant acousto-ultrasonic waveforms were captured at four different material stress states (i.e., 0, 12.406, 24.813 and 39.287 MPa). These waveforms were recorded before the stress level in the material reaches its yield point, when the material was stressed continuously to failure. The captured acousto-ultrasonic wave forms were stored on the hard disk of the computer. For the purpose of discriminating between these three stress states using pattern recognition methodology, three pattern classes (i.e., the resultant acousto-ultrasonic waveforms

belonging to the three different stress states of 0, 24.813 and 39.287 MPa) were chosen for designing a pattern classifier. The acousto-ultrasonic waveforms obtained at these stress states represent the raw data values for the pattern recognition analysis.

The feature extraction, selection and ranking of the selected features were performed using ICEPAK™[1] (see, e.g., sections 3.4.2 & 5.6.1 and references [20,45-46,50]). Important features that can readily discriminate the waveform from other waveforms are ranked in order of their discriminatory power for the present problem of stress evaluation [20,46]. These selected features represent values in various domains whose units of measurement are different. Thus a normalization process is initiated that normalizes the feature vector of each of the class with respect to its mean and variance [20] (see section 3.4.2). Further, the normalized feature vectors are stored as separate files on the hard disk of the computer.

As explained earlier in section 3.4.1, the pattern classification approach adopted in the present thesis depends on prior knowledge with respect to the decision boundaries between different classes. For the purpose of designing the classifier, the normalized feature vectors are further split into training files and evaluation files (see section 3.4.10). The normalized feature values of acousto-ultrasonic waveforms obtained from three of the twelve specimens at different stress levels were used for the training and evaluation process. The remaining nine specimens were treated as 'unknown specimens' and the acousto-ultrasonic waveforms obtained from them were

---

[1] ICEPAK™ is the trade mark of Tektrend International Inc., Montreal, Canada.

used for testing the designed classifier.

Figs.6.4a & 6.4b illustrate a two-dimensional 'feature' space. These features were selected by the software used in this thesis ICEPAK™, using Fisher discriminatory ratio [20] based on their discriminatory power. With reference to Figs.6.4a & 6.4b, class 1 represents the pattern class representing the unstressed state, the value of which was observed to be 0 MPa. Class 2 represents the pattern class representing one of the stressed states, with an observed value of 24.813 MPa. Class 3 represents yet another stressed state, with an observed value of 39.287 MPa. Since it is impractical to project all the combinations of the selected features selected for classification in this problem, only two combinations are shown [20,46] in Figs.6.4a & 6.4b.

Table 6.1 given in the following page, represents the selected features for the classification using Fisher discriminatory ratio.

TABLE 6.1 Normalized features selected using Fisher discriminatory ratio for analysis

Feature Number*	Acousto-Ultrasonic feature Description	Domain of the waveform
4	Greatest peak position	Time
8	3rd greatest peak position	Time
14	Inter-peak distance from 1st to 3rd greatest peaks	Time
66	% of partial power in 2nd octant	Phase
93	Number of peaks above 25% of maximum signal amplitude	Cross-Correlation
75	Number of peaks above 25% of maximum signal amplitude	Cepstral
65	% of partial power in 1st octant	Phase
80	% of total area under greatest peak	Cepstral
92	Number of peaks above 10% of maximum signal amplitude	Cross-Correlation
107	% of partial power in 7th octant	Cross-Correlation
91	Number of peaks above signal base line	Cross-Correlation
81	% of total area under 2nd greatest peak	Cepstral
5	Greatest peak amplitude	Time
83	% of power in the 1st octant	Cepstral
1	Number of peaks above signal base line	Time

*** Corresponds to the identification number appearing in the ICEPAK™ software.**

From Figs. 6.4a & 6.4b, it can be seen that a linear separation between the pattern classes is no longer possible. The classification was performed using linear discriminatory classifier, minimum distance classifier, K-nearest neighbour classifier

and Empirical Bayesian classifier (see, e.g., sections 3.4.3-3.4.7). Only Empirical Bayesian classifier introduced earlier in section 3.4.7, could successfully classify the 'unknown' pattern vectors to their respective class. The three other classification schemes mentioned above could not obtain the correct classification for the 'unknown' specimens.

6.5.1 Training and evaluation of the classifier

The 'training' of the classifier was carried out using three specimens under different levels of uniaxial loading, the results of which are given below.

Table 6.2 Training and evaluation of the classifier

Classification scheme: Empirical Bayesian Classifier

Pattern class	Stress state	Training	Evaluation
Class 1	0 MPa	89.33	89.19
Class 2	24.813 MPa	68.18	62.79
Class 3	39.287 MPa	69.35	70.97

As seen from Table 6.2, the training and evaluation rates for class 1 is fairly satisfactory. For the other two classes (2 & 3), it is fairly moderate to achieve discrimination amongst the different pattern classes. But the real power of the designed classifier is seen only when it is tested with specimens unknown stress states [46]. The results of the testing of the classifier are illustrated in Table 6.3.

6.5.2 Testing of the classifier

TABLE 6.3 Testing of the classifier

Classification scheme: Empirical Bayesian Classifier

Stress level	Pattern class	Specimen #1	Specimens #1-#3	Specimens #1-#6	Specimens #1-#12
0 MPa	1	85.71	63.16	56.30	57.54
24.813 MPa	2	100.0	63.87	69.89	48.23
39.287 MPa	3	87.50	63.71	52.54	61.04

The specimens unknown stress states were grouped into one, three, six and twelve. The waveforms obtained from them were tested with the designed classifier. As seen from Table 6.3, the unknown classification rate is good for sample #1 indicating a well designed classifier and suitably selected features. As the sample size (number of specimens) increases, the classification rate falls down to 63% for the group containing three specimens. The classification rate drops to 56% and 52% for two of the three classes when the sample size is increased to six specimens. When the sample size is further increased to twelve specimens, the classification rate for one of the three classes falls to 48%. This was mainly due to the difficulty in reproducing the acousto-ultrasonic waveforms on different samples rather than on the selection of features or the type of classification function selected.

6.6 Conclusion

Solid polymeric samples made of Polyvinylchloride (PVC) were prepared using flat

specimen configuration for uniaxial tensile testing and acousto-ultrasonic analysis. Twelve specimens were prepared (200 x 25.4 x 4.5)mm and loaded in the universal testing machine to failure. Good correlation was obtained between the normalized acousto-ultrasonic parameter and the normalized tensile stress in the material during the uniaxial tensile loading. Three different elastic stress levels of 0, 24.813 and 39.287 MPa were chosen for classification using pattern recognition methodology. Three samples were used for training and evaluation and the rest were tested using the classifier. A good classification rate was obtained during the training and evaluation process. A classification rate of 90% was obtained while testing one specimen with an unknown stress state and when the sample size increased the overall classification rate dropped to 50%. This drop in the classification rate could be attributed to the problem of signal reproducibility.

CHAPTER 7

FATIGUE TESTING OF A SOLID POLYMER

7.1. Introduction

Polymeric solids are being utilized in the manufacture of an increasing number of cyclic-load bearing structural components (e.g., water and gas transportation system components, gears, hinges, springs, and mechanical arms). In part, this is due to the energy-related trend towards lighter-weight engineering systems and also due to the steady improvement in the mechanical properties of many plastics. Since many loads are cyclic in nature, the deformation and fracture response to cyclic loads (fatigue) is of particular interest.

As discussed in section 4.5, earlier works on the area of fatigue of polymers were purely destructive in nature. σ-N (Stress (σ) - Number of cycles (N)) curves were the starting point and subsequently cracks were initiated. Crack growth with respect to the number of cyclic loadings under a particular stress level was recorded and studied in detail for many polymeric systems [70-78]. Fatigue fractures do occur for many engineering materials, at stresses below the material yield strength.

In the case of both polymers and metals, repeated loading to the same stress level will precipitate damage and eventual failure, even though the stress level is much below the yield strength of the polymer [75,77]. This chapter deals with the experimental study of fatigue using 'unnotched' (i.e., without cracks) specimens. Unnotched specimens are tested assuming that the material is 'defect-free' and are subjected to a particular level of cyclic loading. Fatigue has been known to introduce

irreversible damage and initiates failure at some critical level of damage (as the accumulated damage mechanisms could cause a catastrophic failure of the material) [74,77].

As mentioned in the foregoing chapters, acousto-ultrasonics (a non-destructive testing (NDT) tool) is based on the principle of stochastic ultrasonic wave propagation in a material. Vary [1] has stated that efficient stress wave transfer across the material depends on the integrity and strength of the microstructure. It has also been shown that any reduction in the integrity due to accumulated damages, will result in poor transmission of the stress wave energy across the material [81]. Thus, acousto-ultrasonics could be a viable NDT technique in evaluating fatigue damages.

This chapter contains the experimental investigation aiming at correlating the ultrasonic waveform parameters and the material deterioration state due to an induced fatigue damage in specimens of solid polymers. This is accomplished by means of subjecting a polymeric specimen to cyclic loading, while maintaining the stress level constant. Ultrasonic pulse inputs are injected in the material specimen before subjecting the latter to cyclic loading. The specimen was then subsequently subjected to cyclic loading at a specified stress level. A universal tensile testing machine was employed for the fatigue test. After a prescribed number of cycles, the specimen was unstressed (by bringing the cross-head motion of the universal tensile testing machine to a halt and returning the testing machine to zero loading level). Acousto-Ultrasonic (AU) measurements were taken (as explained in section 5.2.2) and the specimen was once again subjected to cyclic loading, at different cycles of loading (i.e., 0, 1200,

3600 and 4800 cycles of loading) for one particular stress level. The whole operation was repeated in a similar fashion and AU measurements were taken after subjecting the specimen to different cycles of loading till it fails due to fatigue damage.

7.2. Experimental Apparatus and Test Procedure

7.2.1 Material and test specimen

Twenty specimens of Polyvinylchloride (PVC) were prepared with dimensions as shown in Fig.5.1, for performing fatigue loading experiments in the INSTRON Universal Testing Machine (MODEL 4202). The preparation of the specimen and its geometry are explained in section 6.2.1.

7.2.2 Acousto-Ultrasonic testing system

The acousto-ultrasonic (AU) test set-up used for fatigue testing is shown in Fig.5.2 and discussed in section 5.2.2. The hardware parameters are the same as illustrated in Fig.5.3.

7.3 Mechanical Fatigue Testing

The specimen for fatigue testing in cyclic tension mode is shown in Fig.6.1. This was loaded in the Universal testing machine using screw type self-tightening wedge action grips. After initializing the parameters such as gauge length of 110 mm and speed of the cross-head at 100 mm/min, the specimen was loaded in tension. Four identical specimens were tested in a similar fashion. A chart recorder was used to record the stress vs. strain curve. The x-axis of the recorder was set at a scale of 10

mm of chart distance for 2 mm elongation of the specimen. The y-axis of the chart recorder was set at a scale of 10 mm for 400 N of load acting on a cross-sectional area of the specimen of 120.9 mm^2. The specimens tested failed after '0' cycles of loading (i.e., without any fatigue damage at this yield stress). To obtain the σ-N diagram, the cross-head limits were set between 0 and 5.5 KN of loading. After 250 cycles, they were observed to fail catastrophically. Similarly, other specimens were tested at reduced loading levels of 5, 3.75 and 3.25 KN) in cyclic tension to fatigue failure. Fig.7.1 illustrates the σ-N diagram obtained for this experiment.

7.3.1 Acousto-Ultrasonics measurements

The acousto-ultrasonic (AU) waves were injected and captured for specimens loaded in cyclic tension between 0 and 3.75 KN. The waves were let to travel inside the specimen and the resulting stress wave was captured by the receiving transducer located at 25.4 mm distance from the pulsar transducer at '0' cycles of loading at 0 MPa. The coupling fluid "acoustic emission testing gel SC-2" was used for creating an effective continuity between the transducers and the test specimens. Further, after a cyclic loading of 1200 cycles, the cross-head was stopped and the specimen was unstressed (i.e., cross-head was brought to its original position). AU measurements were taken as before and the specimen was further loaded in cyclic tension. In a similar fashion, AU measurements were taken at 2400, 3600 and 4800 cycles of loading. The specimen was finally seen breaking at 4860 cycles. In an identical fashion four specimens were tested. The waveforms obtained were stored on the hard disk of the computer. All other parameters concerning both the acousto-

ultrasonic and tensile testing were maintained constant for all specimens.

7.4 Results and Discussion

Fig.7.1 illustrates the stress (σ) vs. number of cycles to failure (N) for the Polyvinychloride specimens subjected to fatigue failure. These values were obtained when the specimens were cyclically loaded to fatigue failure as explained in section 7.3.1. For the twenty specimens tested, a curve was fitted to the experimental data using a 'least square method'.

Fig.7.2 illustrates the correlation between the normalized acousto-ultrasonic parameter (AUP) and the number of cycles to cause fatigue damage. The acousto-ultrasonic parameter was normalized with respect to its maximum of the average values as per the following equation.

$$AUP_{norm} = \frac{AUP\ measured\ for\ a\ specimen}{Maximum\ of\ the\ average\ value\ of\ AUP} \qquad (7.1)$$

where AUP_{norm} is the normalized value of the acousto-ultrasonic parameter.

These normalizations are carried out to eliminate the material variations and compare the values of stresses obtained from different specimens. It was found that as the number of cycles of loading increases, the values of the normalized AUP decreases.

The correlation obtained in Fig.7.2 between the normalized AUP and the fatigue level at different cycles of loading Polyvinylchloride (PVC) specimens is of the same trend observed by Talreja [81] while evaluating fatigue damage growth in

graphite/epoxy laminates using acousto-ultrasonic measurements (i.e., the normalized AUP decreases with increase in the number of cycles). Dos Reis and McFarland D.M. [32] also obtained correlations of decrease in stress wave factor with increase in fatigue cycles for wire ropes.

7.5 Pattern Recognition Methodology Applied for Signal Analysis

During the cyclic tensile testing (0 and 3.75 KN), as mentioned in section 7.3.1, ultrasonic pulse inputs were injected and the resultant acousto-ultrasonic waveforms were captured after different cycles loading. This is done at 0, 1200, 2400, 3600 and 4800 cycles of loading for a specimen under 0 MPa (i.e., after unstressing the specimen). The resulting acousto-ultrasonic wave forms were stored on the hard disk of the computer. For the purpose of discriminating the 'fatigue damaged' states using pattern recognition methodology, five pattern classes (i.e., the resultant acousto-ultrasonic waveforms belonging to five different cyclic loading levels of 0, 1200, 2400, 3600 and 4800 cycles) were chosen for designing a pattern classifier. The acousto-ultrasonic waveforms obtained at these fatigue states represent the raw data values for the pattern recognition analysis.

Important features that can readily discriminate the waveform from other waveforms are ranked in order of their discriminatory power for the present problem [20,46]. These selected features represent values in various domains whose units of measurement are different. Thus, a normalization process is initiated that normalizes the feature vector of each of the class with respect to its mean and variance [20] (see

section 3.4.2). Further, the normalized feature vectors are stored as separate files on the hard disk of the computer.

As explained in section 3.4.1, the pattern classification approach adopted in the present thesis depends on prior knowledge with respect to the decision boundaries between different classes. For the purpose of designing the classifier, the normalized feature vectors are further split into training files and evaluation files, as discussed earlier in section 3.4.10. The normalized feature values of acousto-ultrasonic waveforms obtained from one of the four samples at different fatigue cyclic levels were used for the training and evaluation process. The remaining three samples were treated as 'unknown samples' and the acousto-ultrasonic waveforms obtained from them were used for testing the designed classifier.

Figs.7.3 & 7.4 illustrates a two-dimensional 'feature' space. These features were selected automatically by the software used in this thesis ICEPAK™, using Fisher discriminatory ratio [20] and based on the class separability (Figs.7.3 & 7.4).

In Figs.7.3 & 7.4, class 1 represents the pattern class representing the unfatigued state (0 cycles of loading). Class 2 represents the pattern class representing one of the fatigued states, with an observed value of 1200 cycles. Class 3 represents yet another fatigued state (2400 cycles of loading). Classes 4 and 5 represent fatigue levels of 3600 and 4800 cycles of loading respectively. Two combinations of the features are shown in Figs. 7.3 and 7.4. The pattern classes are projected onto this features space. Table 7.1 represents the selected features for the classification using Fisher discriminatory ratio as explained in section 3.4.2.

Table 7.1 Features selected for classification

Feature No.	Acousto-Ultrasonic feature	Domain of the waveform
41	Greatest peak amplitude	Power
77	Greatest peak amplitude	Cepstral
79	2nd greatest peak amplitude	Cepstral

7.5.1 Training, evaluation and testing of the classifier

Table 7.2 Results for training, evaluation and testing of the classifier

Classification scheme: K-Nearest Neighbour

Pattern class	Fatigue state	Training (%)	Evaluation (%)	Testing (%)
Class 1	0 Cycles	100.0	100.0	100.0
Class 2	1200 Cycles	100.0	100.0	100.0
Class 3	2400 Cycles	100.0	100.0	100.0
Class 4	3600 Cycles	100.0	100.0	98.11
Class 5	4800 Cycles	100.0	100.0	100.0

Table 7.2 represents the classification rates obtained for the 5-class classifier, designed for discriminating various fatigue levels. As seen from Table 7.2, the training, evaluation and testing rates are good for the designed classifier.

7.6 Conclusion

Solid polymeric specimens made of Polyvinylchloride (PVC) were prepared using flat specimen configuration for fatigue testing in cyclic tension mode and acousto-ultrasonic analysis. Twenty samples were prepared (200 x 25.4 x 4.5)mm and loaded in the Universal testing machine to fatigue failure. Good correlation was obtained between the normalized acousto-ultrasonic parameter and the number of cycles required to cause fatigue damage. Five different fatigue damage levels (0, 1200, 2400, 3600 & 4800 cycles) were chosen for classification using pattern recognition methodology. One specimen state was used for training and evaluation and the three others were tested using the classifier. A good classification rate of 98%-100% was obtained during the training, evaluation and testing process.

CHAPTER 8

TESTING FOR A MACROMECHANICAL DEFECT IN A SOLID POLYMERIC SPECIMEN

8.1. Introduction

Solid Polymeric materials are being utilized in an increasing number of load bearing structural components. This has resulted in a number of components that have to be mechanically fastened to each other to fulfil the requirements of the structure. Macromechanical defects such as rivet holes, fasteners etc., reduce the strength-related properties of any engineering material.

For fastening or riveting two solid polymeric materials to one other, it is necessary to drill holes in them causing a macromechanical defect state. During such operations, as in metals, discontinuities in the microstructure of the material can cause reduction in the strength of the structural component.

This chapter evaluates the possibility of investigating this phenomenon non-destructively, using acousto-ultrasonics. For the purpose of initiating a defect, holes of varying diameters were drilled at the geometric centre of rectangular Polycarbonate (PC) specimens (Fig.8.1). These specimens were then subjected to acousto-ultrasonic examinations and subsequently loaded to failure in uniaxial tensile testing mode. The acousto-ultrasonic waveforms obtained from the specimens were utilized for designing a pattern classifier that could effectively distinguish between the variations in the strength of various specimens containing different defect sizes. The strength of each specimen is calculated by dividing the fracture load by the load bearing area of the

specimen. The acousto-ultrasonic parameter (AUP) has been determined and correlated with the tensile strength of the specimens.

8.2. Experimental Apparatus and Procedure

8.2.1 Material and test specimen

An Uniaxial tensile test specimen configuration is adopted for performing tensile loading experiments in the INSTRON Universal Testing Machine (MODEL 4202). Seven groups of Polycarbonate (PC) specimens (each group containing four identical specimens) were prepared with dimensions as shown in Fig.8.1. The specimens were cut by careful machining to obtain defect free boundaries and dimensional accuracy. Close tolerances were maintained as per ASTM D-638 guidelines. To create defects, holes were drilled at the geometric centre of the specimen. The diameter of the hole was varied from one group to another as illustrated in Fig.8.1. The surface of the specimen was guarded against any scratches for visible defects. As mentioned in section 5.2.1, the 'flat specimen configuration', Fig.8.1, was adopted and preferred over the 'dog-bone' type in order to simplify the boundary effects on the mode of stress wave propagation through the specimen.

8.2.2 Acousto-Ultrasonic testing system

A typical AU experiment for characterizing engineering materials is shown in Fig. 5.2. The sending and receiving transducers were aligned with the load bearing axis of the test specimen. This configuration is adopted following the discussions (see e.g., section 5.2.2) (see also references [1,30-37 & 41]. Both the sending and

receiving transducers were placed equidistant from the initiated defect (i.e., along the axis of the specimen and 12.7 mm from the geometric centre of the hole). A sample AU waveform and the chart for test parameters are illustrated in Fig.5.3. The digitized waveform was stored on the computer hard disk in separate data files for later analysis. The hardware parameters, such as the frequency of the wave, gain, couplant etc., were maintained the same as the ones discussed in section 5.2.

8.3 Mechanical Testing

The specimen for uniaxial tensile testing, as shown in Fig.8.1, was loaded in the universal testing machine using screw type self-tightening wedge action grips.

8.3.1 Acousto-Ultrasonics measurements

Ultrasonic input pulses were injected in the material specimen when the stress level was observed to be 0 MPa. The resulting waves were let to travel inside the specimen and the resulting stress wave was captured by the receiving transducer. These waveforms were gathered and stored in separate data files on the hard disk of the computer. Further, the acousto-ultrasonic (AU) measurements were taken from four identical specimens belonging to each group (Fig.8.1) containing the same hole size. All other parameters concerning both the acousto-ultrasonic and tensile testing were maintained constant throughout the experiment. The coupling fluid "acoustic emission testing gel SC-2" was used for creating an effective continuity between the transducers and the test specimens.

After initializing the parameters such as gauge length of 110 mm and speed of the

cross-head at 2.5 mm/min, the specimen was then loaded in tension. The cross head was allowed to stress the specimen continuously till failure. A chart recorder was used to record the stress vs. strain curve. The x-axis of the recorder was set at a scale of 10 mm of chart distance for 2 mm elongation of the specimen. The y-axis of the chart recorder was set at a scale of 10 mm for 400 N of load acting on a cross-sectional area of the specimen of 120.9 mm^2. The specimens were loaded to failure and the fracture load was recorded. Table 8.1 illustrates the fracture load and the tensile strength of the specimen for various defect sizes.

TABLE 8.1 Mechanical testing results

Size of the hole (mm^2)	Average Fracture load (N)	Average ultimate tensile strength (MPa)
0	7021.6	58.076
9.52	6946.6	57.456
11.334	7139.2	59.049
13.223	6815.4	56.370
15.113	6779.8	56.076
16.736	6696.9	55.391
19.04	6516.1	53.895

8.4 Results and Discussion

The acousto-ultrasonic parameter was normalized with respect to the maximum of the average values, obtained for six groups of specimens. That is,

where AUP_{norm} is the normalized value of the acousto-ultrasonic parameter.

$$AUP_{norm} = \frac{AUP\ measured\ for\ a\ given\ specimen}{Maximum\ of\ the\ average\ value\ of\ AUP} \qquad (8.1)$$

The value of tensile strength obtained during uniaxial loading in the test specimen (fracture load divided by the load bearing area) is also normalized with respect to the maximum of the average values, given by

$$\sigma_{norm} = \frac{Value\ of\ the\ tensile\ strength\ in\ a\ specimen}{Maximum\ of\ the\ average\ tensile\ strength} \qquad (8.2)$$

where σ_{norm} is the normalized value pertaining to the tensile strength of the specimen.

These normalizations are carried out to eliminate the material variations and compare the values obtained from specimens. Fig.8.2 illustrates the correlation between the normalized acousto-ultrasonic parameter (AUP) (Eqn. 8.1) and the normalized strength (Eqn.8.2).It was found that as the ultimate tensile strength increases, the values of the normalized AUP increases (Fig.8.2).

Fig.8.3 illustrates the variation of tensile strength with the increase in defect size (i.e., in the form of increase in the diameter of the hole drilled; defect size representing the area of the hole in mm^2 (Fig.8.1)). As shown in Fig.8.3, it is difficult to obtain a correlation between the tensile strength of the material and the size of the defect. Tanary [26] was also unable to obtain any correlation between the size of the defect (in terms of void size) and the shear strength in case of adhesively bonded joints. Wang et.al., [85] were also unable to find a direct correlation between the void size and the fractured load of single lap-shear aluminium joints.

The correlation obtained in Fig.8.2 between the normalized AUP and the

normalized ultimate tensile strength is of the same trend observed by Tanary [26] and Tanary et.al., [37] in evaluating adhesive shear strength of bonded joints (i.e., the normalized AUP increases with the increase in the ultimate strength of bonded joints containing voids). Vary [1,28,41] obtained similar correlations in the case of evaluating the tensile strength of composite specimens. Vary and Lark [86] obtained a similar correlation of increasing stress wave factor with increase in the tensile strength of graphite/epoxy composite laminates. Srivastava and Prakash [86] also obtained similar correlation between the ultimate tensile strength and acousto-ultrasonic stress wave factor for glass/epoxy and graphite/epoxy unidirectional fibre-reinforced composite laminates with varied fiber loading and porosity. The reader is also referred in this regard to references [1,26,28 & 37].

8.5 Pattern Recognition Methodology Applied for Signal Analysis

Acousto-Ultrasonic measurements were taken from the specimens before subjecting them to tensile loading. Ultrasonic pulse inputs were injected in the material specimens and the resultant waveforms were captured for seven different groups of specimens containing holes of differing diameters (Fig.8.1). The resulting acousto-ultrasonic waveforms were stored on the hard disk of the computer. For the purpose of discriminating specimens with different tensile strength using pattern recognition methodology, four pattern classes (i.e., the resultant acousto-ultrasonic waveforms received from four different groups of specimen containing hole diameters of 0, 2.381, 3.175 & 4 mm) were chosen for designing a pattern classifier. The

acousto-ultrasonic waveforms obtained at these pattern classes represent the raw data values for the pattern recognition analysis.

The commercial software used for pattern recognition analysis in this thesis, ICEPAK™[1], selects a total of 108 waveform features [20]. These are in five domains of the wave form (i.e., time, phase, power, cepstral[2] and cross-correlation). These wave forms are automatically selected utilizing feature extraction algorithms [45,50]. To reduce this high dimensionality of features, Fisher discriminatory ratio (see section 3.4.2) is used [20,46].

Important features that can readily discriminate the waveform from other waveforms are ranked in order of their discriminatory power for the present problem. These selected features represent values in various domains whose units of measurement are different (e.g., time and power domains represent two very different values that cannot be compared). Thus a normalization process is initiated that normalizes the feature vector of each of the class with respect to its mean and variance [20] (see section 3.4.2). Further, the normalized feature vectors are stored as separate files on the hard disk of the computer.

As explained in section 3.4.1, the pattern classification approach adopted in the present thesis depends on prior knowledge with respect to the decision boundaries

---

[1] ICEPAK™ is the trade mark of Tektrend International Inc., Montreal, Canada.

[2] cepstral domain provides data on spectral periodicity. i.e., this domain provides information on various wavelet arrival times that are calculated by filtering the time domain signals [1].

between different classes. For the purpose of designing the classifier, the normalized feature vectors are further split into training files and evaluation files (see section 3.4.10). The normalized feature values of acousto-ultrasonic waveforms obtained from one of the specimens in each group was used for the training and evaluation process. The remaining three specimens in each group were treated as 'unknown' specimens and the acousto-ultrasonic waveforms obtained from them were used for testing the designed classifier.

Figs.8.4a & 8.4b illustrates a two-dimensional 'feature' space. These features were selected automatically by the software used, ICEPAK™, using Fisher discriminatory ratio [20] based on their discriminatory power. Table 8.2 represents the selected features for the classification using Fisher discriminatory ratio and manual iterations based on class 'separability' and discrimination, as seen from Figs.8.4a & 8.4b.

TABLE 8.2 Normalized features selected using Fisher discriminatory ratio for analysis

Feature Number*	Acousto-Ultrasonic feature Description	Domain of the waveform
65	% of partial power in 1st octant	Phase
66	% of partial power in 2nd octant	Phase
77	Greatest peak amplitude	Cepstral

*** Corresponds to the identification feature number used in the software.**

In Figs.8.4a & 8.4b, class 1 represents the pattern class representing the specimen group with a hole size of 4 mm. Class 2 represents the pattern class representing the group of specimen with 3.175 mm diameter of hole. Class 3 represents the group with 2.3812 mm diameter of hole, while class 4 represents the group of specimens containing 0 mm diameter of hole (i.e., specimens without any defect). Two combinations of the features are shown in Figs.8.4a & 8.4b and the pattern classes are projected in the feature space.

From figures 8.4a & 8.4b, it can be seen that a linear separation between the pattern classes is no longer possible. After repeated trials with various classification schemes (see section 3.4.4 to 3.4.8), the K-Nearest Neighbour classifier, introduced in section 3.4.7, was chosen. This classifier was found to classify most of the waveforms resulting from 'unknown' samples to their respective pattern classes, than any other classifier (see section 3.4.4-3.4.8). The results of training, evaluation and testing are given below (see section 3.4.9) in Table 8.3. Good classification rates of 92%-100% were obtained during the training and evaluation process. For the case

of testing using unknown samples, recognition rates of 96%-100% were obtained, which is an indication of a well designed classifier.

8.4.2 Training, evaluation and testing of the classifier

TABLE 8.3 Results for training, evaluation and testing of the classifier

Classification scheme: K-Nearest-Neighbour

Defect state	Pattern class	Training (%)	Evaluation (%)	Testing (%)
4 mm hole	1	100.0	100.0	100.0
3.175 mm hole	2	100.0	100.0	100.0
2.3812 mm hole	3	100.0	100.0	100.0
0 mm hole	4	100.0	92.31	96.23

8.6 Conclusion

Solid polymeric samples made of Polycarbonate (PC) were prepared using flat specimen configuration for uniaxial tensile testing and acousto-ultrasonic analysis. Twenty eight specimens were prepared forming seven groups of specimens. Four identical specimens were prepared in each group. Defects were initiated in the specimen in the form of drilled holes. The defect size (i.e., the diameter of the holes drilled) were varied between each group. Good correlation was obtained between the normalized acousto-ultrasonic parameter and the ultimate strength of the specimen. For the purpose of pattern recognition analysis of the test results, one out of four specimens were treated as training and evaluation sample (i.e., the resulting acousto-ultrasonic waveforms from the specimen forming the raw data vector for training and

evaluation). Three other specimens from each group were treated as unknown samples and tested with the designed classifier.

Good training, evaluation and testing results were obtained. This is an indication of a well designed classifier and can be successfully applied for material characterization, once the experimental system is illustrated for material variation and geometry.

Chapter 9

CONCLUSION AND FUTURE RECOMMENDATIONS

Solid polymeric materials can offer considerable advantages over metals, particularly in terms of ease of fabrication and weight saving. Due to these benefits, they are increasingly being used in aerospace components, automotive structures and engineering. This has prompted the need for developing a non-destructive testing (NDT) technique that can accurately characterize the material in terms of its current strength.

The use of destructive techniques, however advanced and accurate, are of limited use in the case of components that are already in the structure. Most NDT techniques developed for evaluating the structural members can readily detect flaws, but it is often difficult to correlate a detected flaw to the overall performance of the structural member. The acousto-ultrasonic (AU) technique, used in conjunction with pattern recognition methodology, could be used to evaluate the mechanical response of polymers.

The acousto-ultrasonic (AU) technique has been used in this thesis to evaluate stress-relaxation, a time-dependent property of polymers. The acousto-ultrasonic parameter (AUP) which measures the relative strength of the ultrasonic wave transmission was correlated with the relaxed stress. Statistical pattern recognition techniques were used to design a discriminating classifier that can correctly identify the relaxed stress state of the material. Good correlation was obtained between the acousto-ultrasonic parameter (AUP) and the relaxed stress. Pattern recognition

methodology applied to the resulting acousto-ultrasonic (AU) waveform, utilizing a K-Nearest Neighbour classification function, resulted in good classification rates for Polyvinylchloride (PVC) and Polycarbonate (PC) specimens undergoing stress-relaxation.

The results of the designed classifier indicate that the acousto-ultrasonic (AU) technique can be used for characterizing stress-relaxation in linear viscoelastic materials. The results of the classification also indicate that statistical pattern recognition methodology could be effectively used for acousto-ultrasonic (AU) signal analysis, once the acousto-ultrasonic (AU) measurement system is calibrated for material variations and specimen geometry.

The acousto-ultrasonic parameter (AUP) is seen to decrease linearly with increase in stress levels. Statistical pattern classifier using an Empirical Bayesian classification function was designed for this purpose.

For fatigue damage, the statistical pattern classifier was designed using K-Nearest Neighbour classification scheme. The designed classifier could correctly classify the waveforms to their respective classes. Good correlation was also obtained between the acousto-ultrasonic (AU) parameter and the fatigue cyclic level for a given level of stress.

For the case of macromechanical defect in the form of holes, the reduction in tensile strength due to such defects was seen to have good correlation with the acousto-ultrasonic parameter. Also, the statistical pattern classifier designed using a K-Nearest Neighbour classification function was able to correctly identify the

reduced strength states.

The above results obtained from the acousto-ultrasonic test set up can be affected by many factors such as the pressure applied to the transducer and the coupling fluid applied between the transducer and the specimen. These factors affect the reproducibility of the AU measurements. Through experimentation and optimization of system parameters, these were chosen so as to reproduce the resulting waveform over different tests.

The factors affecting the resulting waveform require more research regarding their application to acousto-ultrasonic technique so that the reproducibility of measurement could be improved (e.g., using contactless probes and laser generation of ultrasonic waves inside the material).

Variations in the material and geometry of the test specimens also affects the results of acousto-ultrasonic (AU) measurement. The effect of these variations on AU wave propagation should be studied and understood. To do this, it is useful to attempt to trace wave paths, track multiple reflections and refractions, and to gauge the depth of penetration of the AU waves. This would require distinctive analytical and numerical approaches to study the stochastic nature of the AU wave propagation.

REFERENCES

1. Vary A., The Acousto-Ultrasonic Approach, Acousto-Ultrasonics: Theory and Applications, Ed. J.C.Duke Jr., Plenum Press, New-york, 1988, pp.1-21.

2. Halmshaw R., Non-Destructive Testing, Second Edition, Edward Arnold, London, 1991

3. Hagemaier D., Fassbender R., 'Non-Destructive Testing of Adhesive Bonded Structures', SAMPE Quarterly, Vol.9, No.4, 1980, pp.36-58.

4. Alers G.A., Flynn P.L., and Buckley H.J., 'Ultrasonic Technique for measuring the Strength of Adhesive Bonds', Materials Evaluation, Vol.35, No.4, April 1977, pp.77-84.

5. Kline R.A., Hsiao C.P., and Fidaali M.A., 'Nondestructive Evaluation of Adhesively Bonded Joints', Journal of Engineering Materials and Technology, Vol.108, No.3, July 1986, pp.214-217.

6. Curtis G.J., 'Non-destructive Testing of Adhesively Bonded Structures with Acoustic Methods', Ultrasonic Testing, Ed., Szilard J., John Wiley and Sons Ltd., New York, 1982, pp.495-554.

7. Szilard J., 'Physical principles of Ultrasonic Testing', Ultrasonic Testing, Ed. Sizlard J., John Wiley and Sons, New York, 1982, pp.1-24.

8. Thompson D.O., Thompson R.B., Alers G.A., Non-Destructive Measurement of Adhesive Bond Strength in Honeycomb Panels, Materials Evaluation, Vol.32, No.4, April 1974, PP 81-85, pp.92.

9. Rokhlin S.I., 'Evaluation of the Curing of Structural Adhesives by Ultrasonic Interface Waves. Correlation with Strength', Journal of Composite Materials, Vol.17, No.1, January 1983, pp 15-25.

10. Kline R.A., and Hashemi D., 'Ultrasonic Guided - Wave Monitoring of Fatigue Damage Development in Bonded Joints', Materials Evaluation, Vol.45, No.9, Sept.1987, pp.1076-1082.

11. Chapman G.B.II, 'A Nondestructive method of Evaluating Adhesive Bond Strength in Fibreglass Reinforced Plastic Assemblies', Joining of Composite Materials ASTM STP 749, Ed. Kedward K.T., American Society for Testing and Materials, 1981, pp.32-60.

12. Schliekelmann R.J., 'Nondestructive Testing of Adhesively Bonded Joints', Adhesion Fundamentals and Practice, Gordon and Breach Science Publishers Inc., New York, 1969, pp.246-261.

13. Schliekelmann R.J., 'Nondestructive Testing of Adhesively bonded Metal-to-Metal Joints-2', Non-destructive Testing, Vol.5, No.3, June 1972, pp.142-153.

14. Highmore P.J., Szilard J. 'Resonance Methods', Ultrasonic Testing, Ed. Szilard J., John-Wiley & Sons Ltd., New York, 1982, pp.263-296.

15. Brown A.F., 'Ultrasonic Spectroscopy', Ultrasonic Testing, Ed. J.Szilard, John-Wiley & Sons Ltd., New York, 1982, pp.167-216.

16. KrautKramer J., and KrautKramer H., Ultrasonic Testing of Materials, 3rd Ed., Springer-Verlag, Berlin and New York, 1983.

17. Rose J.L., Meyer P.A., 'Ultrasonic Procedure for Predicting Adhesive Bond Strength', Materials Evaluation, Vol. 31., No.6, June 1973, pp.109-114.

18. Lloyd, E.A. and Wadhawani D.S., 'Ultrasonic Spectroscopy and the Detection of Hygrothermal Degradation in Adhesive Bonds', Adhesion 4, Ed. Allen K.W., Applied Science Publishers Ltd., London, 1980, pp.159-174.

19. James R. Matthews and Hay Robert D., 'Acoustic Emission Evaluation', Acoustic Emission, Volume 2, Nondestructive Testing Monographs and Tracts, Gordon and Breach Science Publishers, New York, Ed. James R. Matthews, 1983, pp.1-14.

20. Tektrend Inc., Mtl., Canada., ICEPAK™ Operating Manual, 1991.

21. Stahlkopt K., and Green A., 'Non-Destructive Pressure Vessel Testing by Acoustic Emission', EPRI Journal, Vol.1, No.1, 1976.

22. Bailey C.D., Freeman S.M., and Hamilton J.M., 'Acoustic Emission Monitor Damage Progression in Graphite Epoxy Composite Structure', Material Evaluation, Vol.58, No.8, Aug 1980.

23. Williams R.V., 'Acoustic Emission', Adam Hilger Ltd., Bristol, 1980, pp.71-86.

24. Evans A.G., Linzer M., 'Failure Prediction in Structural Ceramics Using Acoustic Emission', Journal of American Ceramic Society., Vol.56., pp.575-581, 1973.

25. Liptae R.G., 'Acoustic Emission from Composite materials', STP 497, ASTM, Philadelphia, 1972.

26. Tanary S., 'Characterization of Adhesively Bonded Joints Using Acousto-Ultrasonics, Masters Thesis, University Ottawa, Ottawa, Canada, April 1988.

27. Williams J.H. Jr. and Lampert N.R. Ultrasonic evaluation of Impact damaged Graphite

Fiber Composite, Material Evaluation, Vol-38, No.12, Dec.1980, pp.68-72.

28. Vary A., 'Acousto-Ultrasonic Characterization of Fiber Reinforced Composites', Materials Evaluation, Vol.40, No.6, May 1982, pp.650-662

29. Vary A. and Bowels K.J., 'An Ultrasonic Technique for Nondestructive Evaluation of Fibre Composite Quality', Polymer Engineering and Science, Vol.19, No.5, April 1979, pp.373-376.

30. Vary A. and Lark R.F., 'Correlation of Fibre Composite Tensile Strength with the Ultrasonic Stress Wave Factor', Journal of Testing and Evaluation, Vol.7, No.4, July 1979, pp.185-191.

31. Nayeb-Heshmi N., Cohen M.D., Zotos J., and Poormand R., 'Ultrasonic Characterization of Graphite/Epoxy Composite Material Subjected to Fatigue and Impacts', Journal of Nondestructive Evaluation, Vol.5, No.3/4, December 1986, pp 119-131.

32. Dos Reis H.L.M. and McFarland D.M., 'On the Acousto-Ultrasonic Evaluation of Wire Rope Using the Stress Wave Factor Technique', British Journal of Nondestructive Testing, Vol.28, No.3, May 1896, pp.155-156.

33. Williams J.H.Jr., Hainsworth, J, and Lee S.S., 'Acousto-Ultrasonic Nondestructive Evaluation of Double Braided Nylon Ropes Using the Stress Wave Factor', Fibre Science and Technology, Vol.21, No.3, 1984, pp.169-180.

34. Dos Reis H.L.M. and McFarland D.M., 'On the Acousto-Ultrasonic Characterization of Wood Fiber Hardboard', Journal of Acoustic Emission, Vol.5, No.2, April-June 1986, pp.67-70

35. Phani K.K, Niyogi S.K., Maitra A.K., and Roychaudhury M., 'Strength and Elastic Modulus of a Porus Brittle Solid: An Acousto -Ultrasonic Study', Journal of Material Science, Vol.21, No.12, Dec.1986, pp.4335-4341.

36. Vary A., 'The Acousto-Ultrasonic Approach', NASA Technical memorandum 89843, April 1987.

37. Tanary S., Haddad Y.M., Fahr A., and Lee, S. Nondestructive Evaluation of Adhesively Bonded Joints in Graphite/Epoxy Composites Using Acousto-Ultrasonics, J. of Pressure Vessel Technology, Dec 1992, pp.344-352.

38. Vary A., 'Concepts and Techniques for Ultrasonic Evaluation of Material and Mechanical Properties', Stinchcomb W.W. (ed.), Mechanics of Non-Destructive Testing, Plenum Press, New York, 1980, pp.123-141.

39. Tektrend Inc., Mtl., Canada., ARIUS™ Operating Manual, 1991.

40. Finkel J., 'Computer Aided Experimentation - Interfacing to Mini computers', John Wiley and Sons, New York, 1975.

41. Vary A., Acousto-Ultrasonics, Nondestructive Testing of FRP Composites, Vol-2, ED. John Summerscales, Elsevier Applied Science, 1990, pp.1-54.

42. Henneke II, E.G., et.al., 'A Study of the Stress Wave Factor Technique for the Characterization of Composite Materials', NASA Contractor Report 3670, February 1983.

43. Karagülle H., Williams J.H., and Lee S.S., Application of Homomorphic Signal Processing to Stress Wave Factor Analysis, Materials Evaluation, 1985, 43(1), pp.1446-1454.

44. Tou J.T and Gonzalez R.C., Pattern Recognition Principles, Addison Wesley, Massachusets, 1974.

45. Fukunga, Introduction to Statistical Pattern Recognition, Academic Press., 1972.

46. Hay D.R., Chan R.W.Y, Siddiqui K., Hay J.R., Theory of Operations and Background, Artificial Intelligence, Tektrend International Inc., Mtl., Canada.

47. Meisel W.S., Computer Oriented Approaches to Pattern Recognition, Mathematics in Science and Engineering, Academic Press, 1972.

48. Fu K.S., Introduction, Digital Pattern Recognition, Ed. Fu K.S., 1980, pp.1-44.

49. James H., Williams Jr., Samsar S. Lee., 'Pattern Recognition Characterization of Micromechanical and Morphological Material States Via Analytical Quantitative Ultrasonics', Material Analysis by Ultrasonics - Metals, Ceramics, Composites, Ed., Vary, A., 1987.

50. Andrews H.C., Introduction to Mathematical Techniques in Pattern Recognition, Wiley-Interscience, John Wiley and Sons Inc., New York, 1972.

51. Duda R.O. and Hart P.E., Pattern Classification and scene analysis, Wiley, New York, 1973.

52. Chen C.H., Statistical Pattern Recognition, Hayden Book Co., Washington D.C., 1973.

53. Haddad Y.M., 'On the Theory of Viscoelastic Solid', Res Mechanica, 25, 1988, pp.225-259.

54. Christensen R.M, 'Theory of Viscoelasticity, Academic Press, New york, 1971

55. George E. Mase, 'Schaum's Outline of Theory and Problems of Continuum Mechanics', Mcgraw Hill, New york, 1970.

56. Ferry J.D., Viscoelastic Properties of Polymers, 2nd Edn., Wiley, New York, 1970.

57. Ward I.M., Mechanical Properties of Solid Polymers, 2nd Edn., John-Wiley & Sons, 1983.

58. Alfrey T., Mechanical Behaviour of High Polymers, Interscience Publishers, New York, 1948.

59. William M.L., Landel R.F., and Ferry J.D., 'The Temperature Dependence of Relaxation Mechanisms in Amorphous Polymers and Other Glass-forming Liquids', Journal of American Chemical Society, Vol.77, 1955, pp.3701-3707.

60. Mercier J.P., Alkonis J.J., Litt.M., Tobolsky A.V., 'Viscoelastic Behavior of the polycarbonate of Bisphenol A Journal of Applied Polymer Science, Vol.9, 1965, pp.447-459.

61. Pericles S. Theocaris, Viscoelastic properties of Epoxy Resins Derived from Creep and Relaxation Tests at Different Temperatures, Rheologica Acta, Band 2, Heft 2, 1965.

62. Schwarzl F. and Staverman A.J., Time-Temperature dependence of Linear Viscoelastic Behaviour, Journal of Applied Physics, Vol. 238, 1952, pp.839-841.

63. Kolsky H., 'The Propagation of Stress waves in Viscoelastic Solids', Applied Mechanics Review, Vol.11, No.9, 1958, pp.465-467.

64. Kolsky H., International Symposium on Stress Wave Propagation in Materials, Interscience Publishers, New York, 1960.

65. Kolsky H., Structural Mechanics, Pergamon Press, Oxford, 1960.

66. Gross B., Mathematical Structure of the Theories of Viscoelasticity, Hermann, Paris, 1953.

67. Nadai A., Theory of Flow and Fracture of Solids, Mcgraw-Hill, New York, 1950

68. Ogorkiewicz R.M. (Ed.), 'Engineering Properties of Thermoplastics', Wiley-Inter Science, London, 1970.

69. Rosen B. (Ed.), Fracture Process in Polymeric Solids, Wiley-Inter Science, 1964.

70. Thomas A.G., 'Rupture of Rubber V. Cut Growth in Natural Rubber Vulcanizates', Journal of Polymer Science, Vol.31, 1958, pp.467-480.

71. Lake G.J., and Thomas A.G., 'The strength of Highly Elastic Materials', Proc. Roy. Soc. A., Vol.300, 1967, pp.108-119.

72. Rivlin R.S., and Thomas A.G., 'Rupture of Rubber. I. Characteristic Energy for Tearing', Journal of Polymer Science, Vol.10, 1953, pp.291-318.

73. Rodriguez F., Principles of Polymer Systems, McGraw-Hill, New York, 1970.

74. Hertzberg R.W., Deformation and Fracture Mechanics of Engineering Materials, Wiley-Inter Science, New York, 1976.

75. Ewalds H.L., Wanhill R.J.H., Fracture Mechanics, Edward Arnald Ltd., Baltimore, U.S.A., 1983.

76. Williams J.G., Stress Analysis of Polymers, 2nd Edn., Ellis Horwood, Chichester, 1980.

77. Hertzberg R.W., and Manson J.A. Fatigue of Engineering Plastics, 'Academic Press', New York, 1980.

78. Pitman G.L., and Ward I.M., 'The Molecular Weight Dependence of Fatigue Crack Propagation in Polycarbonate', Journal of Material Science, Vol.15, 1980, pp.635-645.

79. Williams J.G., 'A Model of Fatigue Crack Growth in Polymers', Journal of Material Science, Vol.12, 1977, pp.2525-2533.

80. Vary A., 'Acousto-Ultrasonics - An Update', 'Acoustic Emission: Current Practice and Future Directions', ASTM STP 1077, Sachse W., Roget J., Yamaguchi K. (Eds.), American Society for Testing and Materials, Philadelphia, 1991.

81. Talreja R., Govada A., and Henneke II, 'Quantitative Assesment of Damage-Growth in Graphite/Epoxy Laminates by Acousto-Ultrasonic Measurements, Thompson D.O. and Chimenti D. (eds.), Review of Progress in Quantitative Non-Destructive Evaluation, Plenum Press, New York, 1984, pp.1099-1106.

82. Dos Reis H.L.M. and Kautz H.E., 'Non-Destructive Evaluation of Adhesive Bond Strength Using the Stress Wave Factor Technique', Journal of Acoustic Emission, Vol.5, No.4, Oct-Dec 1986, pp.144-147.

83. Green J.E. and Rodgers J., 'Acousto-Ultrasonic Evaluation of Impact-Damaged Graphite Epoxy Composites', 27th National SAMPE Symposium, May 4-6 1982, pp.428-439.

84. Hemann J.H. and Baaklini G.Y., The Effect of Stresses on Ultrasonic Pulses in Fiber Reinforced Composites, SAMPE, Vol.22, No.4, July-Aug.1986, pp.9-13.

85. Wang T.T., Ryan F.W., and Schonhorn H., 'Effect of Bonding Defects on Shear Strength in Tension of Lap Joints Having Brittle Adhesives', J. Applied Polymer Sci., Vol.16, No.8, Aug.1972, pp.1901-1909.

86. Srivastava V.K. and Prakash R., 'Prediction of Material Property Parameter of FRP Composites using Ultrasonic and Acousto-Ultrasonic Technique', Composite Structures, 1987, Vol.8, pp.311-321.

87. Russell-Floyd R. and Phillips M.G., 'A Critical Assessment of Acousto-Ultrasonics as a Method of Nondestructive Examination for Carbon-Fibre-Reinforced Thermoplastic Laminates' NDT International, Vol.21, No.4, 1988, pp.247-257.

APPENDIX A

Specification* for the materials used in the experiment

Material property	Polycarbonate (PC)	Polyvinylchloride (PVC)
Specific gravity	1.2	1.35-1.45
Tensile strength at yield (p.s.i)	8000 - 9500	5000 - 9000
Modulus of elasticity in tension x 10^5 p.s.i	3.2	3.5 - 6.0
Compressive strength (p.s.i)	11000	8000 - 13000
Flexural strength (p.s.i)	11000 -13000	10000 - 16000
Effect of sunlight	Slight colour change	Darkens on prolonged and intense exposure
Clarity	Transparent	Opaque

* Material specifications were provided by the supplier, Cadillac Plastic (Canada) Limited, Ottawa, Canada.

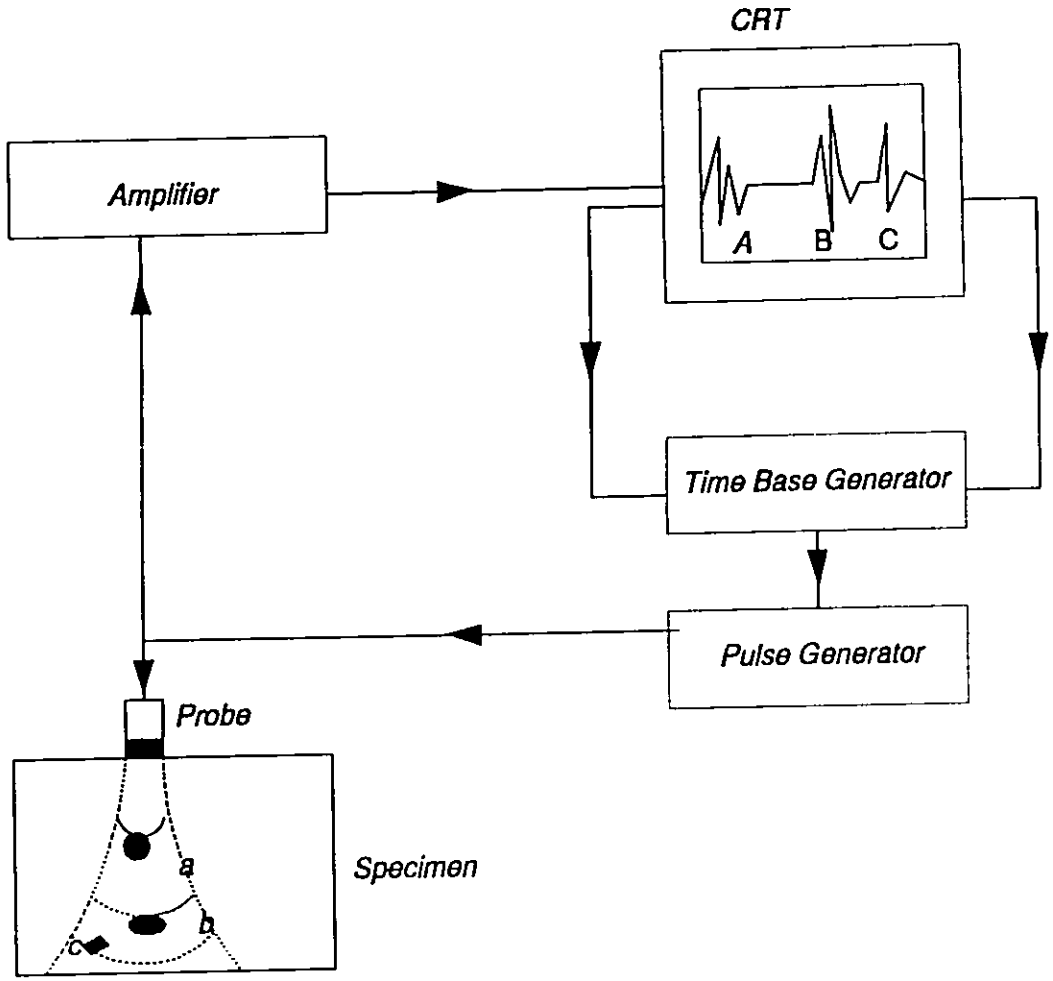

2.1 Ultrasonic pulse echo technique.

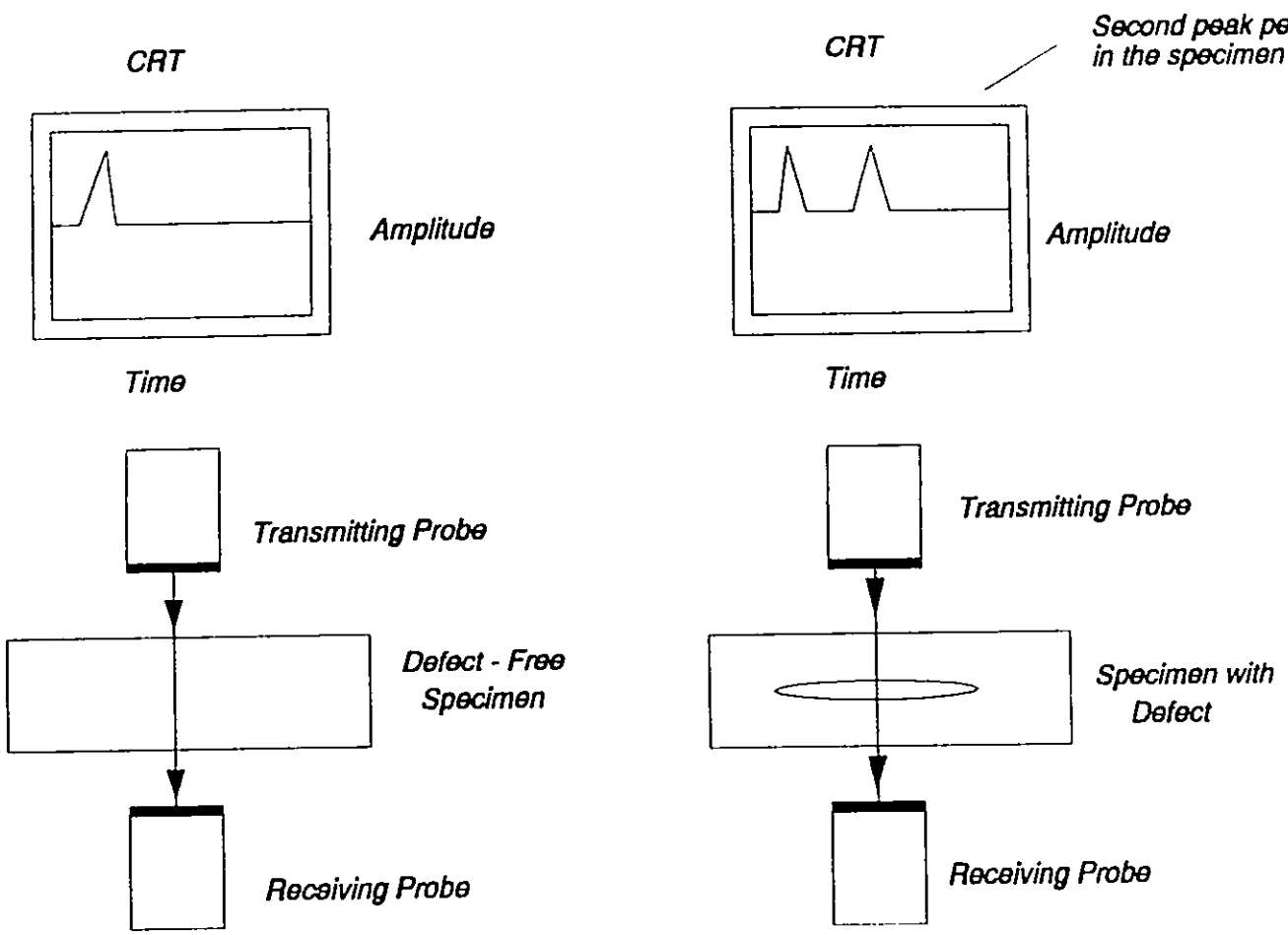

2.2 Ultrasonic through transmission technique.

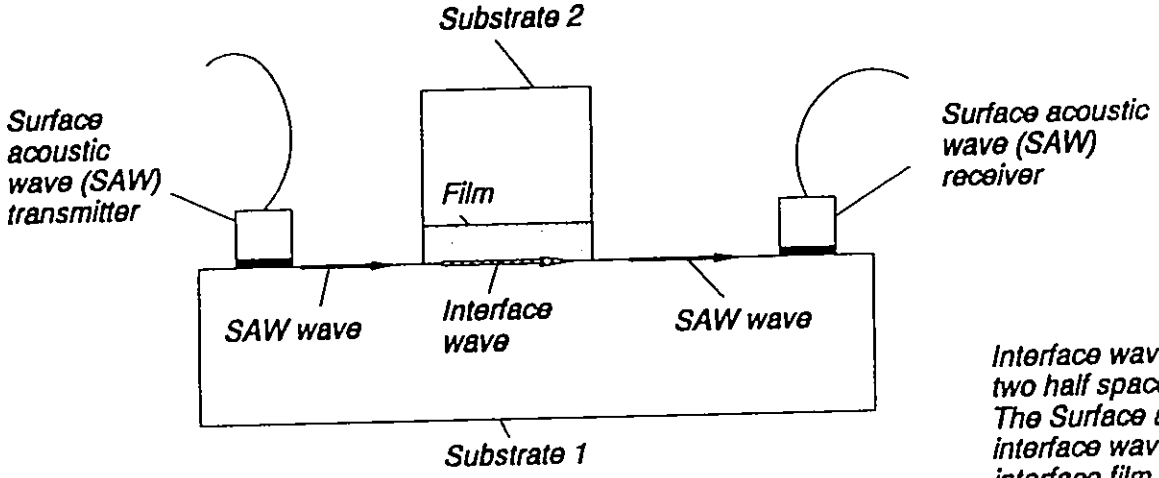

Interface waves were generated in a system of two half spaces seperated by a film of adhesive; The Surface acoustic wave (SAW) generates interface waves when passing through the interface film between the substrates 1 and 2.

2.3 Interface and plate waves technique.

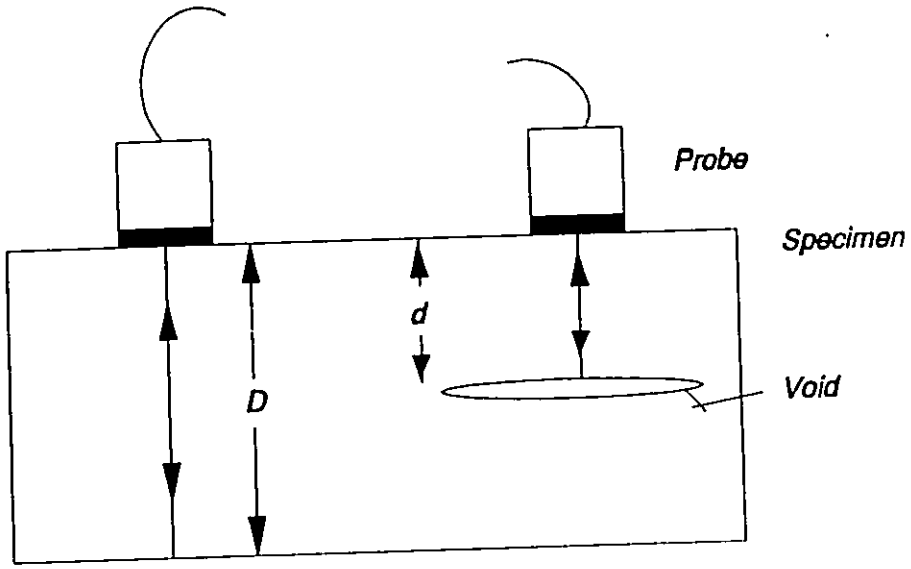

2.4 Ultrasonic resonance technique.

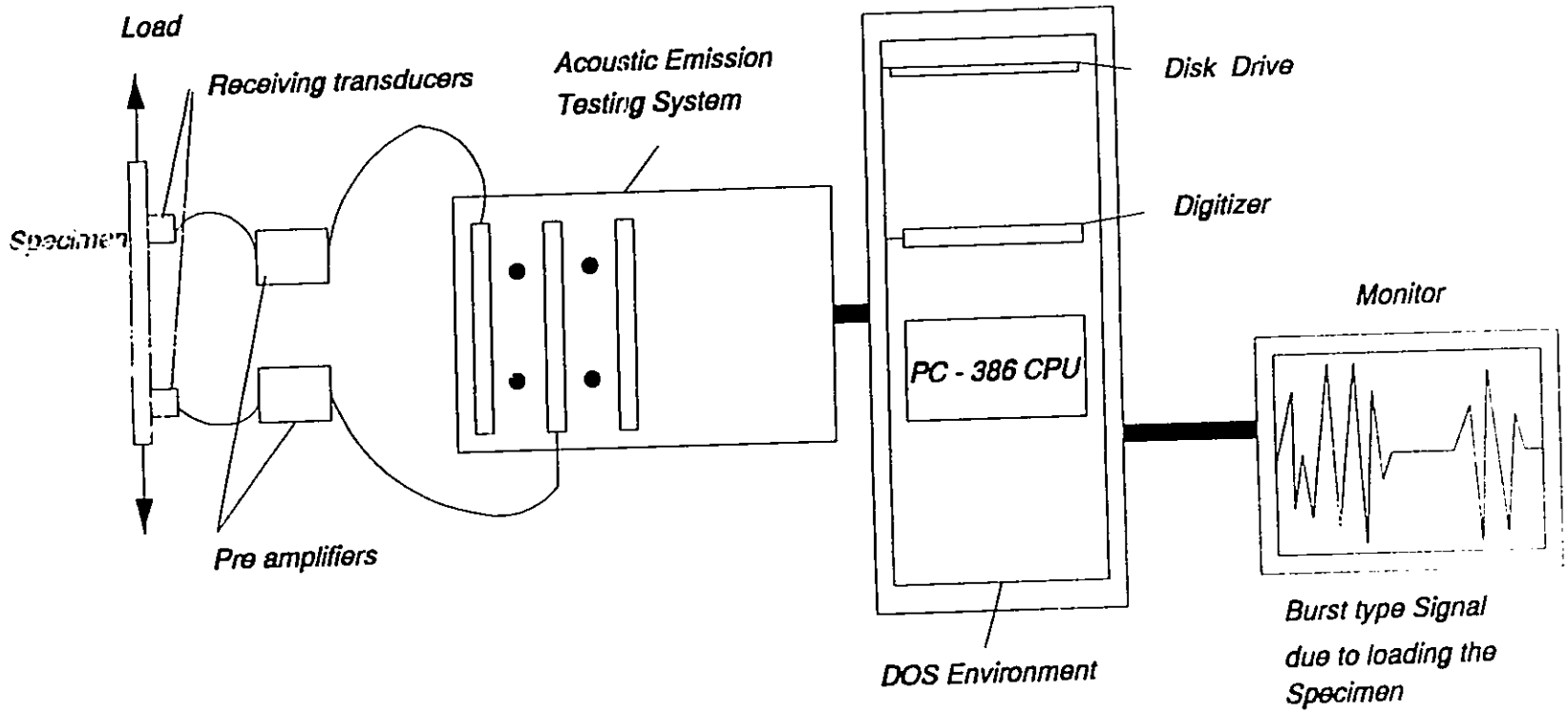

2.5 Acoustic emission testing system.

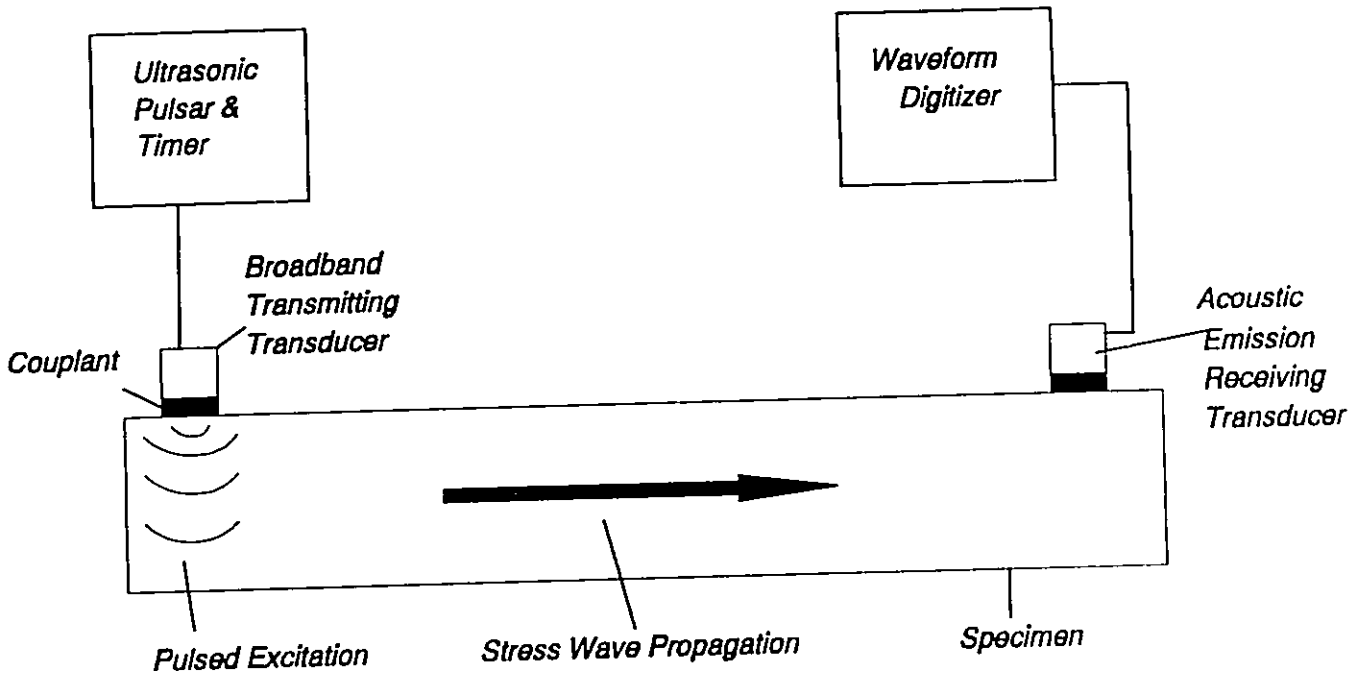

2.6 A schematic diagram of the acousto-ultrasonic test set-up.

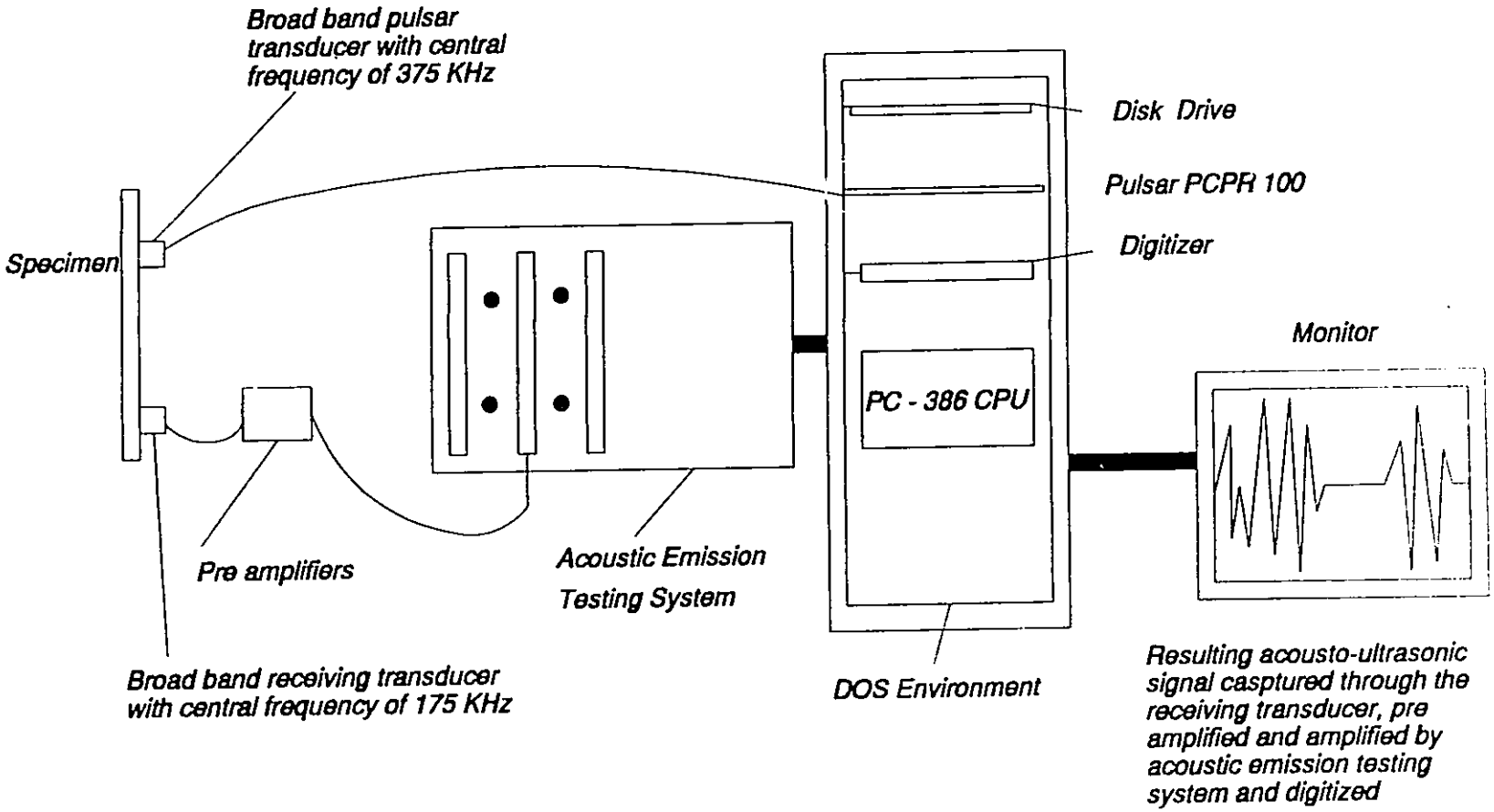

2.7 Acousto-ultrasonic set-up.

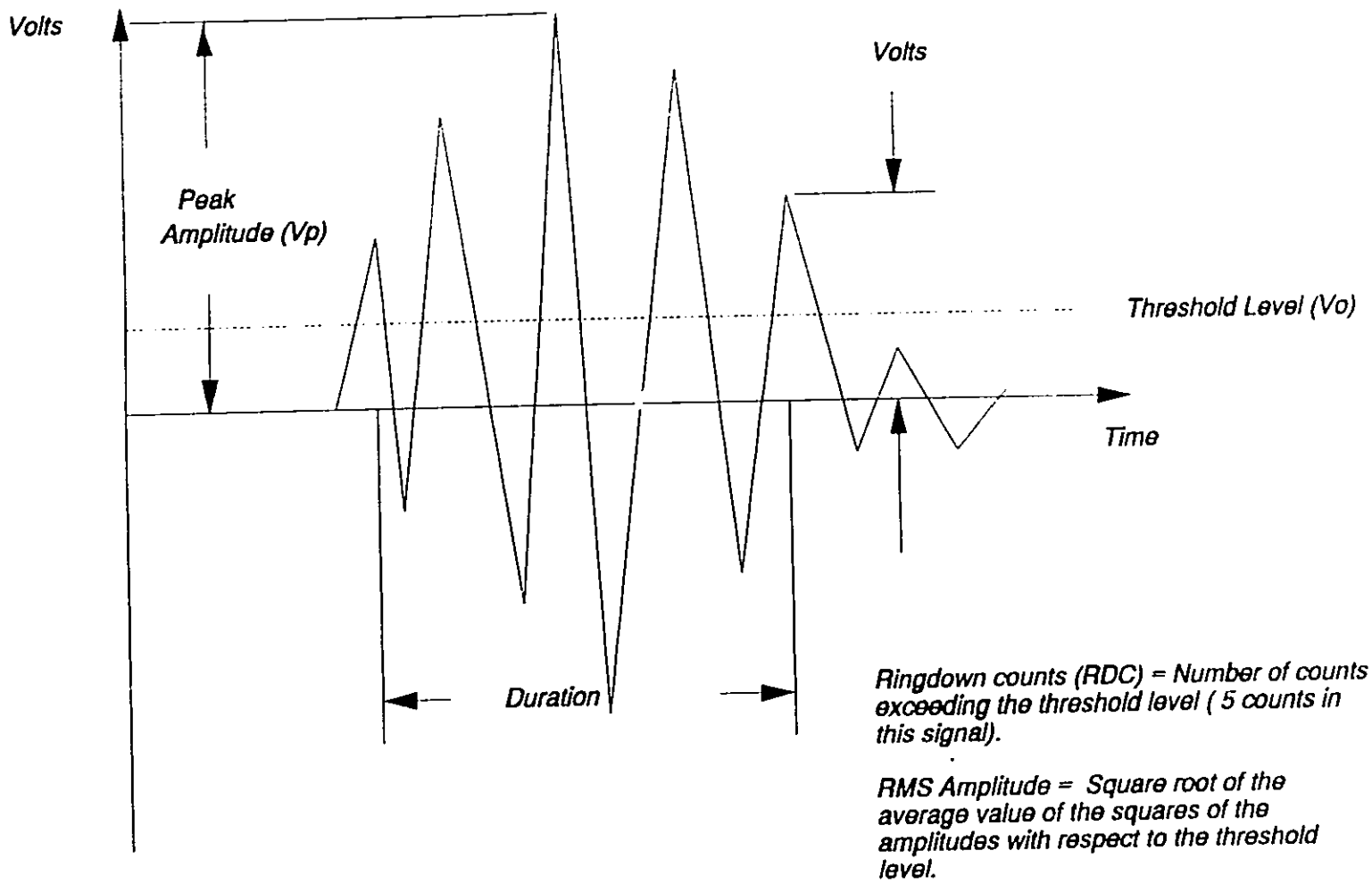

2.8 Measurement of acousto-ultrasonic waveform parameters.

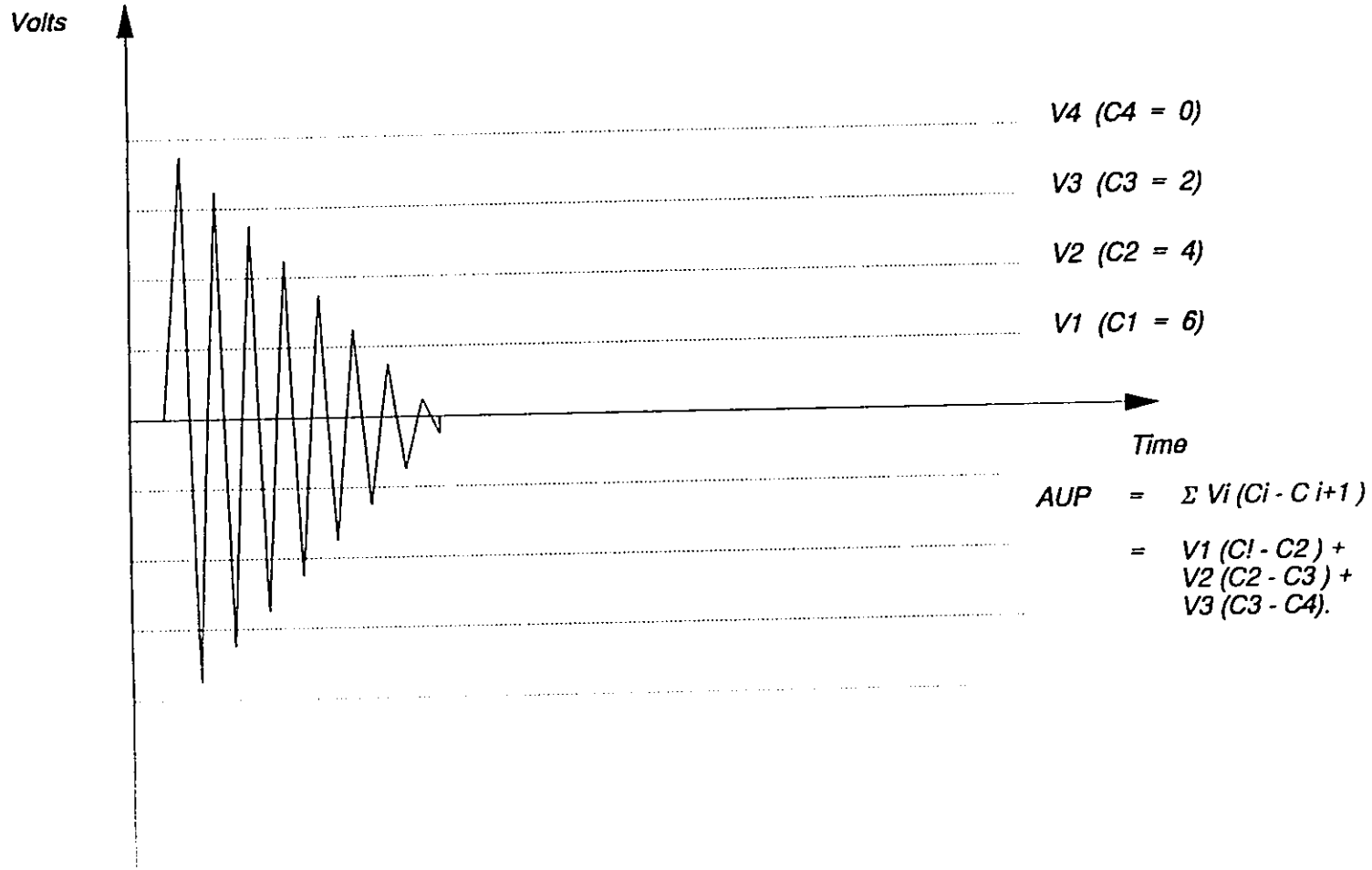

2.9 Calculation of acousto-ultrasonic parameter (AUP) [26,37].

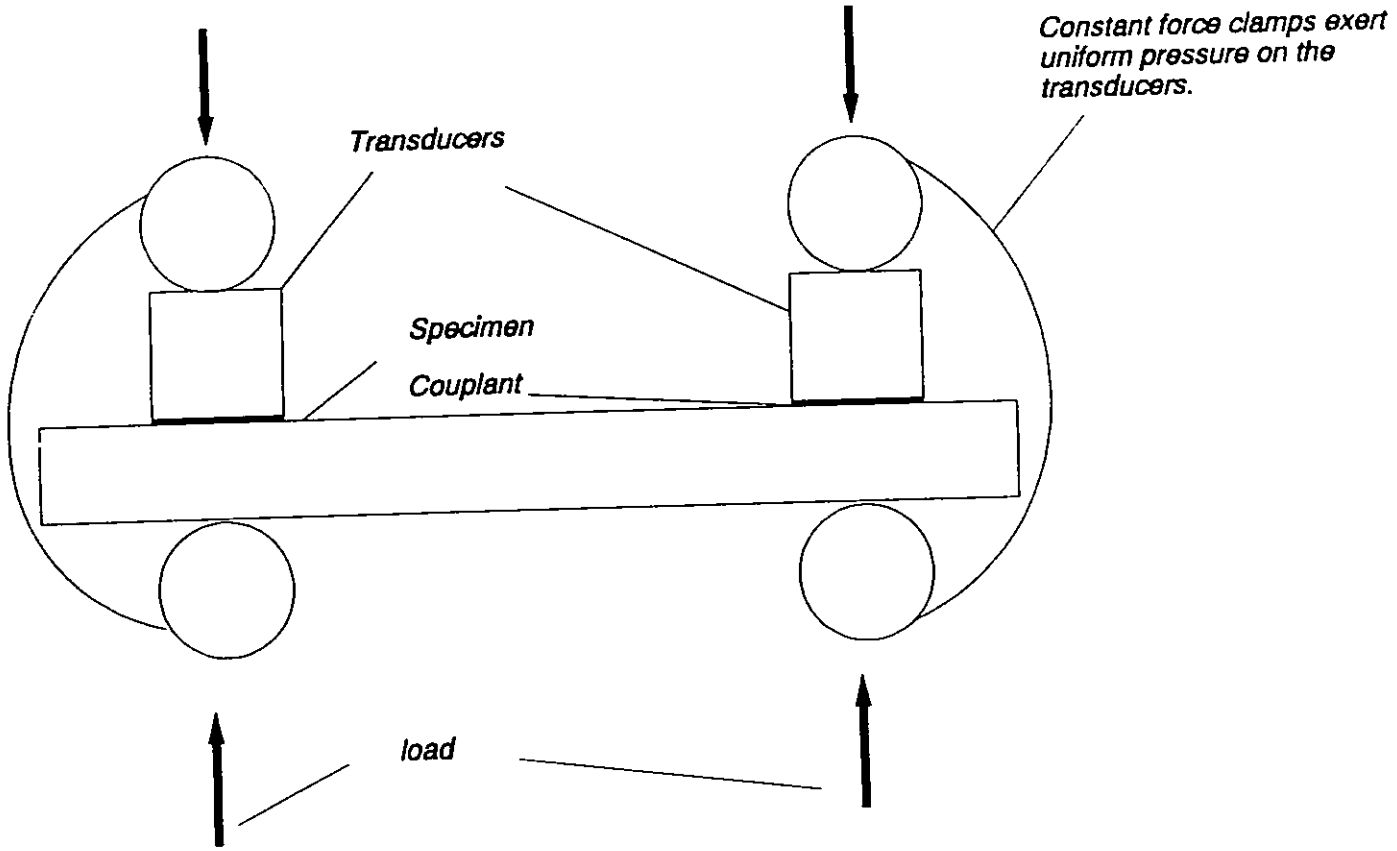

2.10 Illustration of constant force clamps for acousto-ultrasonic set-up.

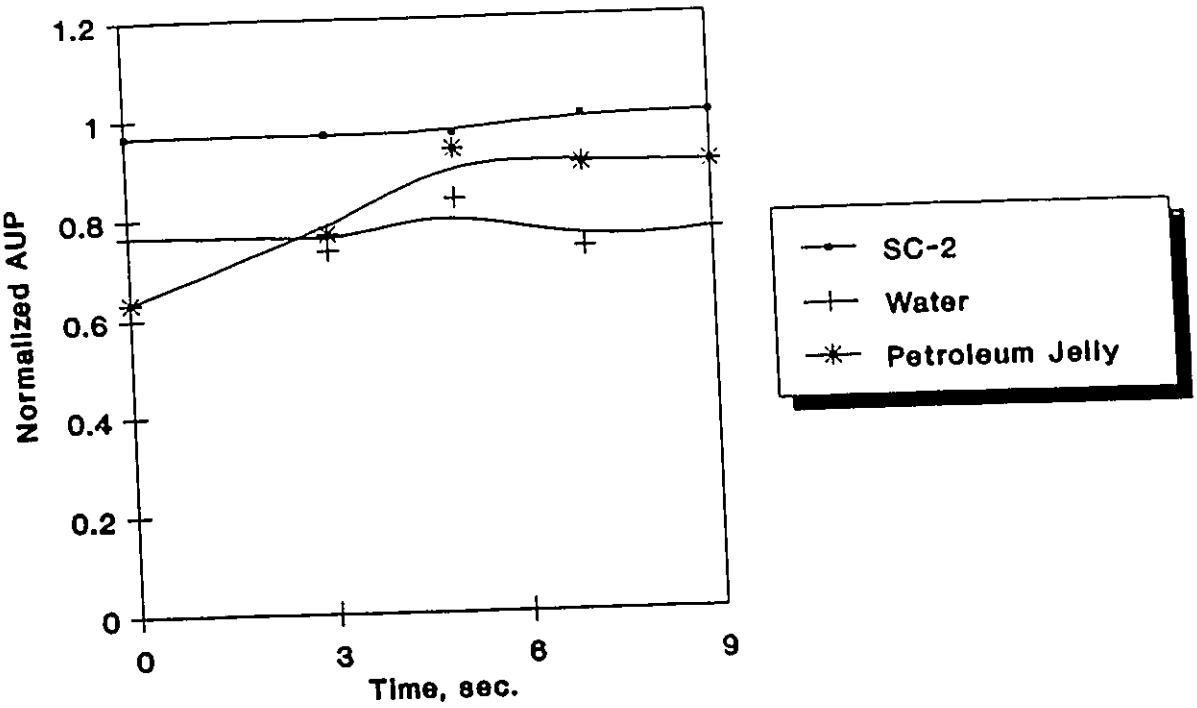

2.11 Variation of acousto-ultrasonic parameter (AUP) with the change in the coupling medium between transducers and the specimen.

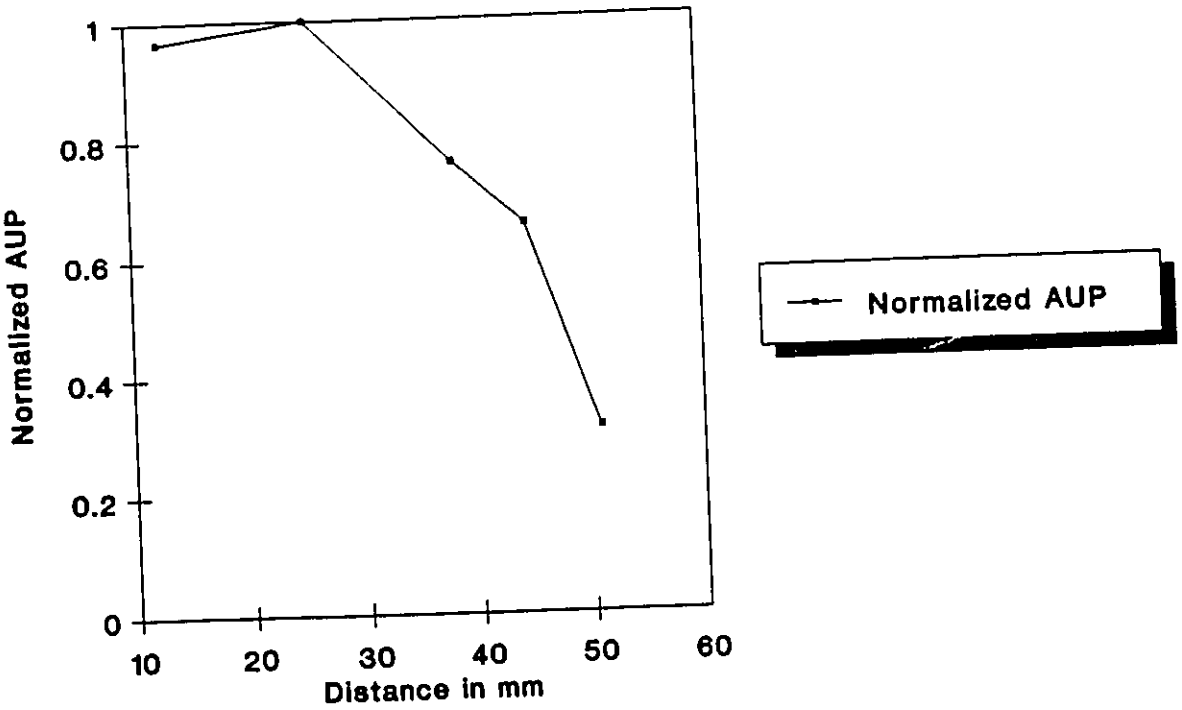

2 12 Variation of AUP with inter-transducer distance.

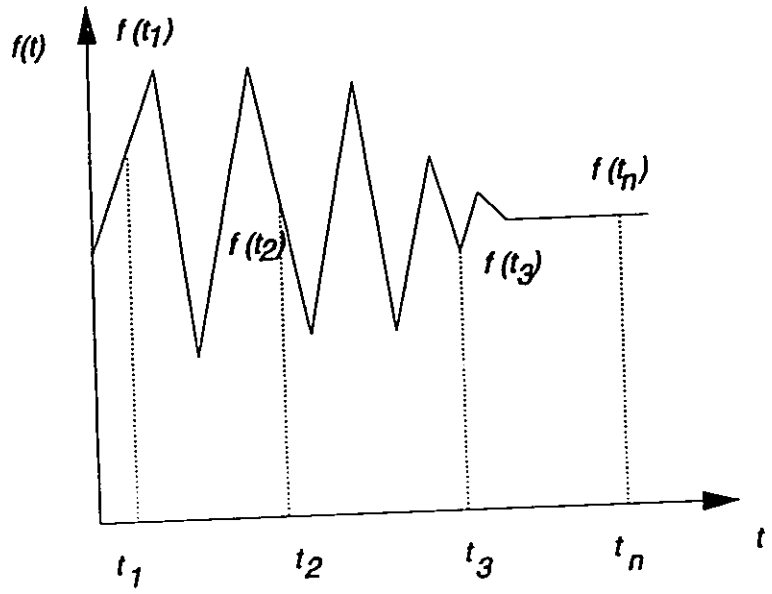

$$X = \begin{bmatrix} x_1 \\ x_2 \\ \vdots \\ x_n \end{bmatrix} \qquad x_i = f(t_i)$$

3.1 ***A sample of the received acousto-ultrasonic signal as the raw data vector for pattern classification.***

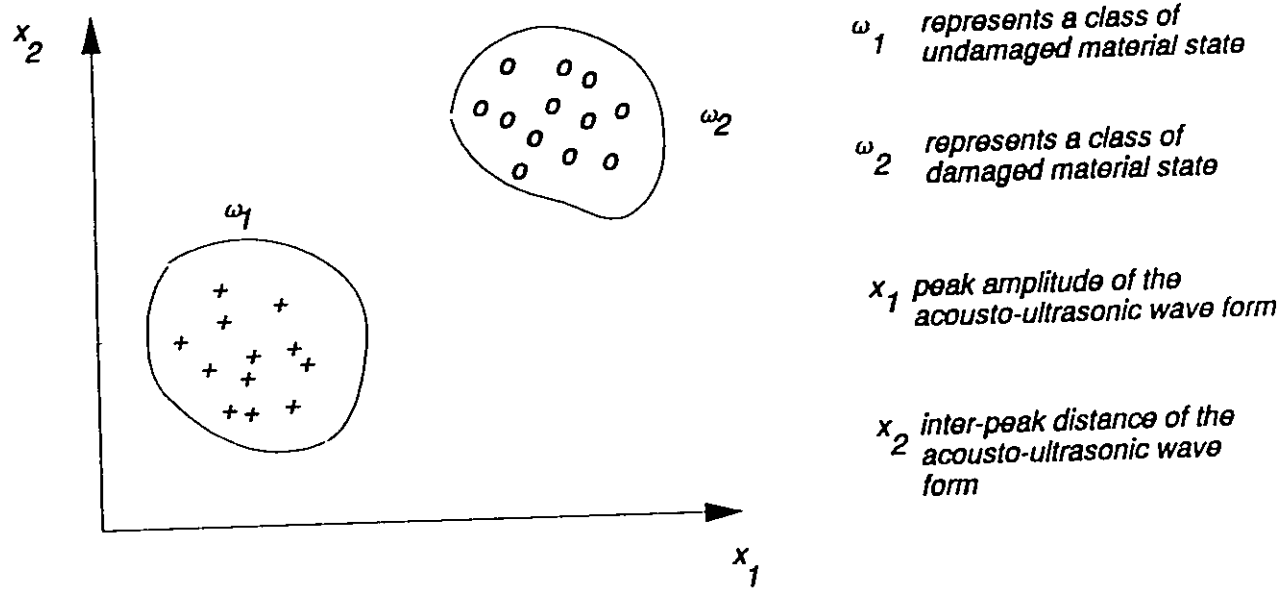

3.2 Two disjoint pattern classes.

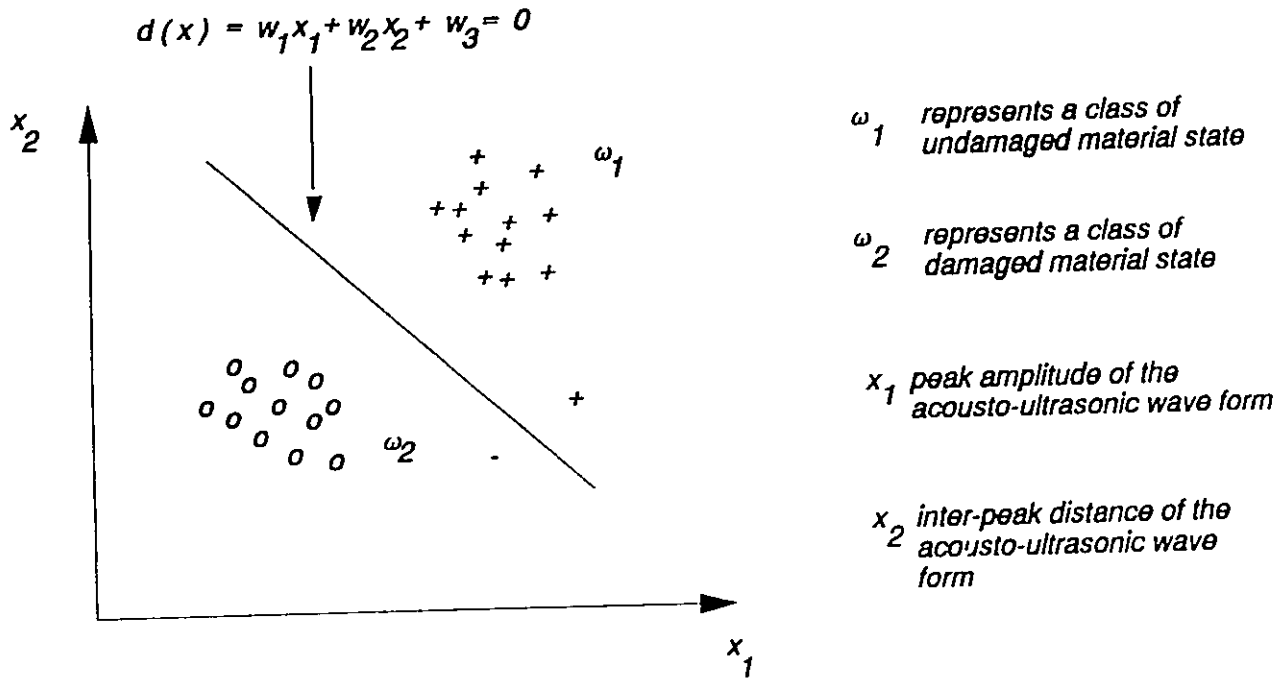

3.3 A simple decision function for two pattern classes.

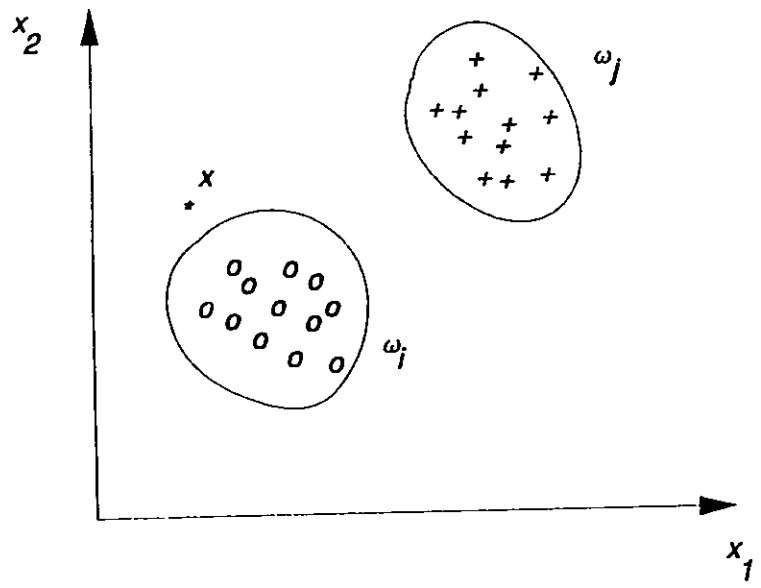

x_1 *peak amplitude of the acousto-ultrasonic wave form*

x_2 *inter-peak distance of the acousto-ultrasonic wave form*

3.4a Patterns classifiable by proximity concept.

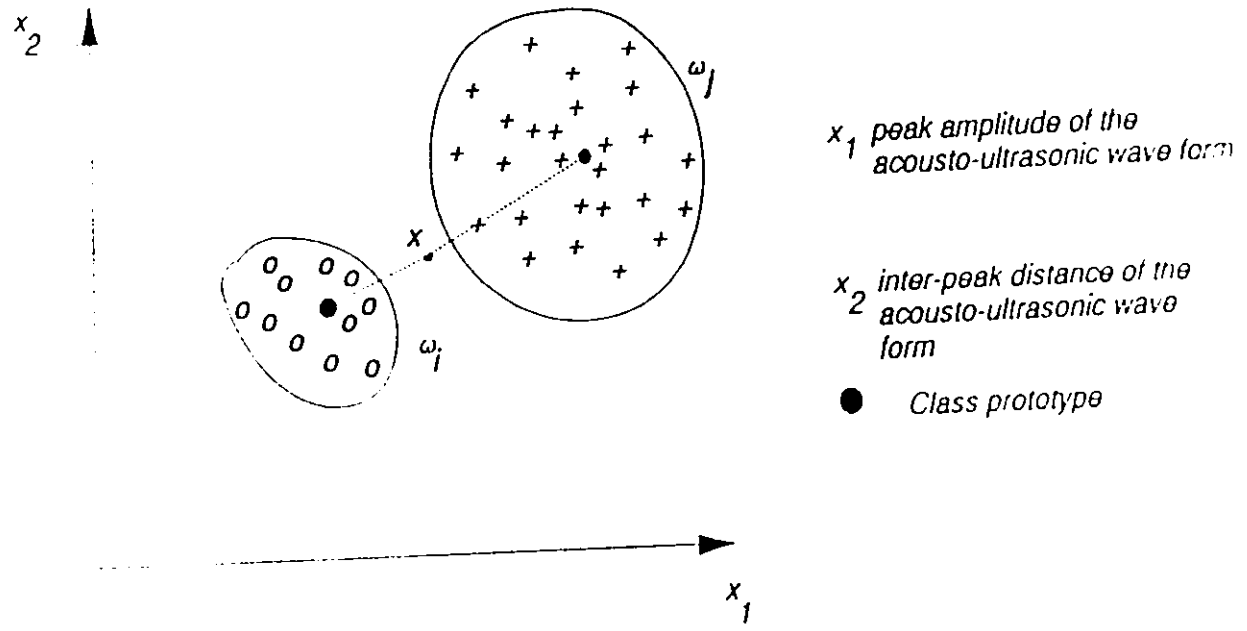

3.45 Minimum distance classifier applied to classes with varying sizes

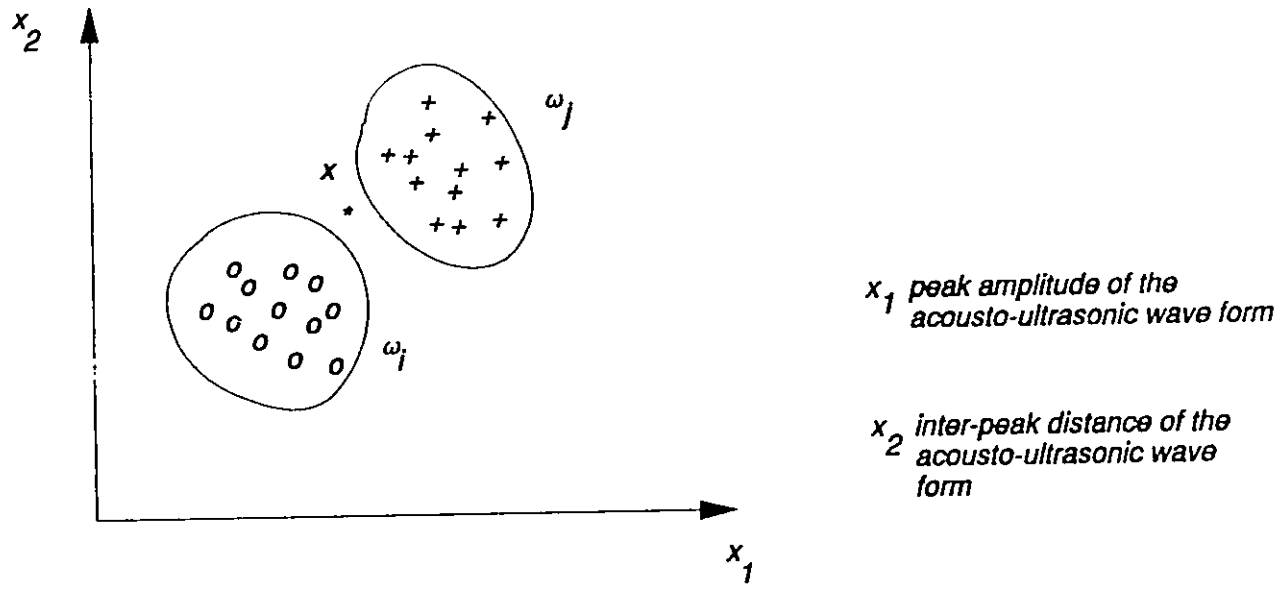

3.5 Patterns not easily classifiable by proximity concept

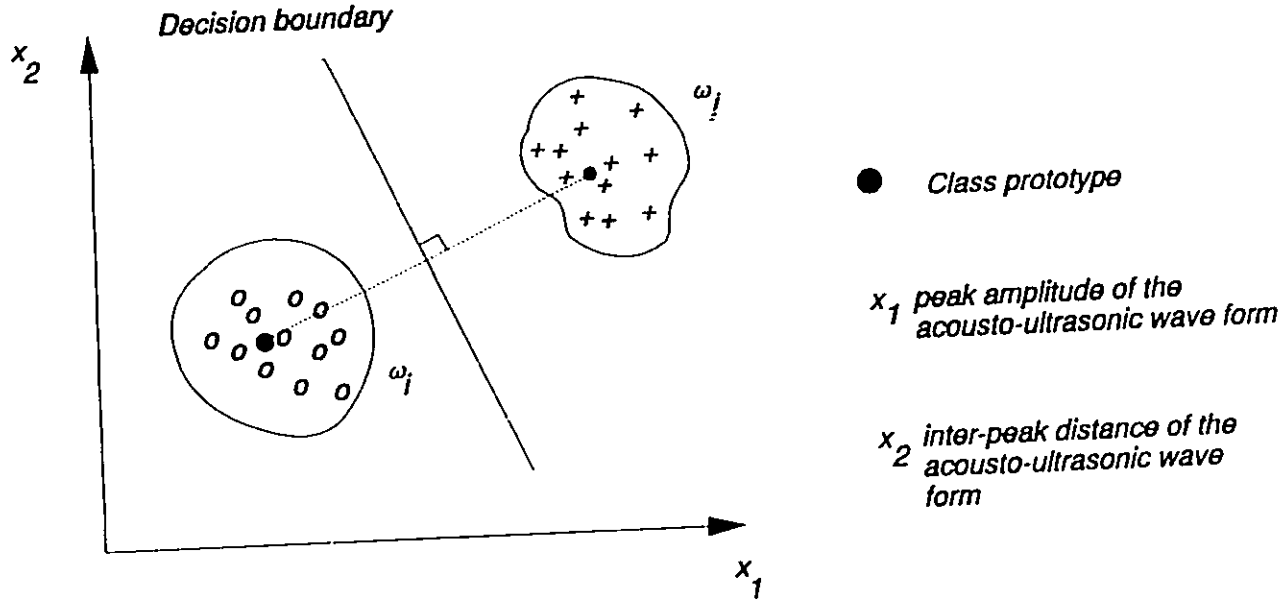

3.6 ***Decision boundary of two classes characterized by minimum distance classification approach.***

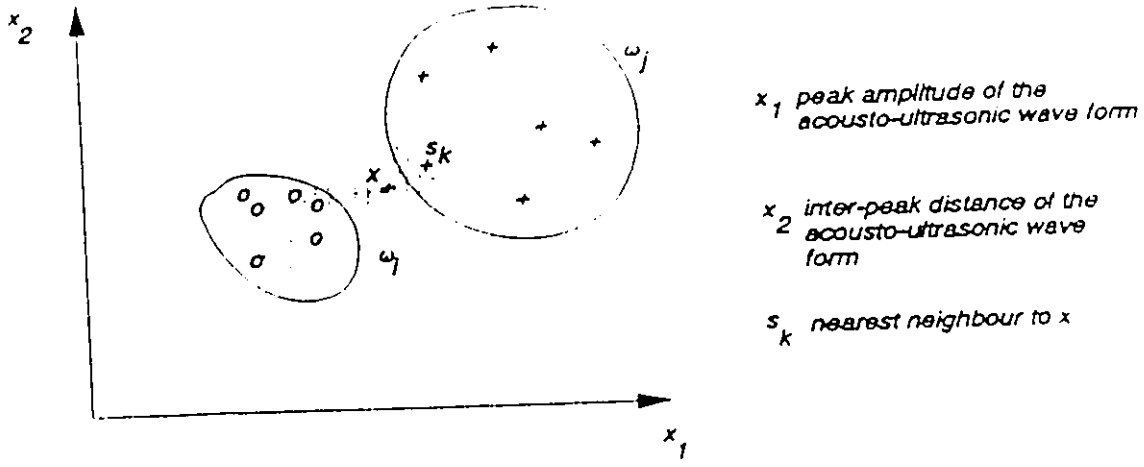

3.7 Nearest Neighbour classifier

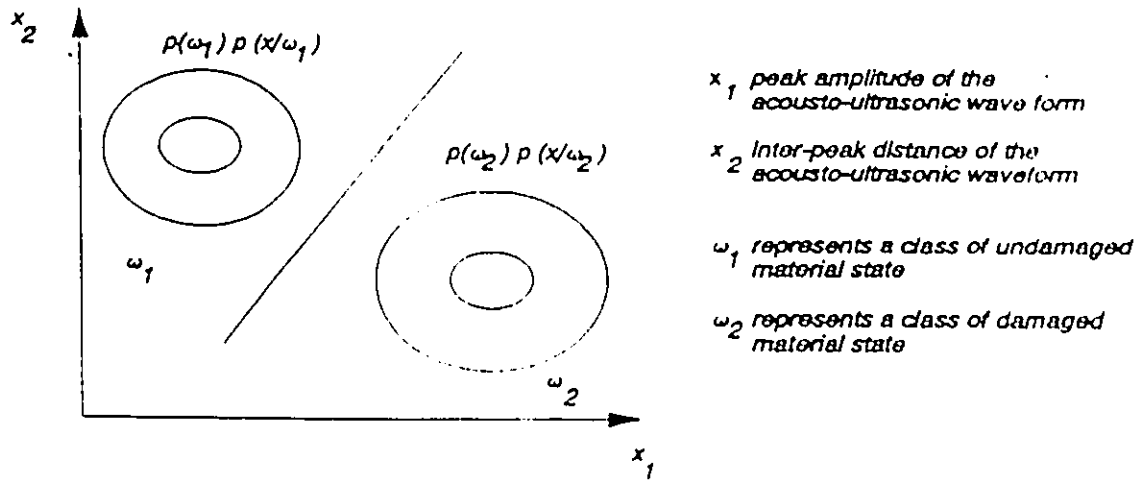

3.8 Empirical Bayesian classifier.

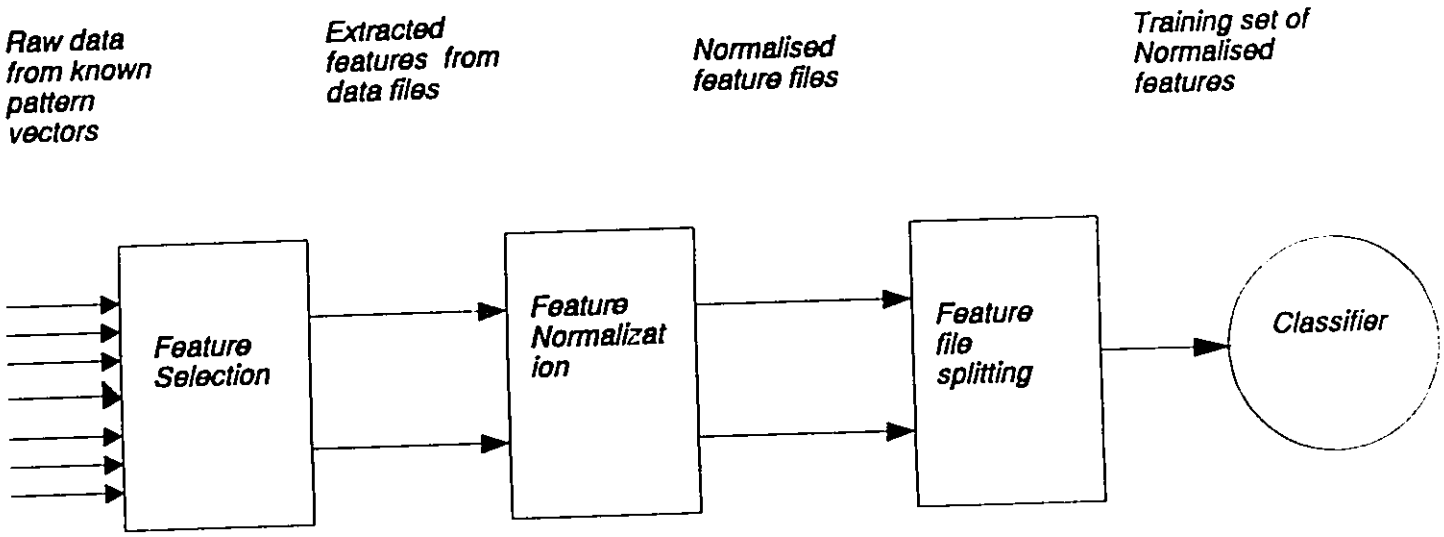

3 9 ***Schematic illustration of the training processes in a pattern classifier using normalized feature values.***

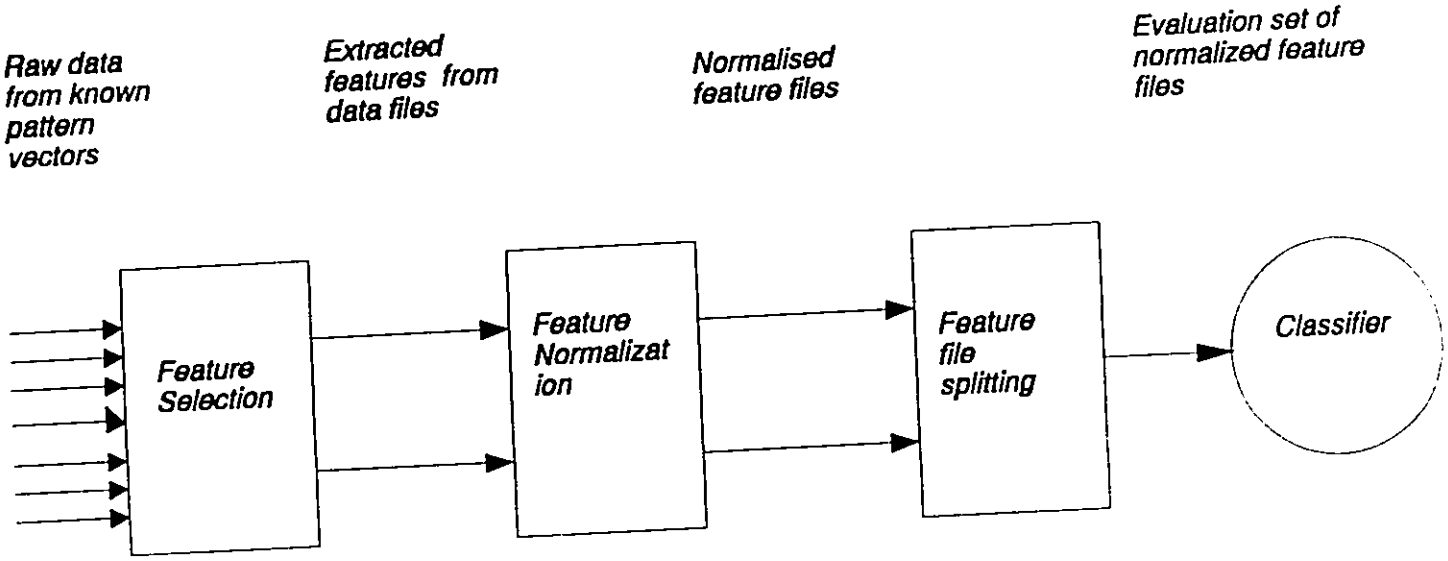

3 10 *Schematic illustration of the evaluation process in a pattern classifier using normalized feature values.*

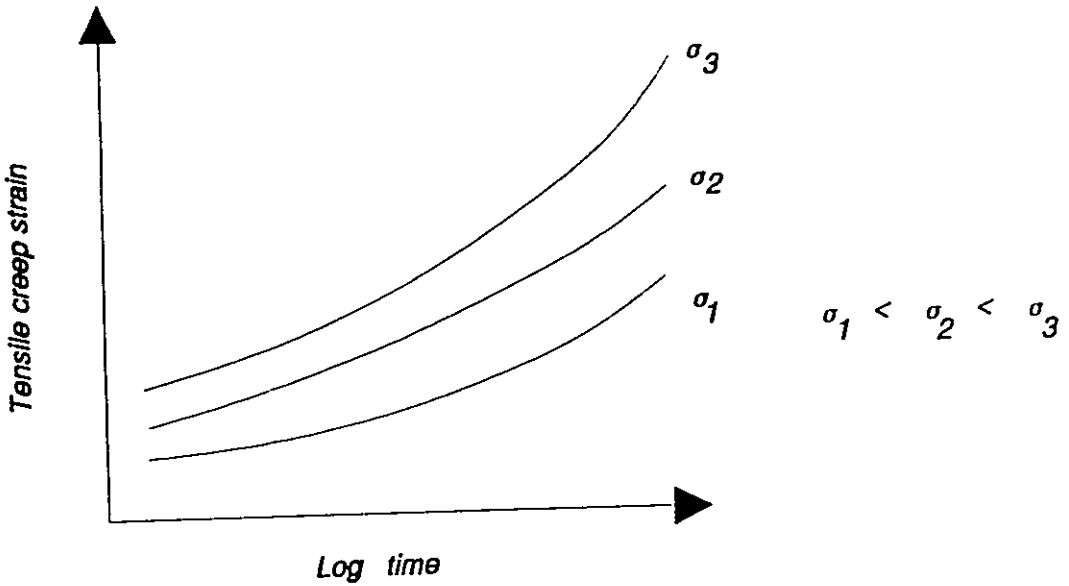

4.1 Creep curves.

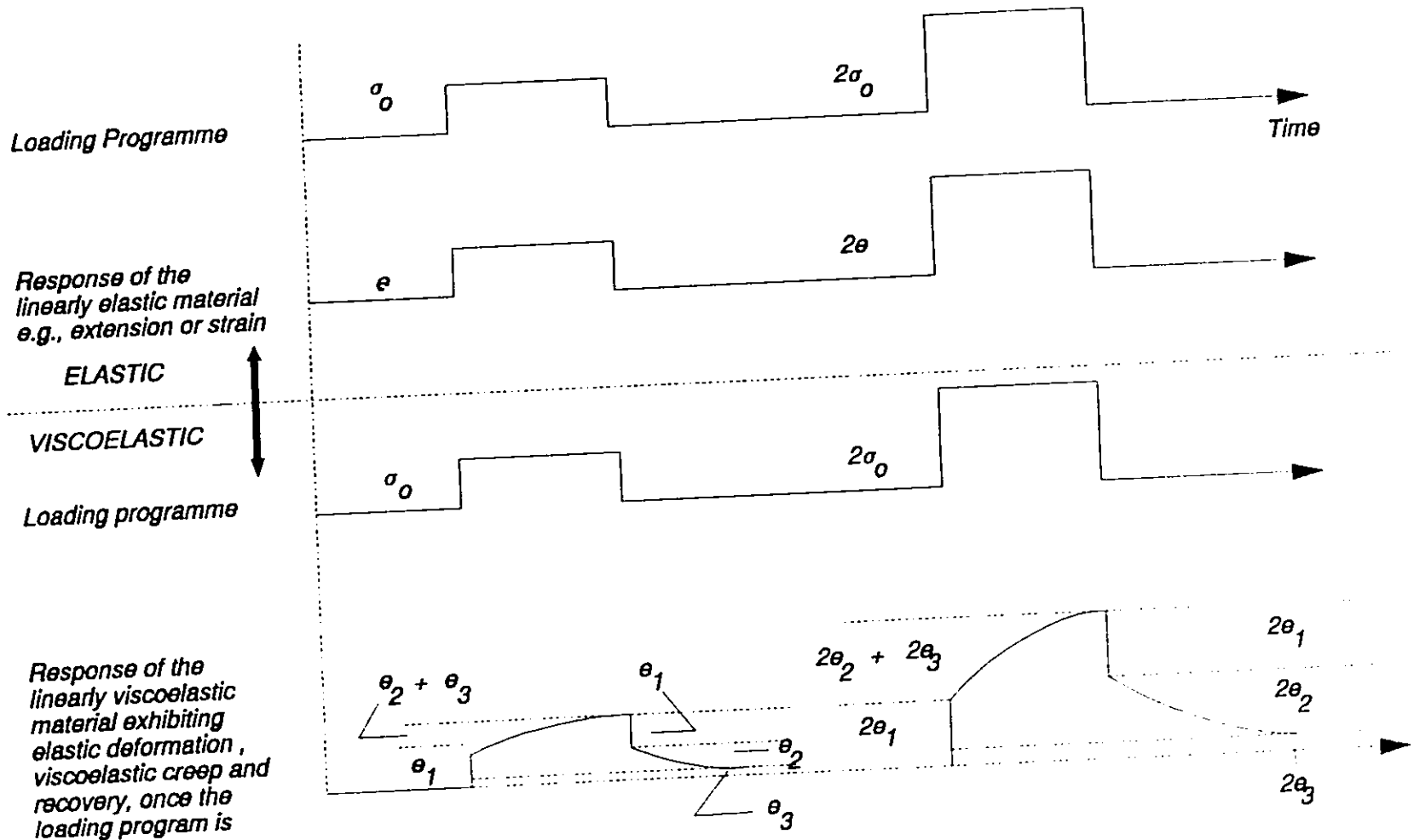

4.2 Comparison between a linearly elastic and linearly viscoelastic material response for the same type of loading program.

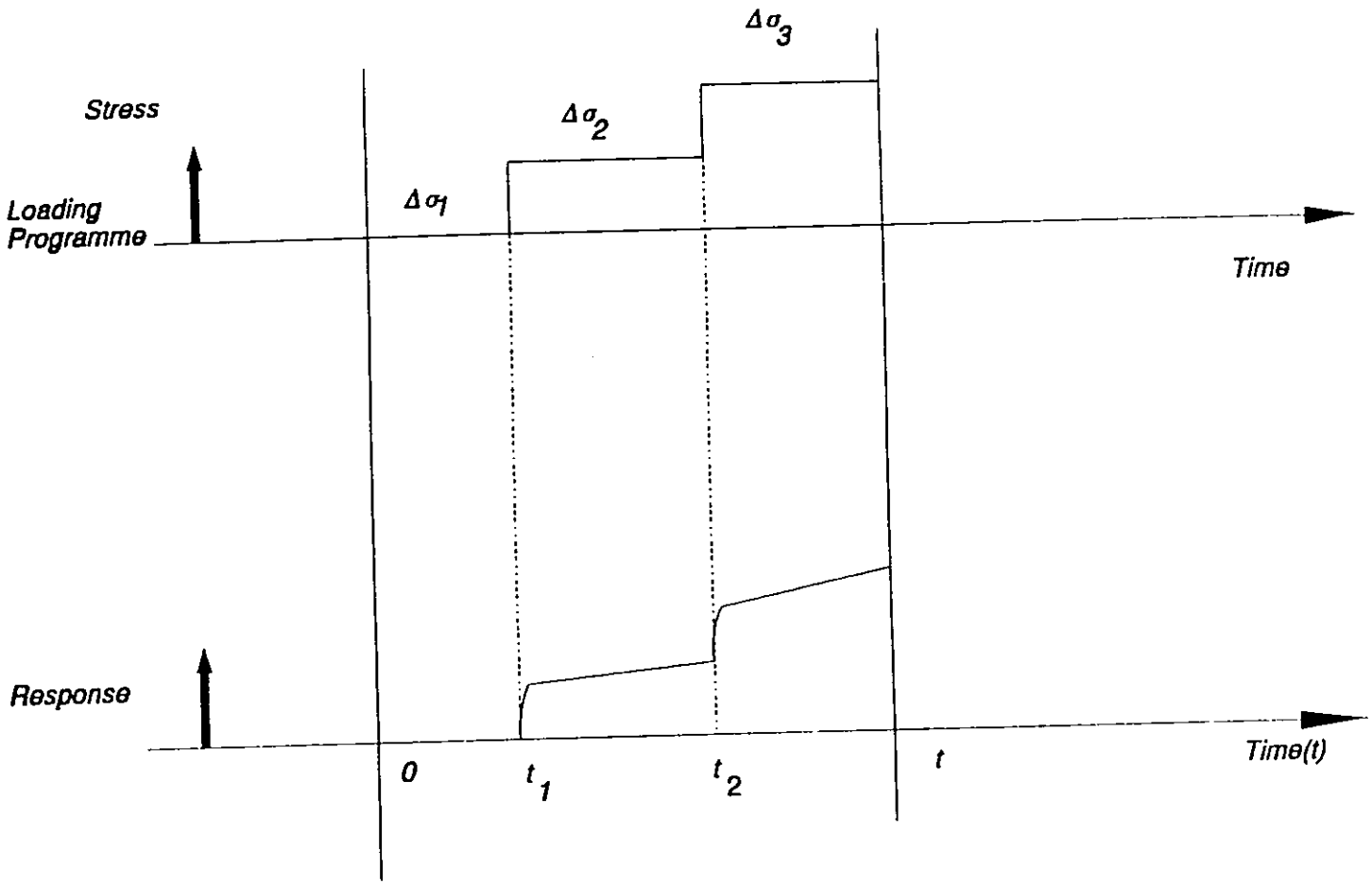

4.3 Boltzmann's superposition principle

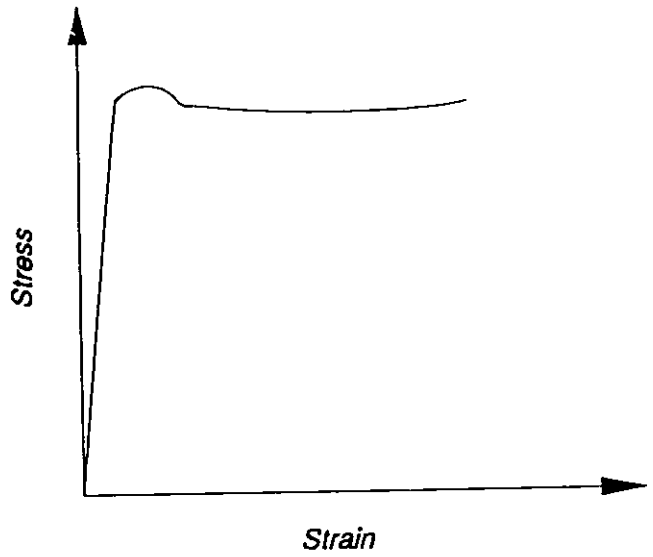

4.4 Schematics of a stress-strain relationship for a solid polymer undergoing uniaxial tension.

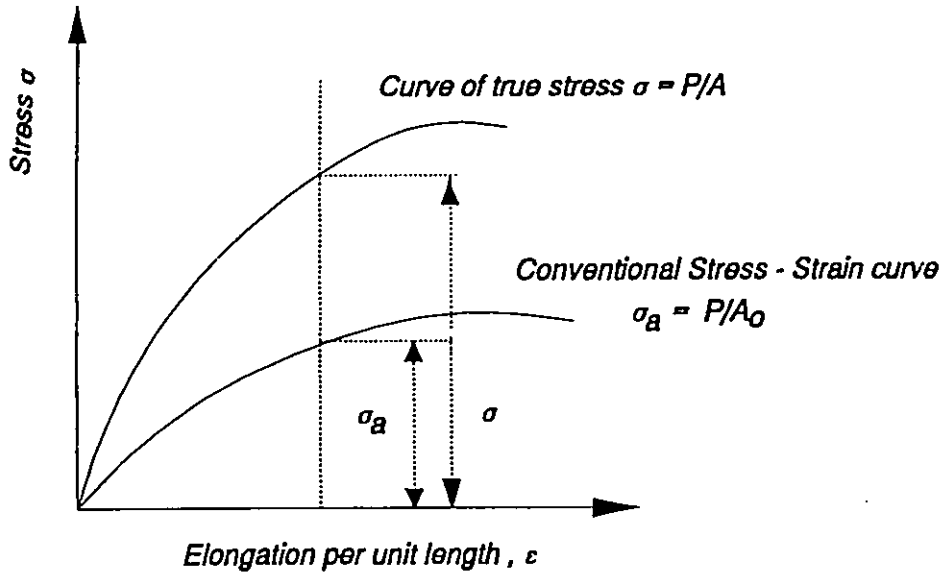

4.5 Conventional (engineering) and true stress-strain curves for a solid polymer undergoing uniaxial tension test.

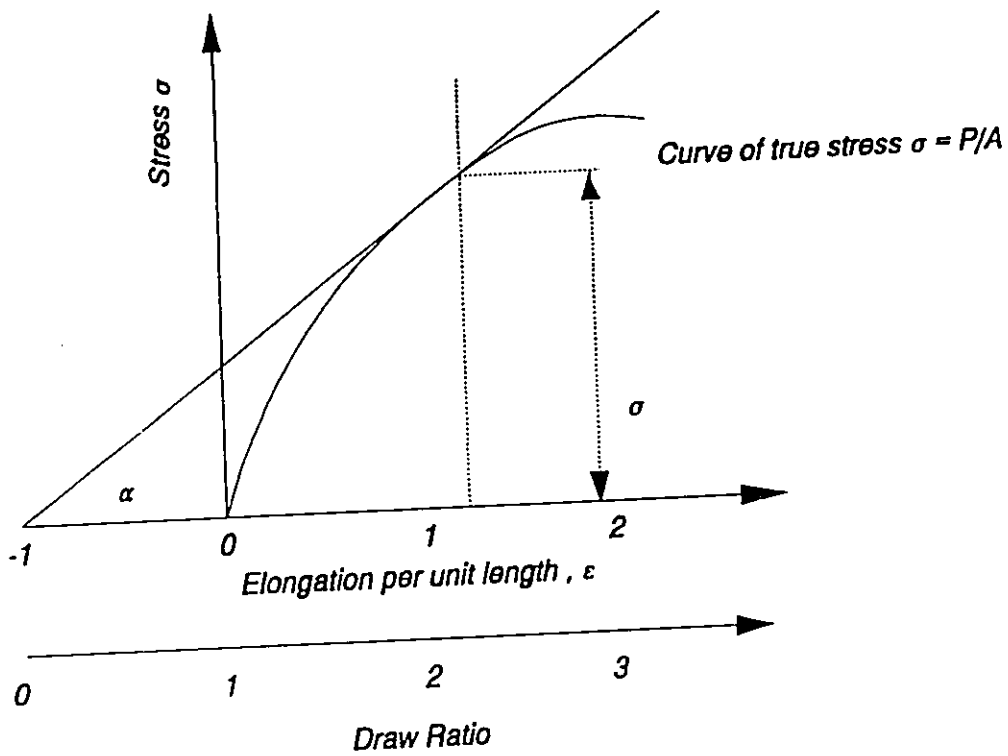

4.6 **The Conside're construction [57].**

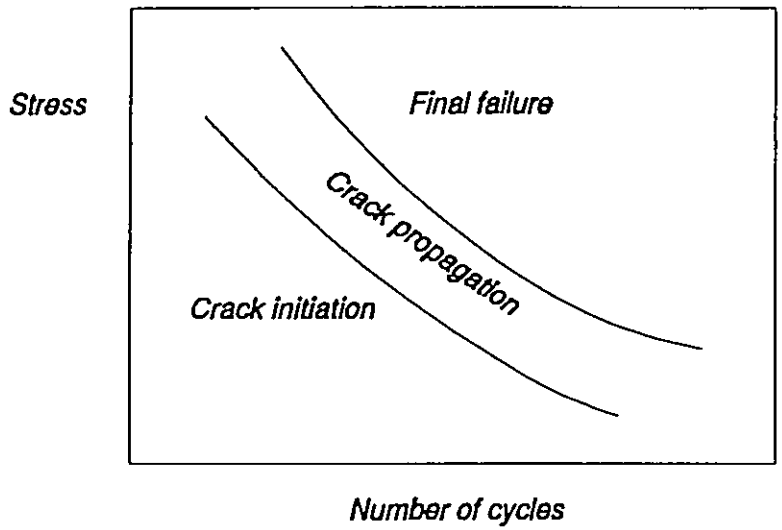

4.7 Fatigue response of a solid polymer.

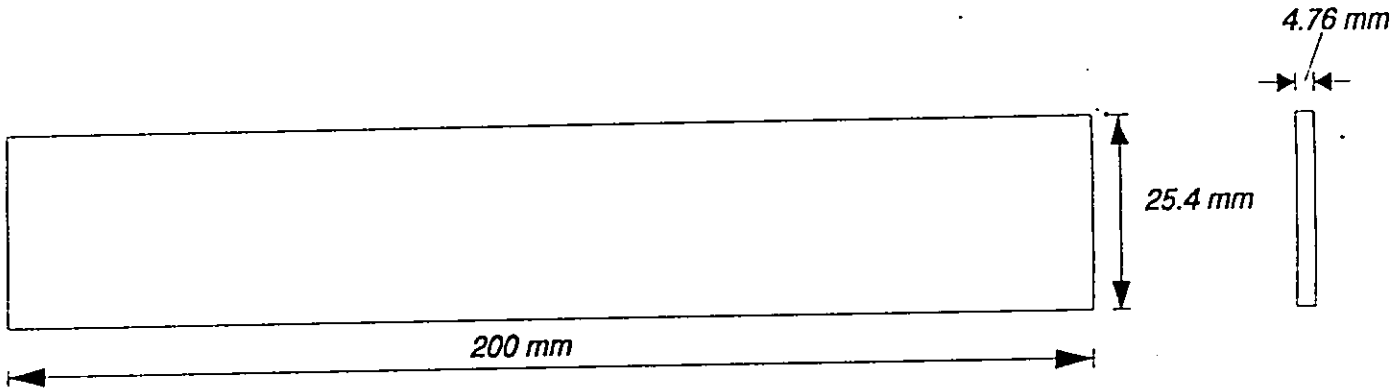

Material	*Polycarbonate (PC) and Polyvinylchloride (PVC)*
Manufacturing Method	*Band saw cutting and milling for finer finish as per ASTM STD D-638M-91a*
Purpose	*For stress-relaxation testing in uniaxial tensile testing.*

5.1 Specimen for uniaxial tensile stress-relaxation testing.

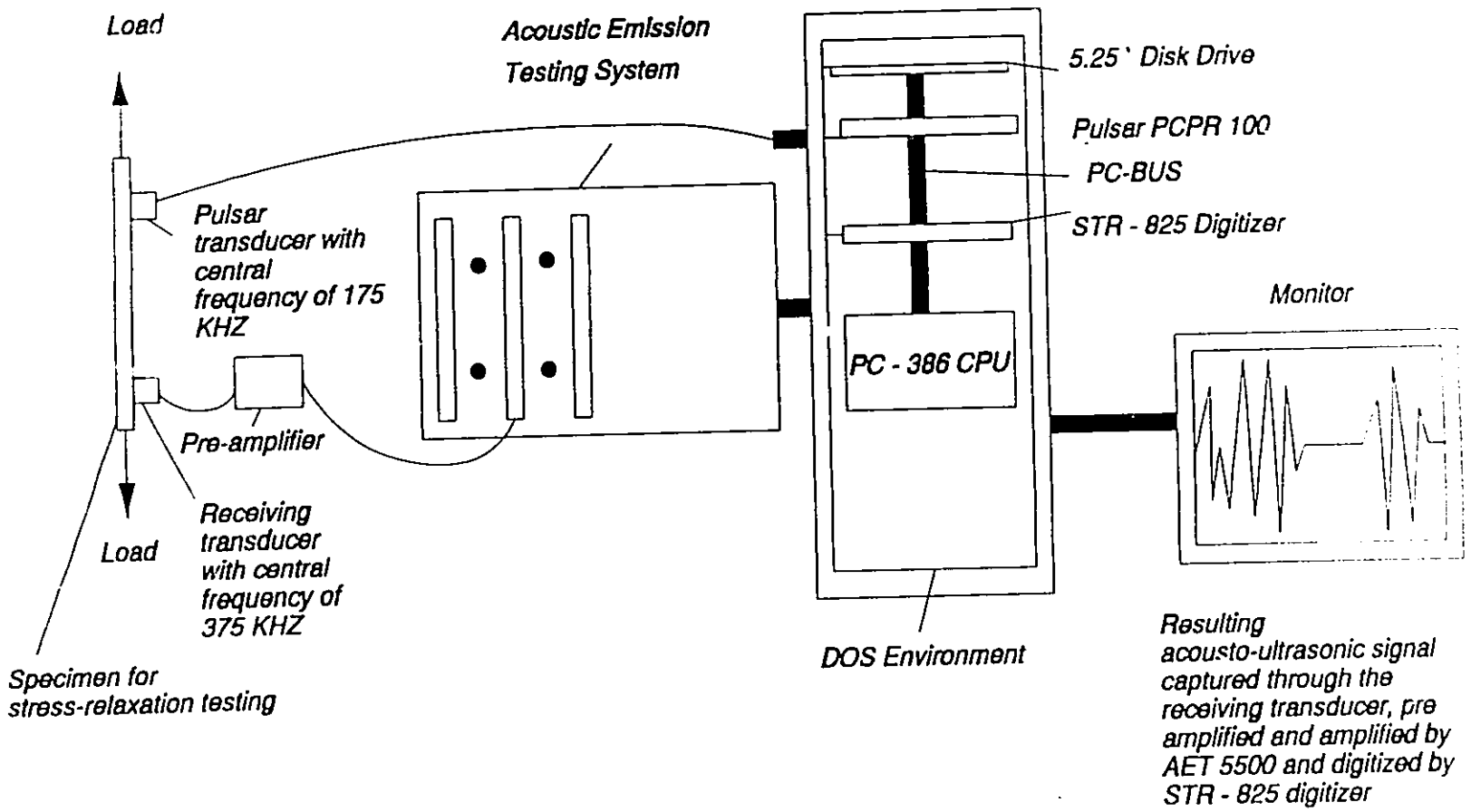

5.2 Acousto-ultrasonic experimental set-up.

TEST PARAMETER CHART

Acousto-Ultrasonic (AU) Test Parameter	Value	Description
Voltage Range	0 to +12V	The AU signal is displayed in the signal window as a time-dependent voltage function between the limits of 0 and +12 volts
Gain	60 decibels	Amplification factor
Frequency of the AU Wave	750 KHz	Frequency of the AU wave determined by the input pulse to the broad band piezo-transducer
Central Frequency of the Broad Band Receiver	175 KHz	Frequency of the receiving transducer
Sampling Rate	3.125 MHz	Rate of digitization of the AU wave form
Calibration of X-axis of the Signal Window	64 microsec / division	The X-axis is labelled as microseconds and the wave form is displayed in real time
Calibration of Y-axis of the Signal Window	32 millivolt/ division	The Y-axis is labelled as millivolts and the acousto-ultrasonic signal is digitized at discrete points as a function of voltage
Active Number of Windows	1	The portion of screen PC-386 converted into real time oscilloscope
Active Number of Channels	1	The number of independent channels in the acoustic emission receiver
Active Number of Gates	1	The number of independent gates used for digitization

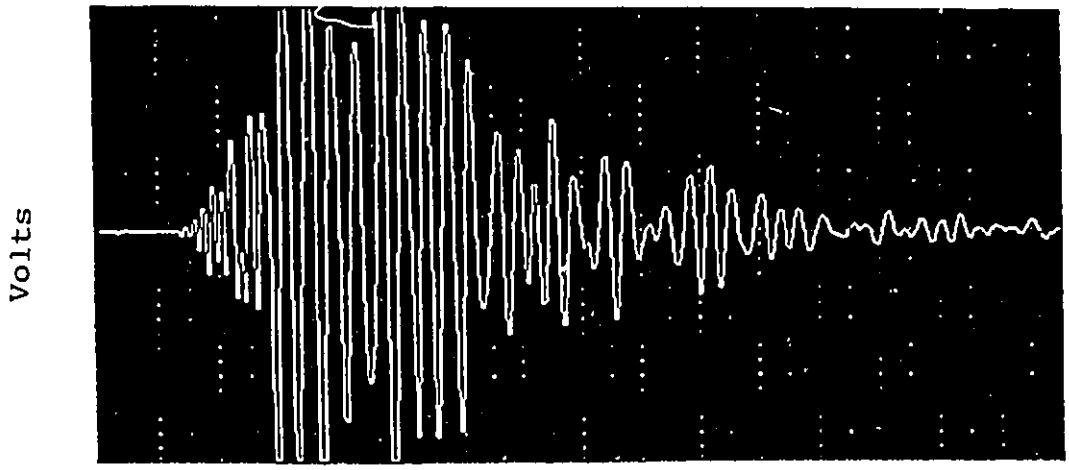

5.3 A sample of acousto-ultrasonic wave form with test parameters chart.

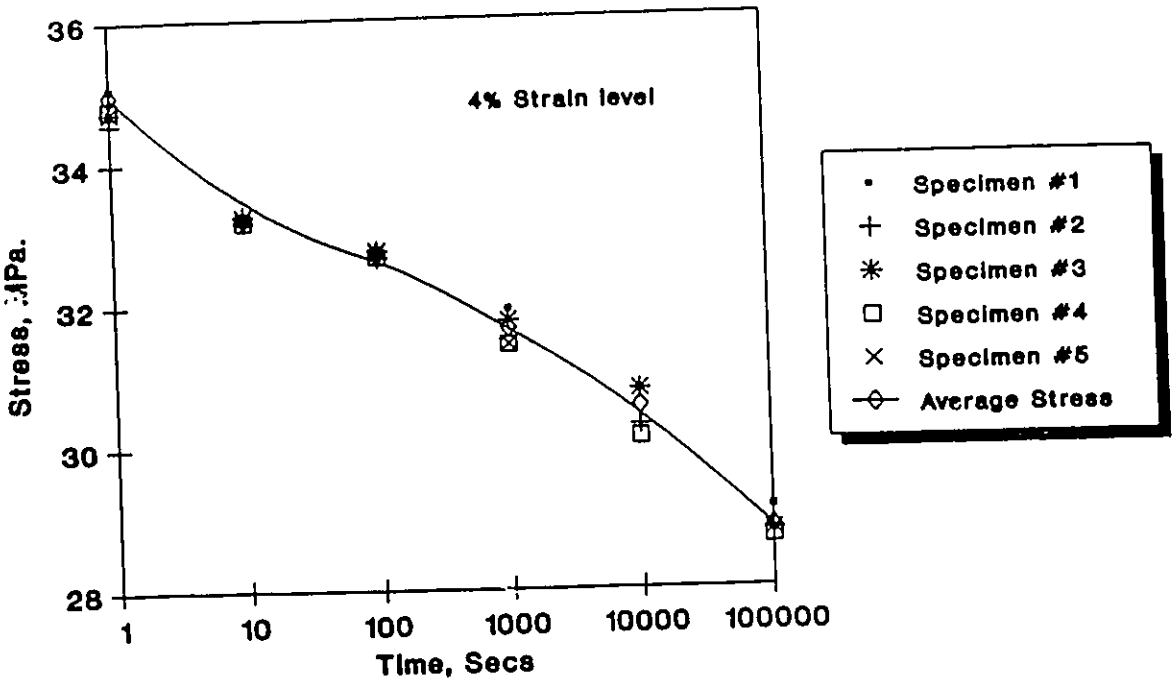

5.4 *Stress-relaxation curves for Polycarbonate (PC) specimens under 4% uniaxial (tensile) strain.*

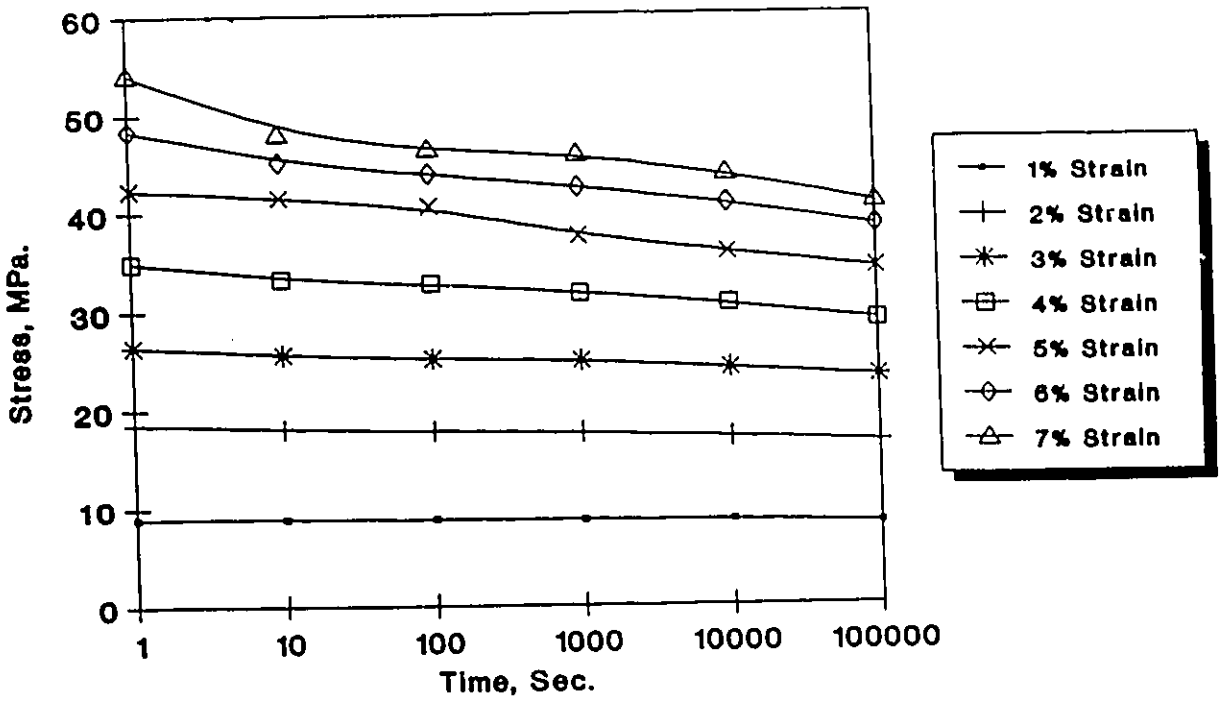

5.5 *Stress-relaxation curves for Polycarbonate (PC) specimens under different uniaxial (tensile) strain levels of 1% - 7%.*

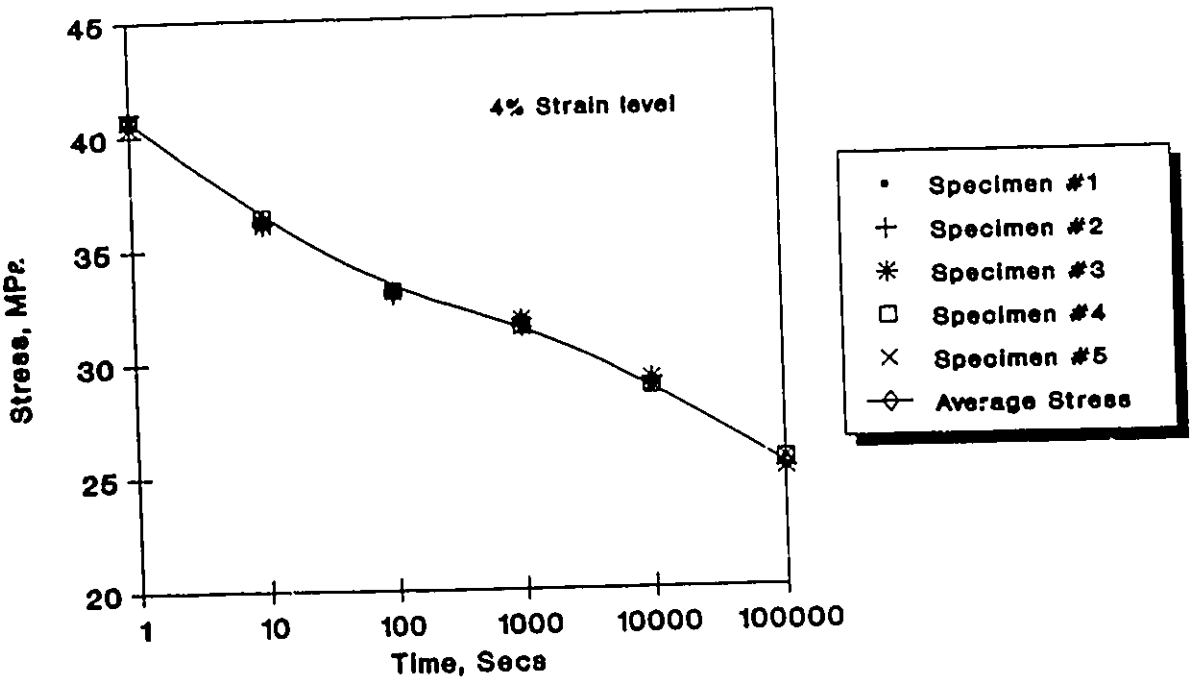

5.6 ***Stress-relaxation curves for Polyvinylchloride (PVC) specimens under 4% uniaxial (tensile) strain.***

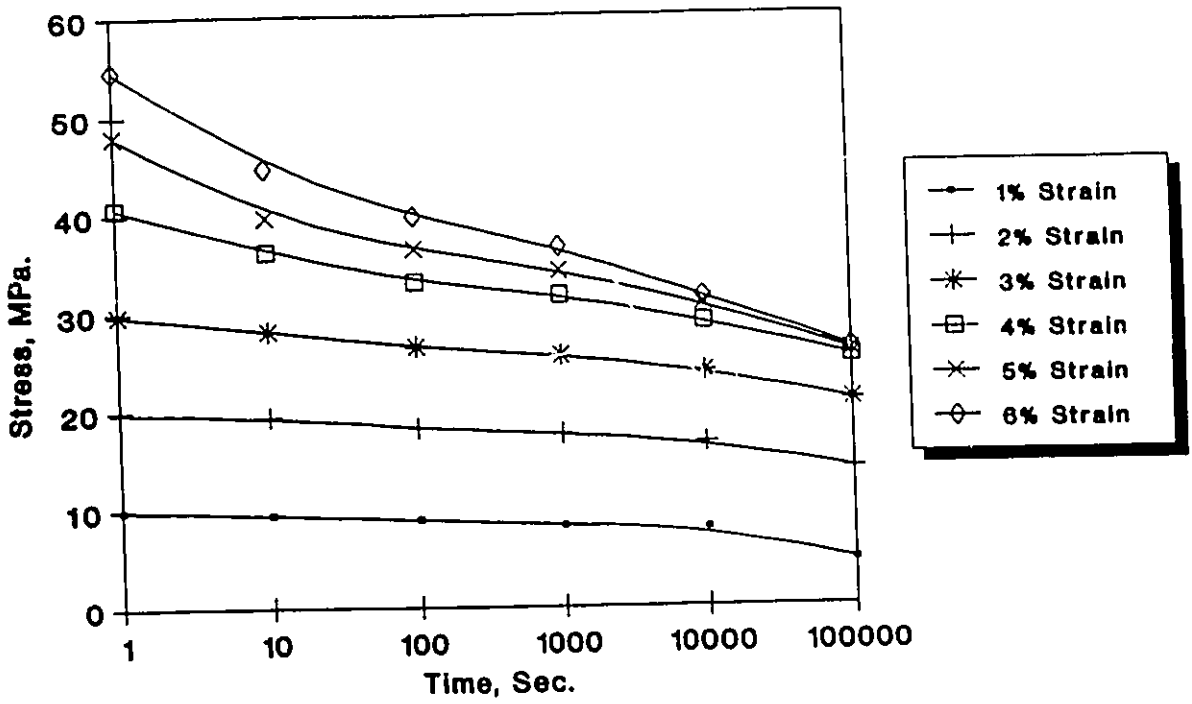

5.7 ***Stress-relaxation curves for Polyvinylchloride (PVC) specimens under different uniaxial (tensile) strain levels of 1% - 6%.***

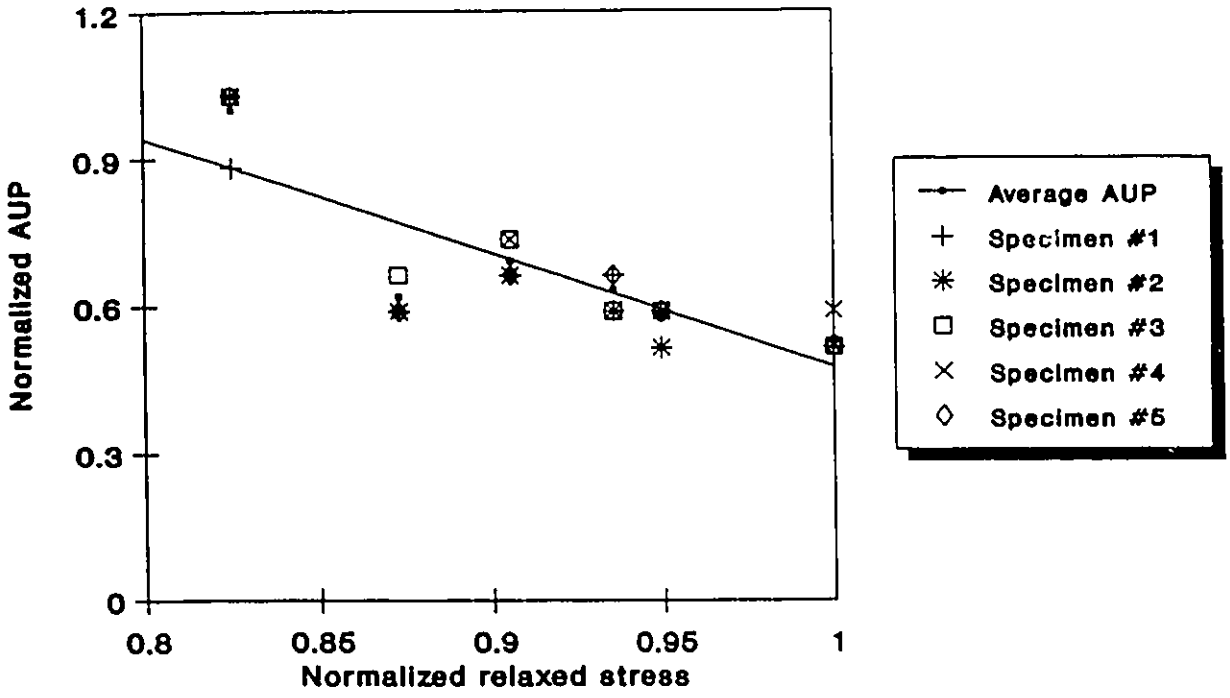

5.8a *Correlation between the normalized relaxed stress and the normalized acousto-ultrasonic parameter (AUP) of the waveform at different stress levels for Polycarbonate (PC) specimens.*

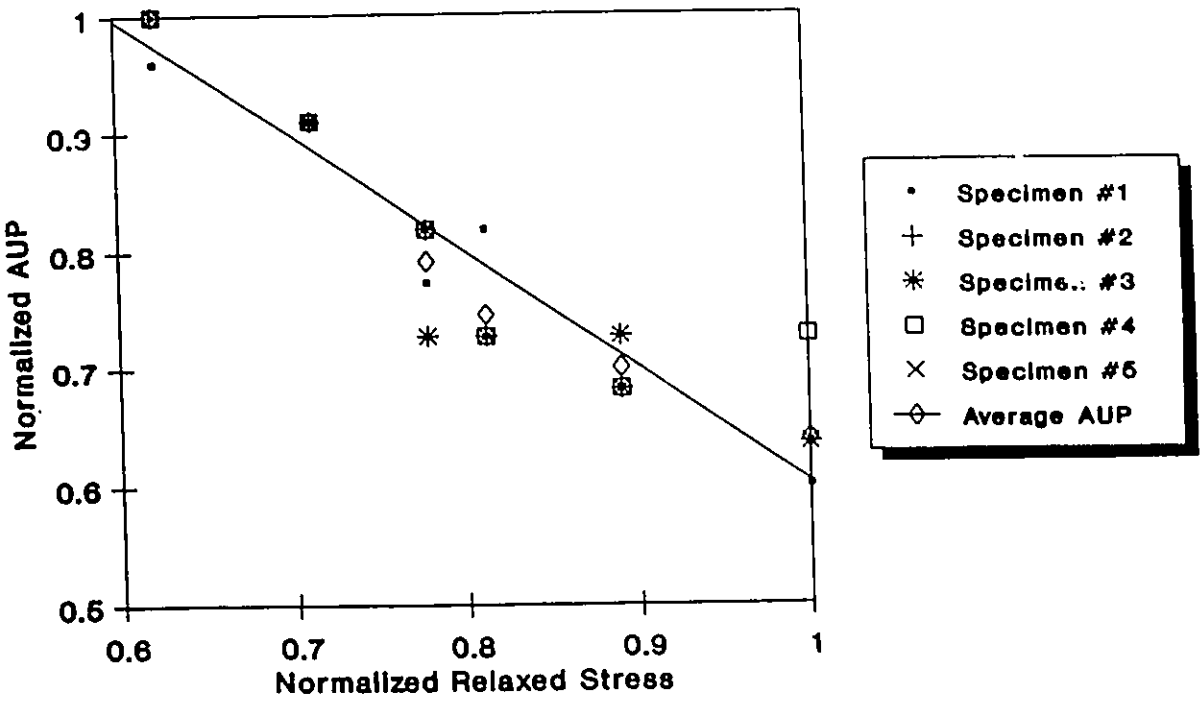

5.8b *Correlation between the normalized relaxed stress and the normalized acousto-ultrasonic parameter (AUP) of the waveform at different stress levels for Polyvinylchloride (PVC) specimens.*

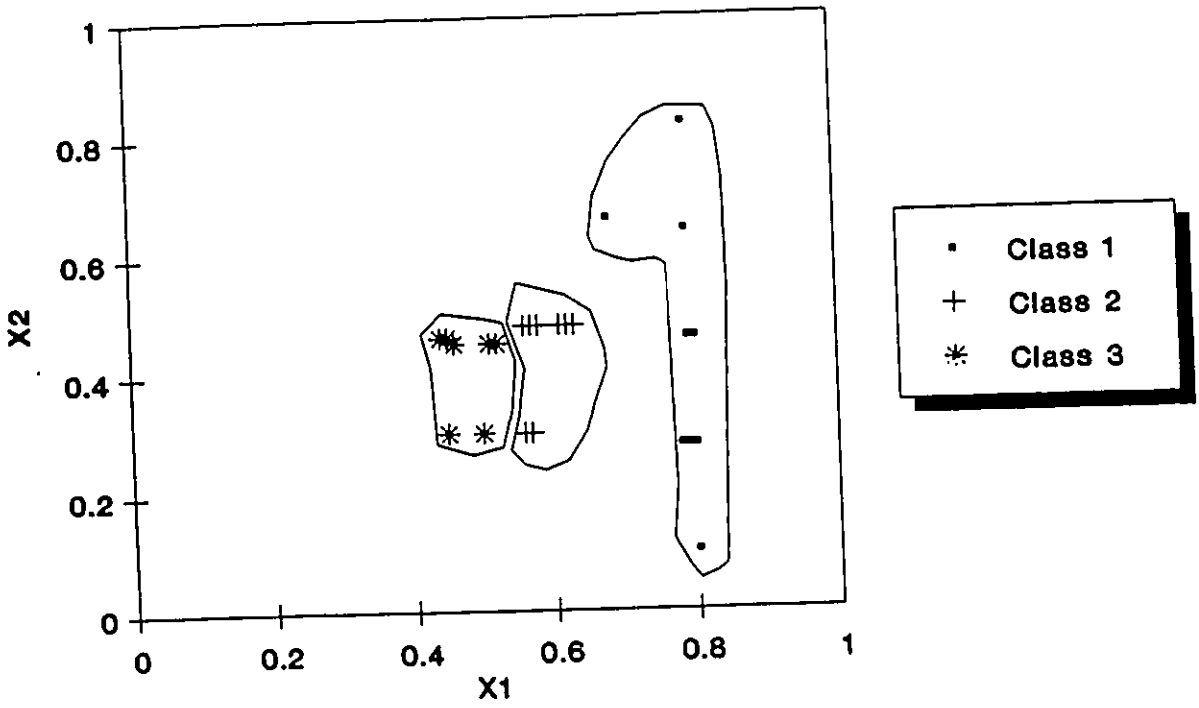

X_1 : Normalized second greatest peak amplitude in power domain.
X_2 : Normalized number of peaks above the signal base line in power domain.

5.9a *Plot illustrating the seperation of pattern classes in a two-dimensional feature space for Polycarbonate (PC) specimens.*

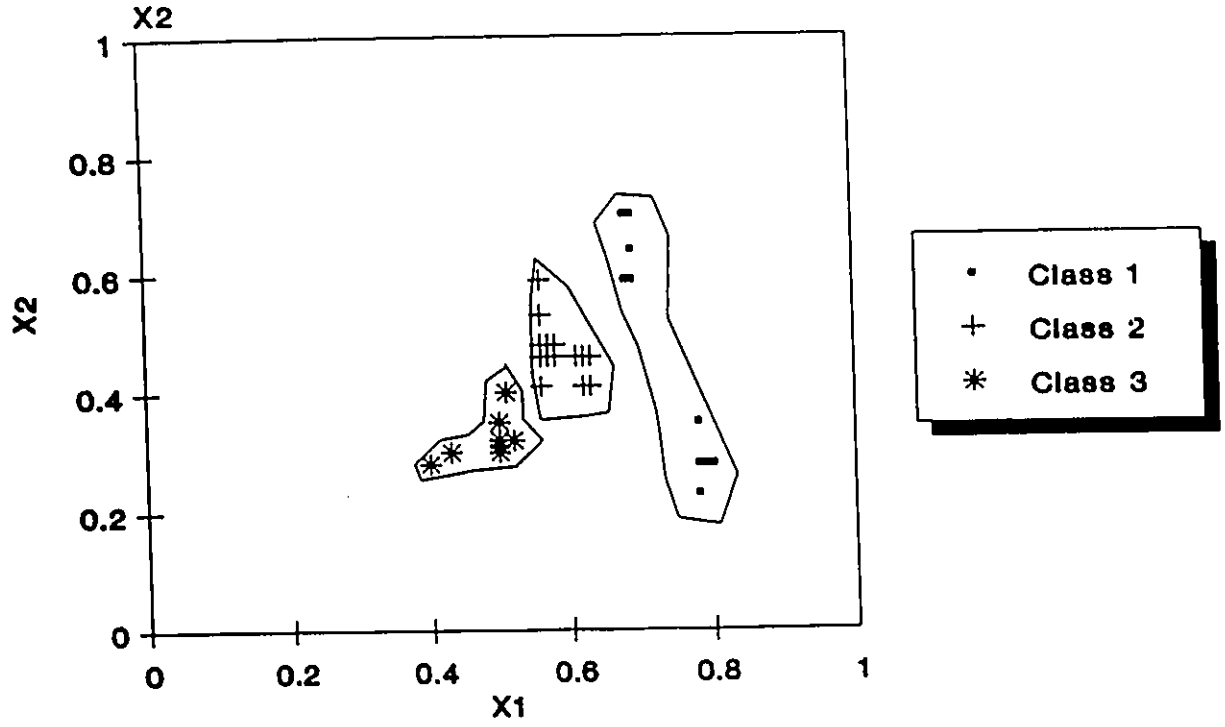

X_1 : Normalized value of second greatest peak amplitude in power domain.

X_2 : Normalized percentage of partial power in third octant.

5.9b *Plot illustrating the seperation of pattern classes in a two-dimensional feature space for Polycarbonate (PC) specimens.*

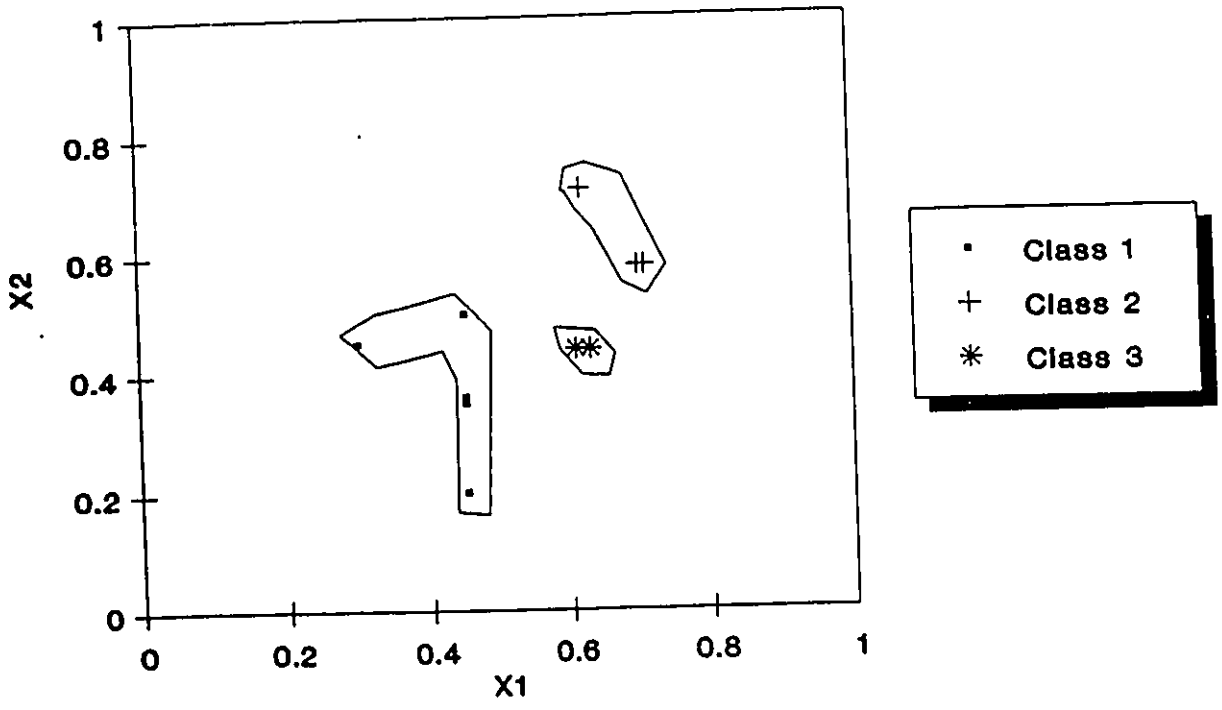

X_1 : Normalized inter-peak distance from first to second greatest peaks in time domain.

X_2 : Normalized greatest peak position in phase domain.

5.9c *Plot illustrating the seperation of pattern classes in a two-dimensional feature space for Polyvinylchloride (PVC) specimens.*

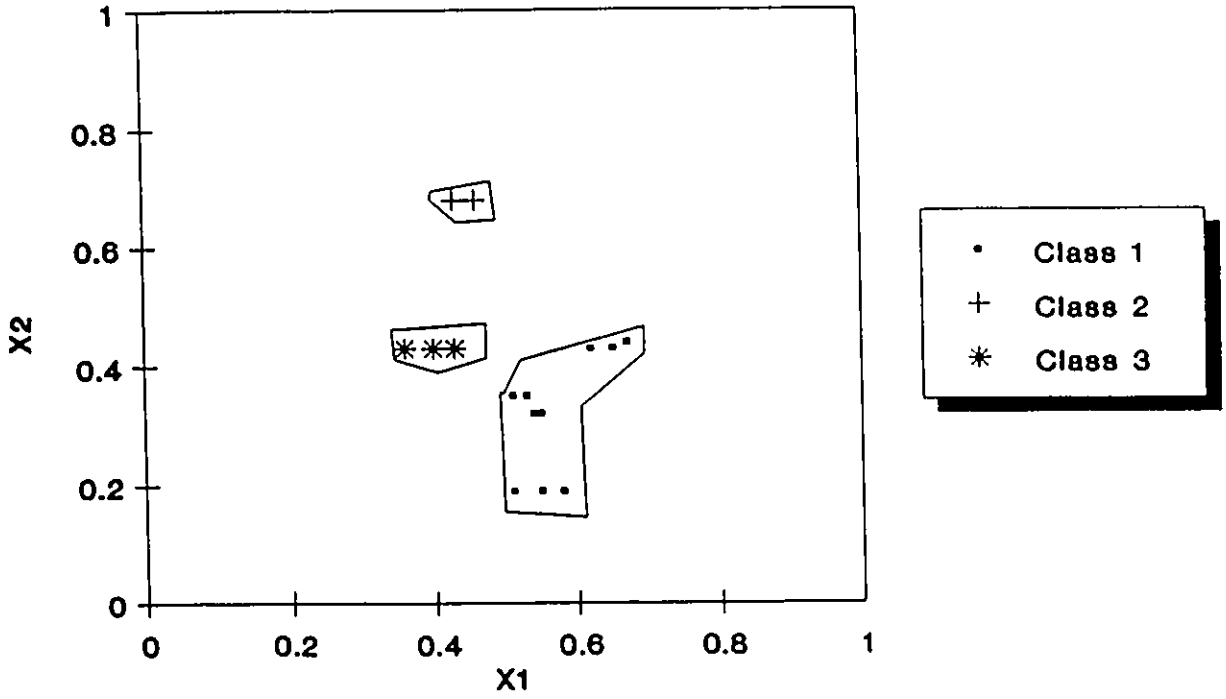

X_1 : Normalized second greatest peak amplitude in power domain.
X_2 : Normalized greatest peak position in phase domain.

5.9d *Plot illustrating the seperation of pattern classes in a two-dimensional feature space for Polyvinylchloride (PVC) specimens.*

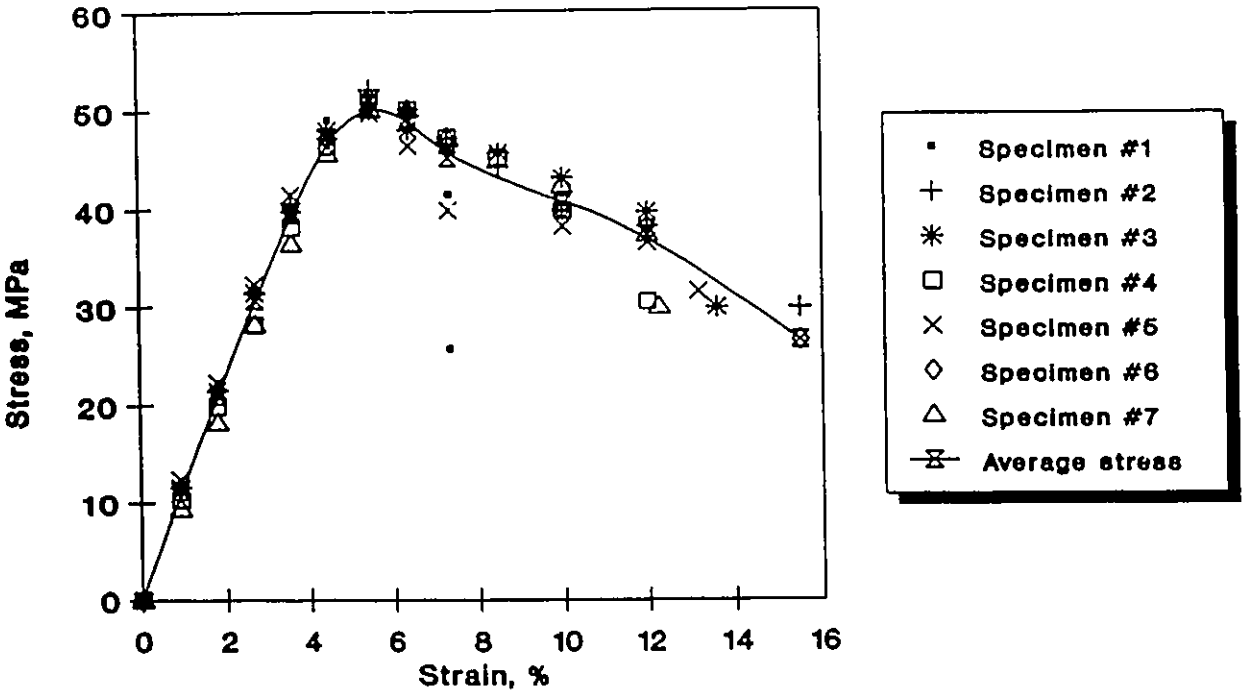

6.1 ***Stress-Strain diagram for uniaxial tension test for Polyvinylchloride (PVC) specimens at a cross head speed of 2.5 mm/min.***

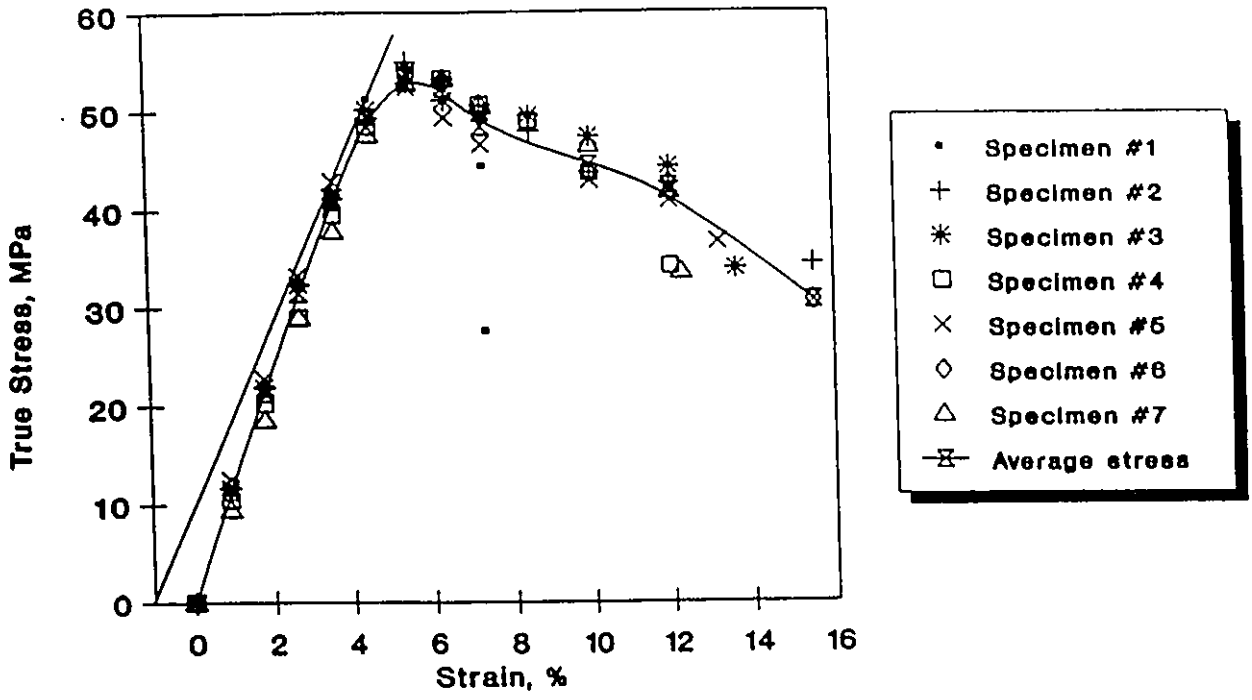

6.2 ***The Conside're construction for the ultimate strength of the PVC specimen under Uniaxial tension test.***

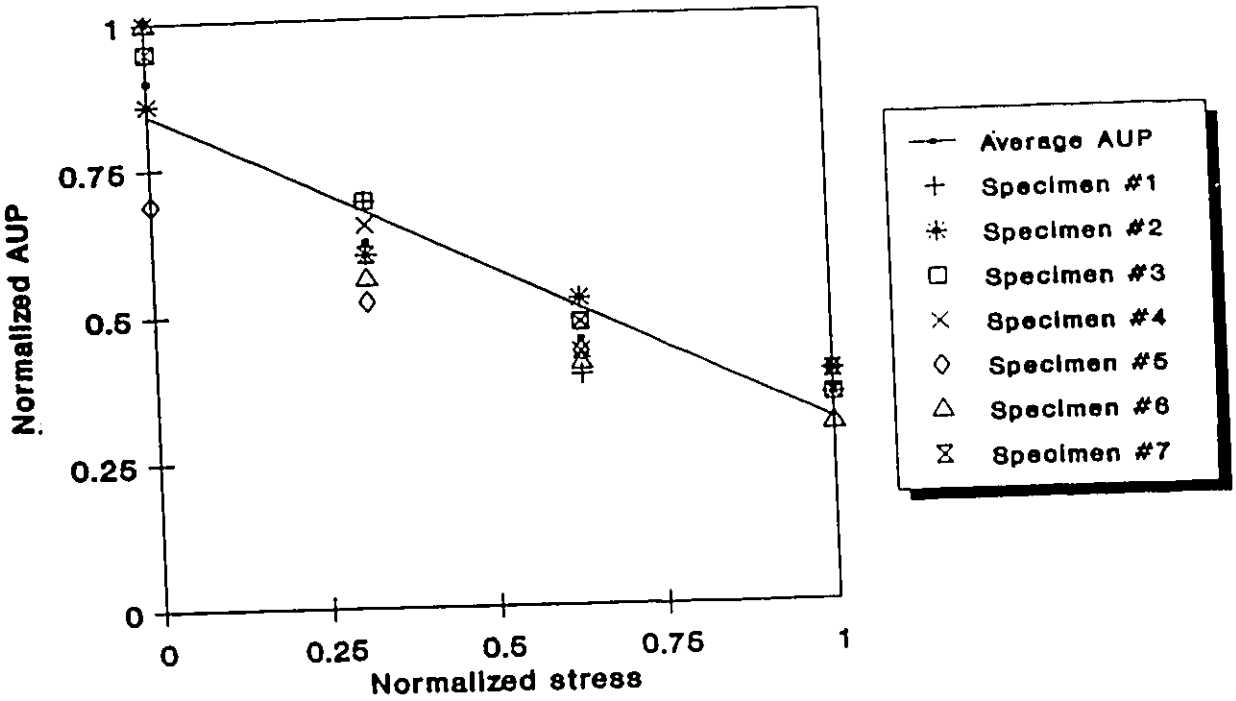

6 3 Correlation between the normalized stress and the normalized acousto-ultrasonic parameter (AUP) of the waveform at different stress levels.

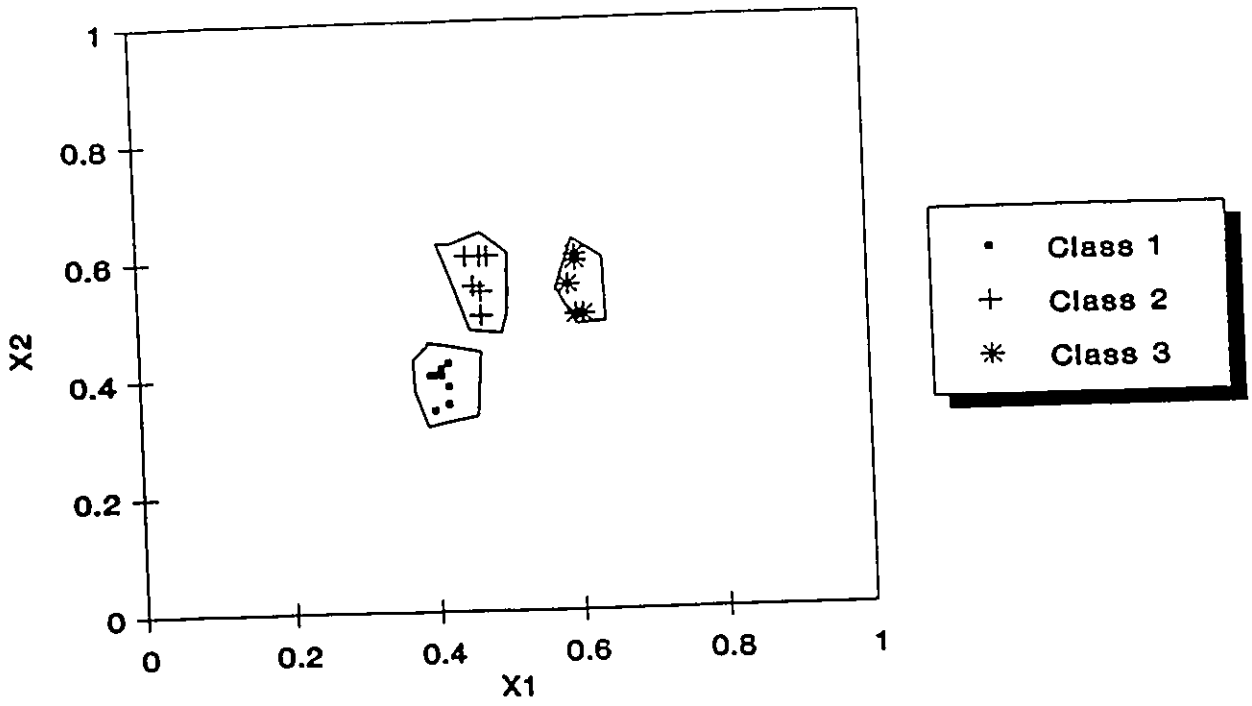

X_1 : Normalized greatest peak position in time.
X_2 : Normalized third greatest peak position in time.

6.4a *Plot illustrating the separation of pattern classes in a two-dimensional feature space.*

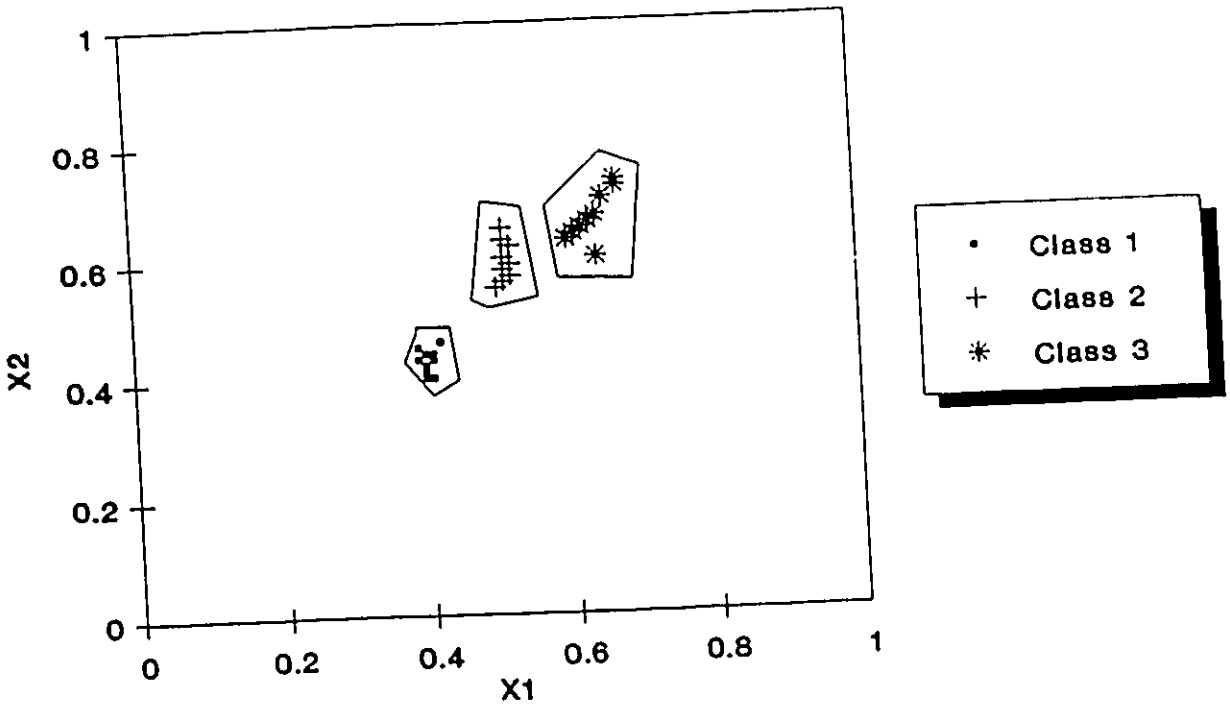

X_1 : Normalized greatest peak position in time.
X_2 : Normalized value of the percentage of partial power in second octant in phase domain.

(6.41) *Plot illustrating the separation of pattern classes in a two-dimensional feature space.*

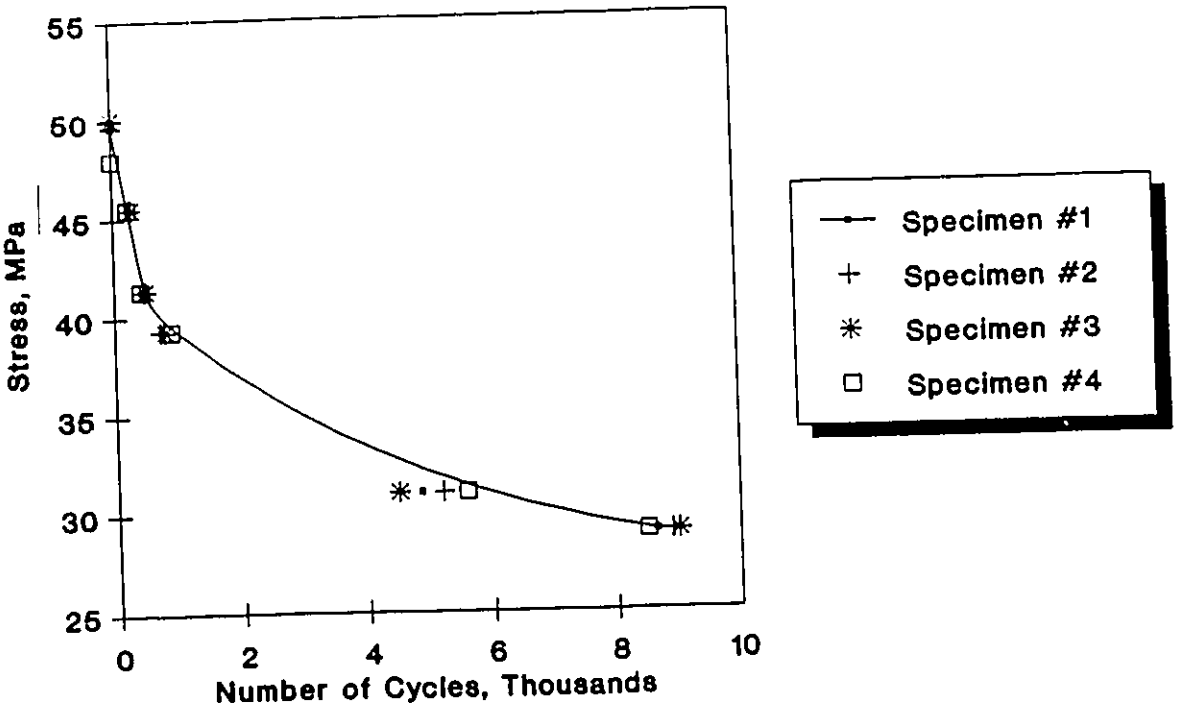

7.1 Stress (σ) - Number of cycles for failure (N) diagram for fatigue testing.

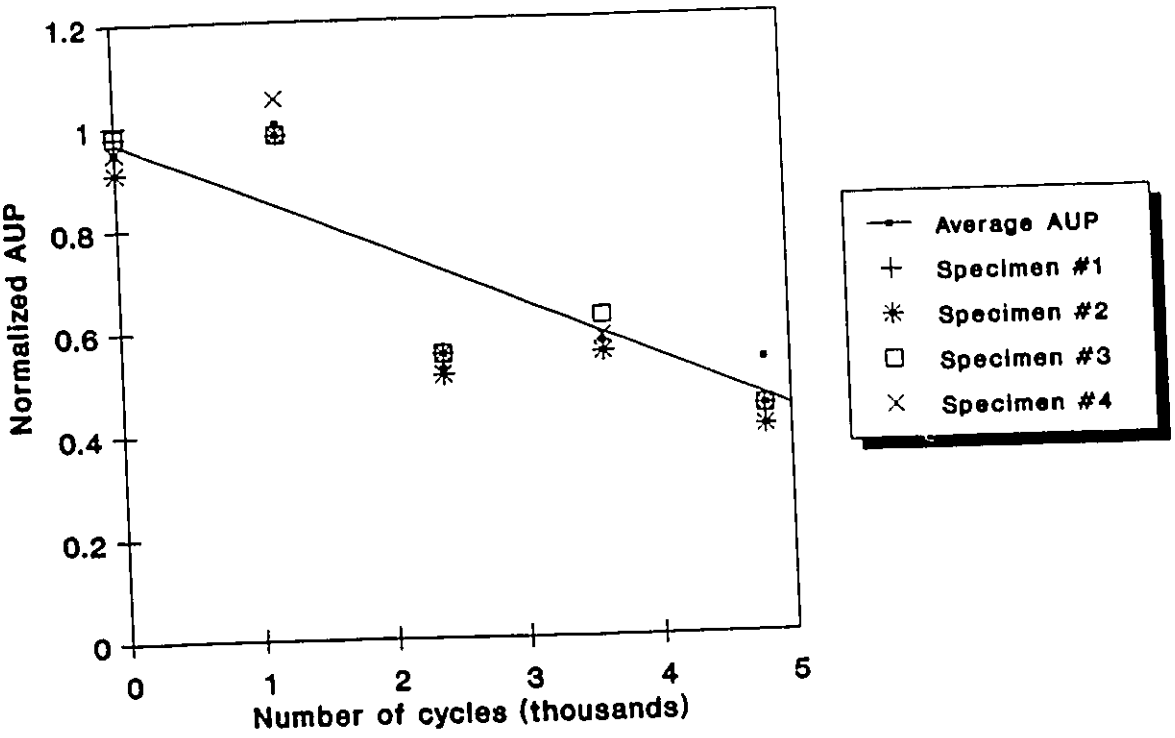

7.2 Correlation between the normalized acousto-ultrasonic parameter and cyclic loading levels causing fatigue.

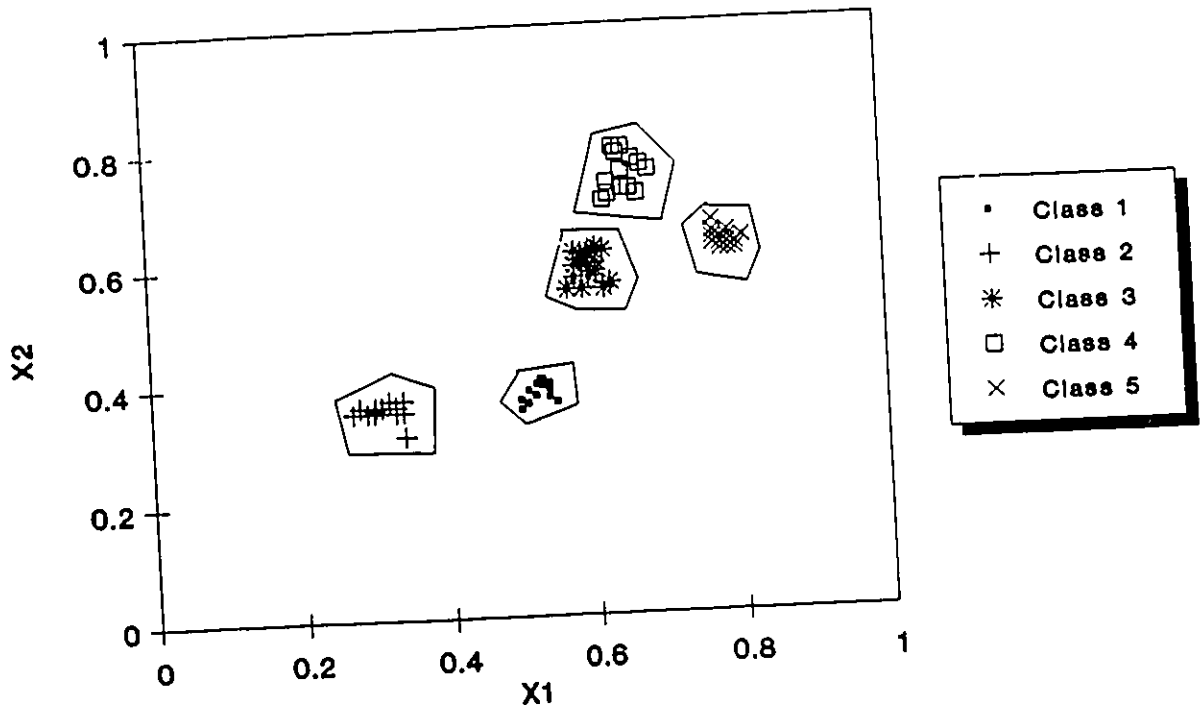

X_1 : Normalized value of greatest peak amplitude in power domain.
X_2 : Normalized value of greatest peak amplitude in cepstral domain.

7.3 Plot illustrating the separation of pattern classes in a two-dimensional feature space.

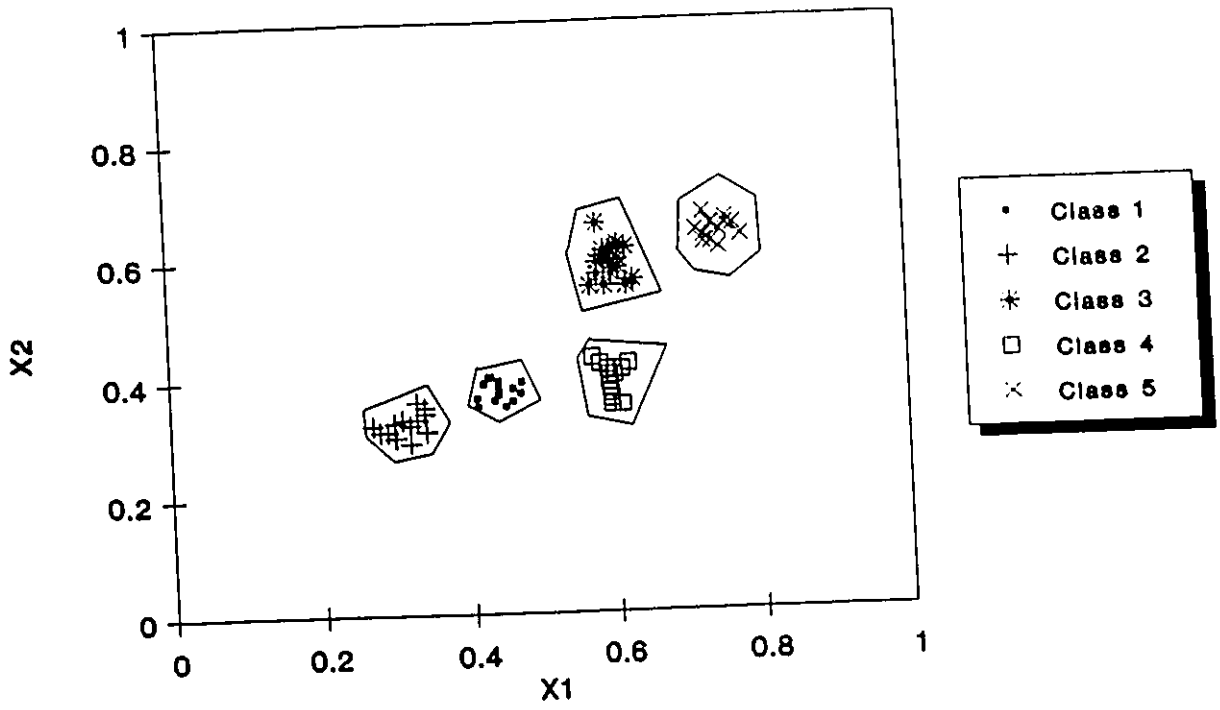

X_1 : Normalized value of greatest peak amplitude in power domain.
X_2 : Normalized value of second greatest peak amplitude in cepstral domain.

7.4 Plot illustrating the separation of pattern classes in a two-dimensional feature space.

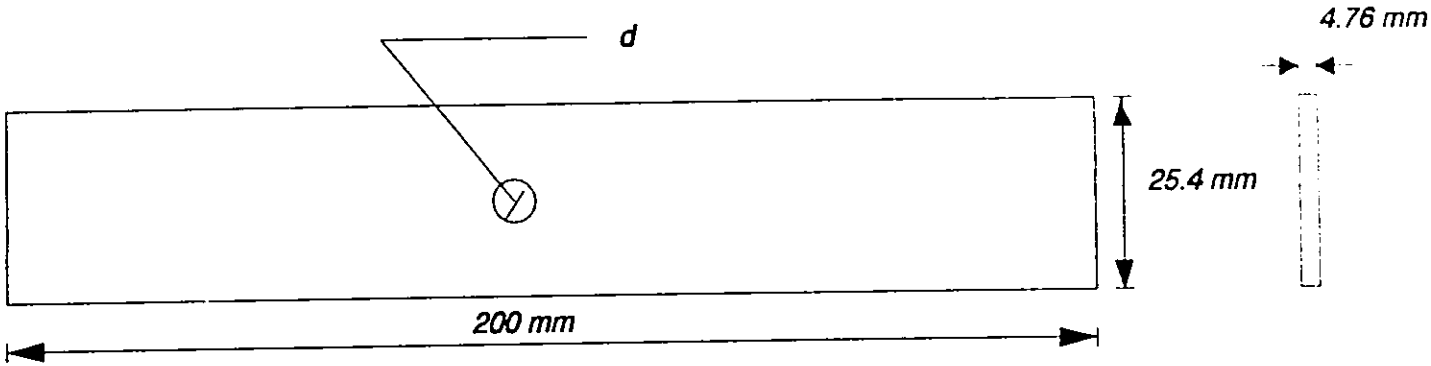

Material	*Polycarbonate (PC)*
Manufacturing	*Bandsaw cutting and milling for finer finish as per ASTM D - 638M-91a ; Defects were created by drilling holes of variying diameter 'd'*
Purpose	*Non-Destructive evaluation of the effect of macromechanical defect on the tensile strength of the specimen in uniaxial tensile testing*

Group	1	2	3	4	5	6	7
'd' in mm	0	2.0	2.381	2.7781	3.175	3.516	4.0

8.1 Specimen for evaluation of reduced tensile strength in uniaxial tensile testing.

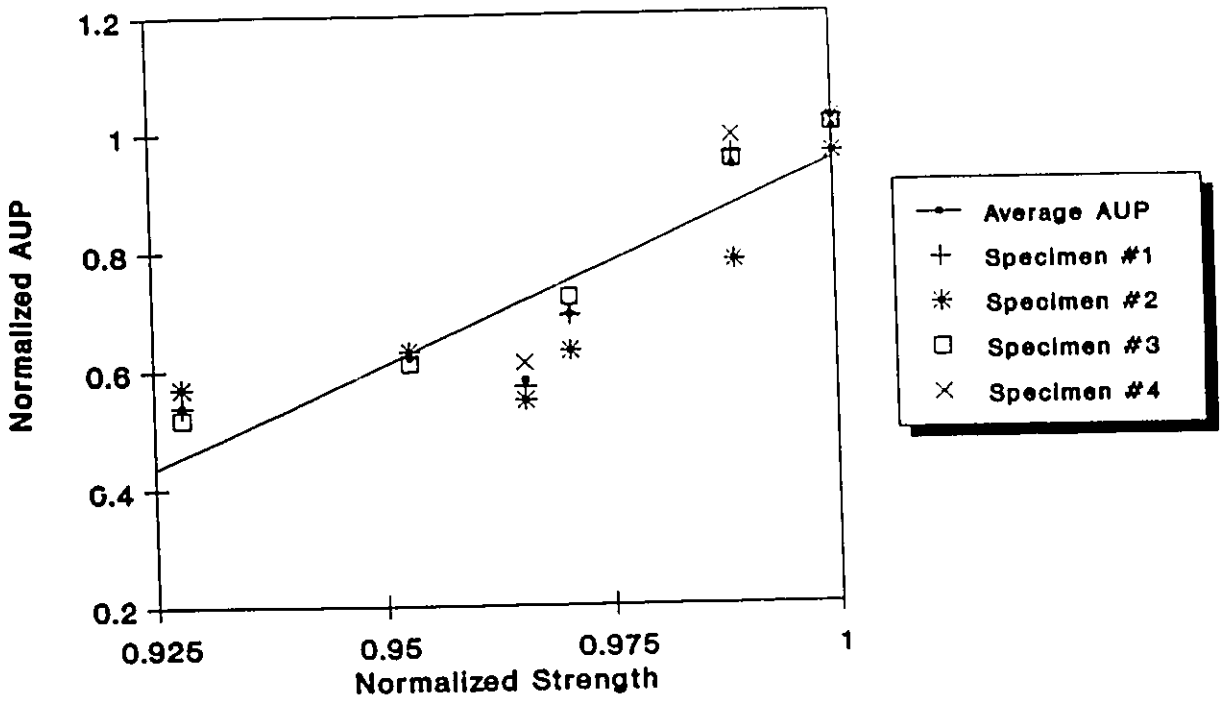

8.2 Correlation between the normalized acousto-ultrasonic parameter and normalized tensile strength.

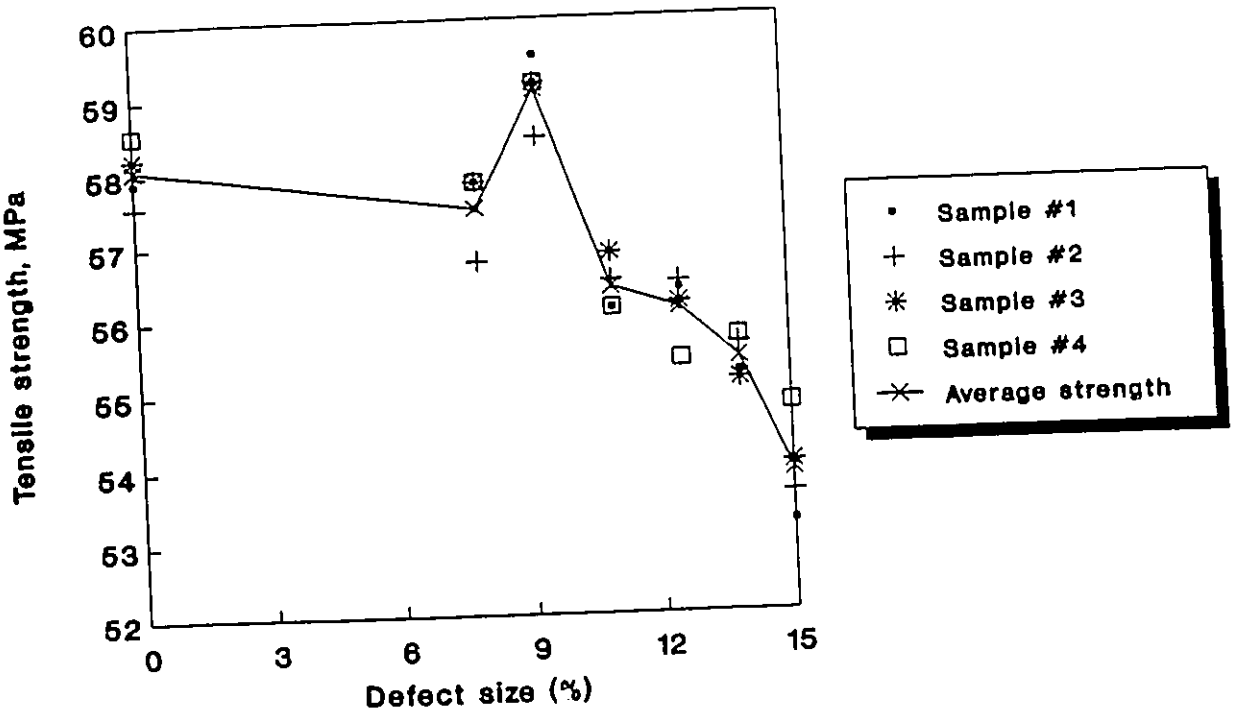

8.3 Correlation between tensile strength and defect size.

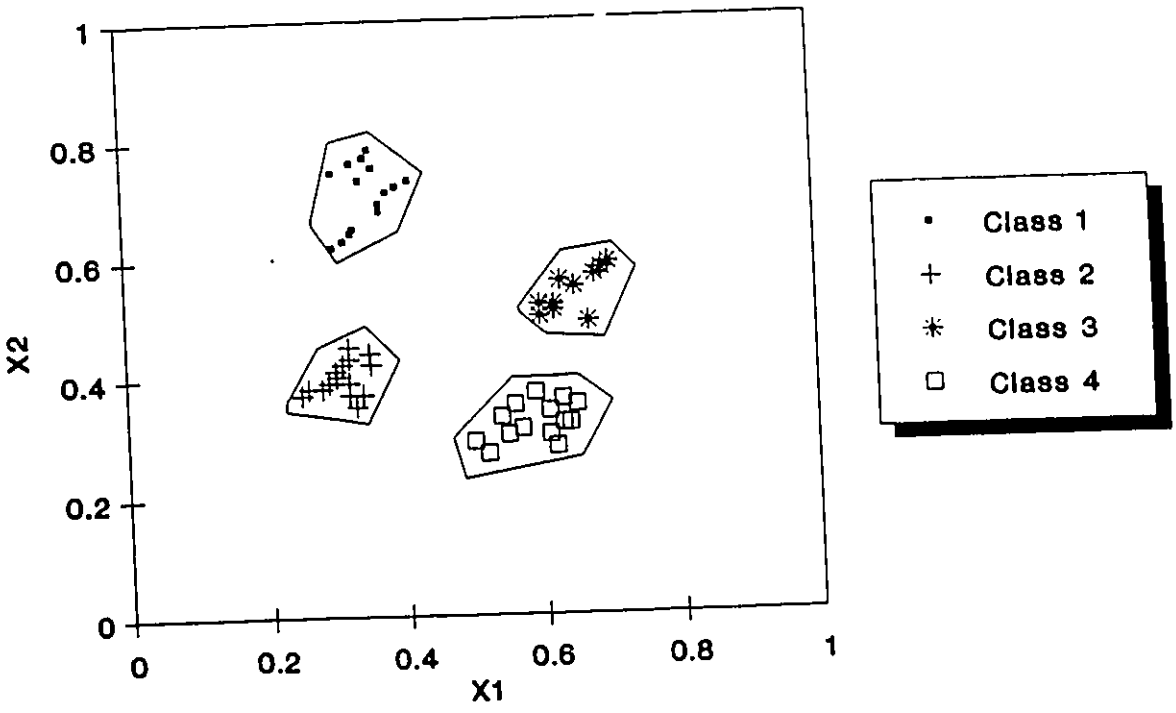

X_1 : Normalized value of greatest peak amplitude in cepstral domain.

X_2 : Normalized value of percentage of partial power in first octant in phase domain.

8.4a Plot illustrating the separation of pattern classes in a two-dimensional feature space.

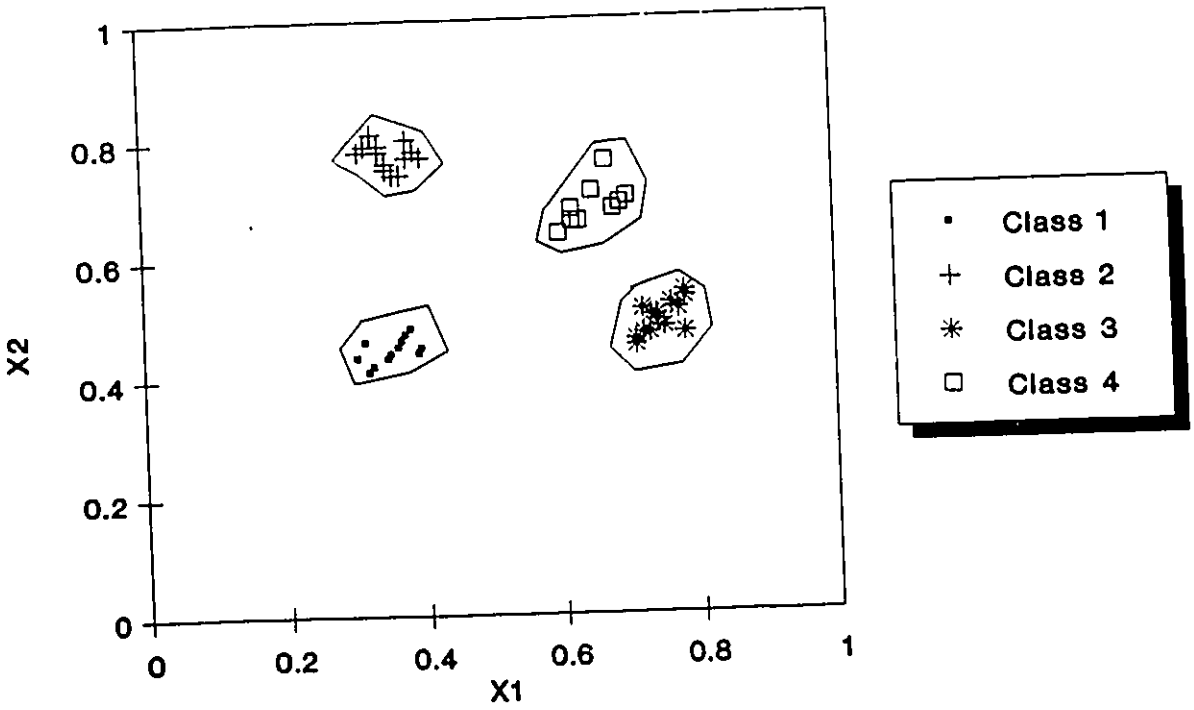

X_1 : Normalized value of greatest peak amplitude in cepstral domain.

X_2 : Normalized value of percentage of partial power in second octant in phase domain.

8.4b Plot illustrating the separation of pattern classes in a two-dimensional feature space.